Metals Handbook Desk Edition Chapter 34,
American Society of Metals, (1985).

34 MECHANICAL TESTING

Edited by Marc A. Meyers, New Mexico Institute of Mining and Technology

The material on torsion testing that appears in this section was reprinted from Workability Testing Techniques, edited by G. E. Dieter, American Society for Metals, 1984. The material on fatigue-crack-growth-rate test methods and fracture-toughness testing was adapted from Application of Fracture Mechanics for Selection of Metallic Structural Materials, edited by J. E. Campbell, W. W. Gerberich and J. H. Underwood, American Society for Metals, 1982. Additional material in this section is based on the Metals Engineering Institute course on Mechanical Testing of Metals, by the M.E.I. Mechanical Testing of Metals Development Committee: W. T. Becker (Chairman), University of Tennessee; J. A. Alic, Office of Technology Assessment; K. T. Bassett, Danly Machine Co.; B. Boardman, Deere & Co.; J. P. Bosscher, Calvin College; T. M. Broughton, Tinius Olsen Testing Machine Co.; J. T. Cammett III, Metcut Research Associates, Inc.; J. Devis, American Society for Metals, retired; G. E. Dieter, University of Maryland; J. L. Herron, Herron Testing Labs; P. M. Mumford, United Calibration Corp.; C. H. Philleo, General Electric Co.; D. Socie, University of Illinois at Urbana-Champaign; J. Woodruff, CMW, Inc.

Introduction to Mechanical Testing

DESIGN of structures and systems requires determination of component dimensions and is based on the appropriate mechanical properties of materials. For static loading at low temperature, design criteria may include:

1. Excessive elastic deformation
2. Initiation of plastic deformation
3. Excessive plastic deformation
4. Unstable crack propagation.

Criterion 1 states that a certain component can undergo a specific maximum elastic strain. The elastic modulus of the material is the important property, because it allows, through Hooke's Law, establishment of the maximum stress. Criterion 2 limits the strains to elastic (recoverable) strains and prohibits plastic strains; the important property of the material is its yield stress. Criterion 3 accepts a certain amount of plastic deformation; important material properties are ultimate strength, uniform elongation, and work hardening. Criterion 4 accepts the possible existence of cracks or defects, and maximum loads are based on fracture toughness.

In conjunction with static loads, most structures are subjected to cyclical loading conditions. When the loads are not constant, the possible damage due to fatigue must be considered and the appropriate fatigue properties must be considered along with the static design requirements.

At high temperature, the mechanical properties of metals are time-dependent and the properties used at low temperatures are not applicable. Under high-temperature conditions, metals tend to deform with time, and the appropriate mechanical properties of interest are creep properties.

In this section, procedures for evaluating the mechanical properties of metals—i.e., the response of a metal to a particular imposed loading condition—are reviewed.

STANDARDIZED TESTS

In the United States, most common mechanical tests have been standardized by the American Society for Testing and Materials (ASTM). In other countries, similar standards have been developed by the appropriate standardization agencies. If a mechanical test is being conducted by the manufacturer, user or testing laboratory, and if the results are used outside the organization, it is imperative that the procedures outlined in ASTM standards be followed and that this is specified in the presentation of the results. For internal work, comparative studies and research studies, specific procedures which may differ from those of ASTM can be developed on approval of all parties; in such instances, specific test conditions should be specified. For specific information on ASTM standards, test methods, definitions, specifications and recommended practices, the reader is referred to ASTM. Each year a new edition of the Book of Standards is published. Because modifications and revisions may be introduced on an annual basis, it is not wise to use obsolete editions. For reference, the appropriate ASTM specifications which are applicable to this section are listed in Table 1. In this table, those standards that have been approved as American National Standards are given. These standards (except for those under the headings "Corrosion" and "Erosion and Wear") are presented in the 1983 Annual Book of ASTM Standards. Additional information can be obtained in the Special Technical Publications (STP's) published by ASTM, a number of which are listed under "Additional Reading" at the end of this article, together with other useful sources of information.

MECHANICAL TESTING MACHINES

Numerous machines have been designed to perform the wide variety of mechanical tests listed in Table 1. In each of the following articles, test machines which are designed for a specific test are described in the separate section of that article devoted to that particular test. In this article, the basics of "universal testing machines," which can be used for tension, compression, formability and fatigue tests, are reviewed.

A wide variety of universal testing machines, produced by several manufacturers, are available. The basic elements of a universal testing machine are shown schematically in Fig. 1. In most modern machines, load is measured with a load cell (i.e., force transducer). Most load cells consist of a deflecting member which is instrumented with strain gages and which is coupled to a signal-conditioning system. The voltage output of the signal-conditioning system varies linearly with load and is used as input to a display or recording system.

The various universal testing machines differ primarily in how the displacement-control (or force-control) system operates. Displacement is usually imposed by either a mechanical or a hydraulic system.

Hydraulic (Open-Loop) Machines. Conventional hydraulic test equipment operates largely on the basis of open-loop control. Figure 2 shows a typical system of this type that is used to position the piston rod of a hydraulic actuator. An oper-

Table 1. ASTM procedures for mechanical testing

Subject	Reference
Bend and flexure testing	
Methods for:	
Bend Testing for Metallic Flat Materials for Spring Applications	E855-81
Guided Bend Test for Ductility of Welds	E190-80
Semi-Guided Bend Test for Ductility of Metallic Materials	E290-81
Methods and Definitions for:	
Mechanical Testing of Steel Products	A370-77
Calibration of mechanical testing machines, extensometers and strain gages	
Methods of Calibration of:	
Force-Measuring Instruments for Verifying the Load Indication of Testing Machines	E74-81
Methods of Verification of:	
Extensometers, and Classification of	E83-67 (1980)
Testing Machines	E4-83
Test Methods for:	
Performance Characteristics of Bonded Resistance Strain Gages	E251-67 (1980)
Compression testing	
Methods for:	
Compression Testing of Metallic Materials at Room Temperature	E9-81
Pin-Type Bearing Test of Metallic Materials	E238-68 (1978)
Practice for:	
Compression Tests of Metallic Materials at Elevated Temperatures with Conventional or Rapid Heating Rates and Strain Rates	E209-65 (1981)
Ductility and formability testing	
Methods for:	
Bend Testing for Metallic Flat Materials for Spring Applications	E855-81
Conducting a Ball Punch Deformation Test for Metallic Sheet Material	E643-78
Ductility Testing of Metallic Foil	E796-81
Test Method for:	
Tensile Strain-Hardening Exponents (n-Values) of Metallic Sheet Materials	E646-78
Definitions on mechanical testing	
Definitions of Terms Relating to:	
Mechanical Testing of Steel Products	A370-77
Methods of Mechanical Testing	E6-81
Elastic properties	
Test Methods for:	
Poisson's Ratio at Room Temperature	E132-61 (1979)
Shear Modulus at Room Temperature	E143-61 (1979)
Static Determination of Young's Modulus of Metals at Low and Elevated Temperatures	E231-69 (1981)
Young's Modulus, Tangent Modulus, and Chord Modulus	E111-82
Hardness testing	
Test Methods for:	
Brinell Hardness of Metallic Materials	E10-78
Hardness Conversion Tables for Metals (Relationship Between Brinell Hardness, Vickers Hardness, Rockwell Hardness, Rockwell Superficial Hardness, and Knoop Hardness)	E140-79
Indentation Hardness of Metallic Materials by Portable Hardness Testers	E110-82
Mechanical Testing of Steel Products	A370-77
Microhardness of Materials	E384-73 (1979)
Rapid Indentation Hardness Testing of Metallic Materials	E103-61 (1979)
Rockwell Hardness and Rockwell Superficial Hardness of Metallic Materials	E18-79
Vickers Hardness of Metallic Materials	E92-82
Practice for:	
Scleroscope Hardness Testing of Metallic Materials	E448-82
Impact testing	
Methods for:	
Mechanical Testing of Steel Products	A370-77
Notched Bar Impact Testing of Metallic Materials	E23-82
Linear thermal expansion test	
Test Methods for:	
Linear Expansion of Metals	B95-39 (1979)
Linear Thermal Expansion of Rigid Solids with a Vitreous Silica Dilatometer	E228-71 (1979)
Linear Thermal Expansion of Rigid Solids with Interferometry	E289-70 (1979)
Machinability of test method	
Method for:	
Machining Performance of Ferrous Metals Using an Automatic Screw/Bar Machine, Evaluating	E618-81
Shear and torsion testing	
Methods for:	
Shear Testing of Aluminum and Aluminum-Alloy Rivets and Cold-Heading Wire and Rods	B565-76 (1981)
Torsion Testing of Wire	E558-75
Residual stress measurement	
Methods for:	
Determining Residual Stresses by the Hole-Drilling Strain-Gage Method	E837-81
Verifying the Alignment of X-ray Diffraction Instrumentation for Residual Stress Measurement	E915-83
Stress-relaxation tests	
Practice for:	
Stress-Relaxation Tests for Materials and Structures	E328-78
Tension testing	
Methods for:	
Mechanical Testing of Steel Products	A370-77
Tension Testing of Metallic Foil	E345-81
Tension Testing of Metallic Materials	E8-82
Tension Testing Wrought and Cast Aluminum- and Magnesium-Alloy Products	B557-81
Tension Testing Wrought and Cast Aluminum- and Magnesium-Alloy Products [Metric]	B557M-81
Test Method for:	
Plastic Strain Ratio r for Sheet Metal	E517-81
Thickness measurement	
Test Method for:	
Thickness of Thin Foil and Film by Weighing	E252-78
Fatigue	
Definitions of Terms Relating to:	
Constant-Amplitude, Low-Cycle Fatigue Testing	E513-74 (1980)
Fatigue Loading	E912-83
Fatigue Testing and the Statistical Analysis for Fatigue Data	E206-72 (1979)
Fluid Aqueous and Chemical Environmentally Affected Fatigue Testing	E742-81
Practices for:	
Constant-Amplitude Axial Fatigue Tests of Metallic Materials	E466-82
Constant-Amplitude Low-Cycle Fatigue Testing	E606-80
Presentation of Constant-Amplitude Fatigue Test Results for Metallic Materials	E468-82
Statistical Analysis of Linear or Linearized Stress-Life (S-N) and Strain-Life (ϵ-N) Fatigue Data	E739-80
Verification of Constant-Amplitude Dynamic Loads in an Axial Load Fatigue Testing Machine	E467-76 (1982)
Test Method for:	
Constant-Load-Amplitude Fatigue Crack Growth Rates Above 10^{-8} m/Cycle	E647-83
Fracture Testing	
Test Methods for:	
Crack Strength of Slow-Bend Precracked Charpy Specimens of High-Strength Metallic Materials	E812-81
Drop-Weight Tear Tests of Ferritic Steels	E436-74 (1980)
Dynamic Tear Testing of Metallic Materials	E604-83
J_{Ic}, a Measure of Fracture Toughness	E813-81
Plane-Strain Fracture Toughness of Metallic Materials	E399-83
Sharp-Notch Tension Testing of High-Strength Sheet Materials	E338-81
Sharp-Notch Tension Testing with Cylindrical Specimens	E602-81
Practices for:	
Fracture Testing with Surface-Crack Tension Specimens	E740-80
R-Curve Determination	E561-81
Terminology Relating to:	
Fracture Testing	E616-82
Corrosion	
Method for:	
Preparation and Use of Bent-Beam Stress-Corrosion Specimens	G39-73

(continued)

O x le Her (DE)

Table 1. (continued)

Subject	Reference
Corrosion (continued)	
Recommended Practices for:	
Alternate Immersion Stress-Corrosion Testing in 3.5% Sodium Chloride Solution	G44-75
Making and Using the C-Ring Stress-Corrosion Cracking Test Specimen	G38-73
Making and Using U-Bend Stress-Corrosion Test Specimens	G30-72
Performing Stress-Corrosion Cracking Tests in a Boiling Magnesium Chloride Solution	G36-73
Preparation and Use of Direct Tension Stress-Corrosion Test Specimens	G49-76
Susceptibility of Stainless Steels and Related Nickel-Chromium-Iron Alloys to Stress-Corrosion Cracking in Polythionic Acids, Determining	G35-73
Erosion and Wear	
Method of:	
Vibratory Cavitation Erosion Test	G32-77
Test Method for:	
Abrasiveness of Ink-Impregnated Fabric Printer Ribbons	G56-77
Terminology Relating to:	
Erosion and Wear	G40-77

Subject	Reference
Effect of Temperature on Metals	
Methods for:	
Conducting Drop-Weight Test to Determine Nil-Ductility Transition Temperature of Ferritic Steels	E208-81
Static Determination of Young's Modulus of Metals at Low and Elevated Temperatures	E231-69 (1981)
Practices for:	
Compression Tests of Metallic Materials at Elevated Temperatures with Conventional or Rapid Heating Rates and Strain Rates	E209-65 (1981)
Conducting Creep and Creep-Rupture Tension Tests of Metallic Materials Under Conditions of Rapid Heating and Short Times (Intent to Withdraw)	E150-64 (1981)
Conducting Creep, Creep-Rupture, and Stress-Rupture Tests of Metallic Materials	E139-83
Conducting Time-for-Rupture Notch Tension Tests of Materials	E292-78
Elevated Temperature Tension Tests of Metallic Materials	E21-79
Tension Tests of Metallic Materials at Elevated Temperatures with Rapid Heating and Conventional or Rapid Strain Rates (Intent to Withdraw)	E151-64 (1981)

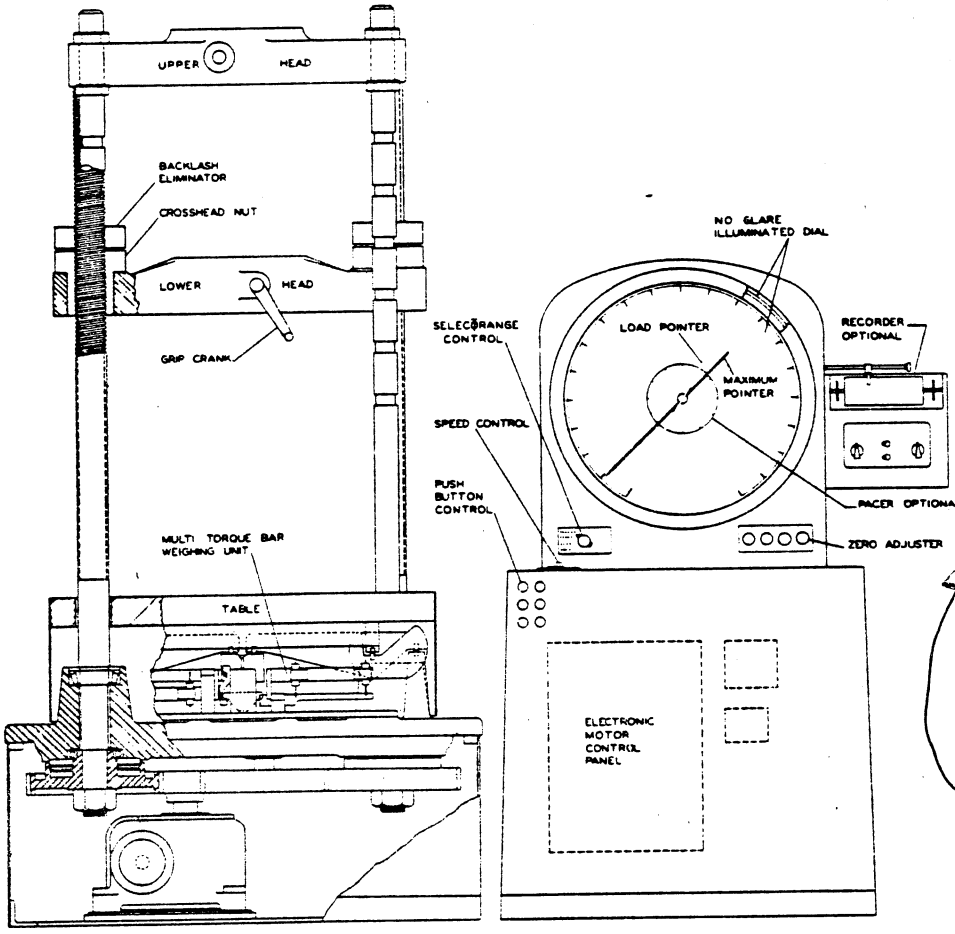

Fig. 1. Schematic drawing of universal testing machine

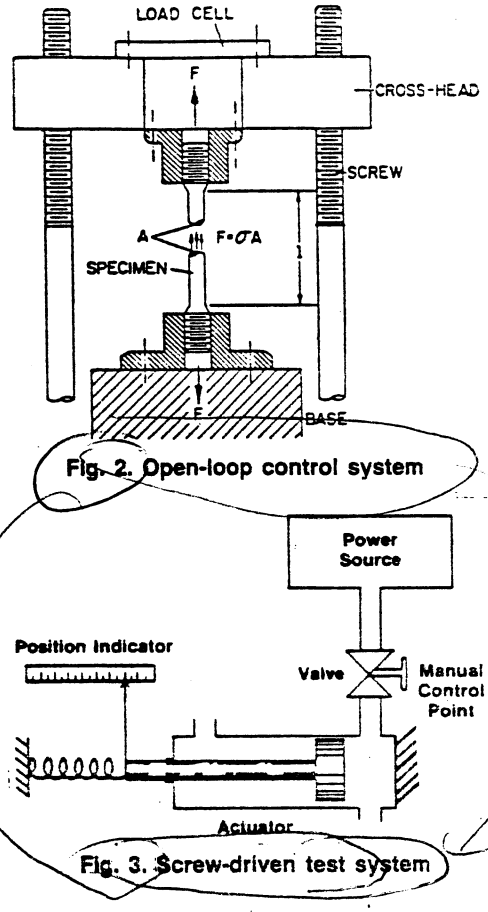

Fig. 2. Open-loop control system

Fig. 3. Screw-driven test system

ator must observe the position indicator and constantly regulate the valve, adjusting for variations in the power source and actuator load to maintain a given position. This is the simplest form of closed-loop control, with the operator closing the loop and thus inserting his response into the loop. If the operator is provided with a suitable indicator, he can also control other parameters, such as velocity or force. If the valve is left unattended, there will be no regulation of position or any other parameter. The Baldwin and Tinius Olsen machines are examples of these machines.

Electromechanical Machines. In electromechanical machines, the cross-head usually is driven vertically by twin screws (Fig. 3). The cross-head velocity is determined by the rotational velocity of the screws. This velocity can be maintained constant throughout the test, in contrast with hydraulic machines, in which the operator continuously adjusts the velocity. These screw-driven machines are reliable, simple to operate, and perfectly suited for routine tensile and compressive testing.

Servo-Hydraulic (Closed-Loop) Systems. A typical closed-loop system that operates in position control is shown in Fig. 4. Without a human operator within the loop, a visual indication of piston position is not necessary. A transducer provides a signal that is proportional to piston position. That transducer signal is connected to a servo controller that compares it to the signal from the manually adjusted command control. The signal from the manual command control is called simple "command"; the signal from the transducer is called "feedback." If command and feedback

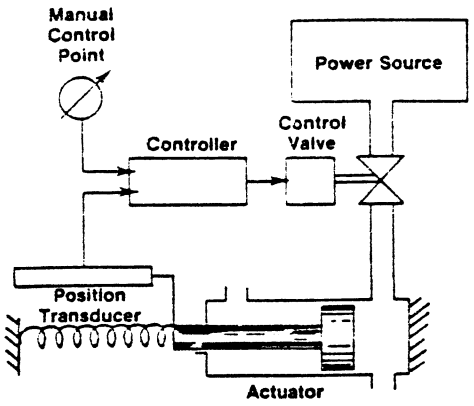

Fig. 4. Closed-loop control system

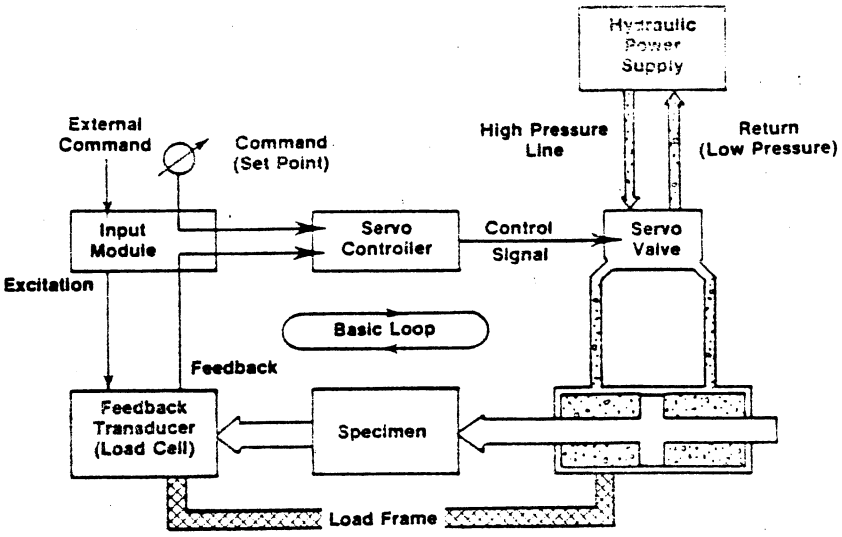

Fig. 5. Basic testing system

are not equal, the actuator is not positioned at the desired, or command, position. The servo controller reacts to relative differences between these signals (both polarity and magnitude) and applies a control signal to the control valve that causes the difference to be corrected. Thus, the system automatically maintains the piston at any given point, even when the power source or the actuator load varies. Servo-hydraulic machines also operate with the strain or load as controlling parameters.

Figure 5 is very similar to Fig. 4 and shows a test specimen as part of the closed servo loop. The force applied to the specimen is sensed by a transducer (load cell) and is controlled by the system. When the specimen is part of the loop, some important considerations are:

- Characteristics of the specimen directly affect the behavior of the system.
- Selection of the proper transducer permits close control of the parameter of interest within the specimen itself. For example, to provide the most precise control of the force applied to the transducer, a load cell (force transducer) is used, or, to control specimen strain, a strain transducer is attached to the specimen.

The following list describes some of the equipment employed in the testing system illustrated in Fig. 5:

- The hydraulic power supply is the source of power for the system. Its output is rated in gallons (litres) per minute at a certain pressure.
- The servo valve, also rated in gallons (litres) per minute, regulates the flow of fluid between the hydraulic power supply and the actuator. The valve opens to power high-pressure fluid to either end of the actuator, depending on the polarity of the electrical input of the valve. When the servo valve is open to permit high-pressure fluid to be admitted to one end of the cylinder, the valve also provides a fluid-return path from the other end of the cylinder to the supply. When the system is in a static condition, the electrical input to the valve is zero and the valve is closed (fluid is not permitted to flow into or out of the actuator). The valve opens in proportion to the magnitude of the input signal and is fully open when the input current reaches the current input rating of the valve.
- The hydraulic actuator has a maximum static-force rating that is determined by the effective area of the piston (area of cylinder bore minus area of piston rod) and the actuating pressure.
- The feedback transducer is any suitable transducer properly coupled to the specimen to sense the quantity being controlled, in this case force. Its electrical output (feedback) is directly proportional to the mechanical input to the transducer and to the specimen. The polarity of the output signal of the transducer is dependent on the direction of the mechanical input. In the case of load cells, the output signal is positive when the input force is tensile. If the input force is compressive, the output signal has a negative polarity.
- The servo controller accepts both the command and feedback signals and reacts to their relative magnitudes and polarities by supplying an output control signal that results from any difference between command and feedback. If command and feedback are equal, the output is zero (the controlled variable is at the command level). If command and feedback are not equal, the output has a polarity that causes the actuator to stroke in the direction required to reduce the error and a magnitude that is proportional to the amount of error.

CALIBRATION

All mechanical testing systems depend on accurate measurement of loads, strains and displacements. Thus, care must be taken to ensure that the transducers are maintained in proper calibration. In the list of ASTM standards presented in Table 1, calibration specifications are included for reference. Specific calibration procedures are usually provided by system manufacturers.

SELECTED REFERENCES

1983 Annual Book of ASTM Standards

Mechanical Measurements, 3rd Ed., by T. B. Beckwith, N. L. Buck and R. D. Marangoin: Addison-Wesley, Reading, MA, 1982

ADDITIONAL READING

Reproducibility and Accuracy of Mechanical Tests, ASTM STP 626, 1977

Recent Developments in Mechanical Testing, ASTM STP 608, 1976

The Making, Shaping, and Treating of Steel, 9th Ed., by H. E. McGannon: U. S. Steel, 1971, Chapter 49, p 1214

Novel Techniques in Metal Deformation Testing, edited by R. H. Wagoner: TMS-AIME, Warrendale, PA, 1983

Hardness Testing

HARDNESS is a term that has different meanings to different people: it is resistance to penetration to a metallurgist, resistance to wear to a lubrication engineer, a measure of flow stress to a design engineer, resistance to scratching to a mineralogist, and resistance to cutting to a machinist. Although these various definitions of hardness appear to differ significantly in character, they are all related to the plastic flow stress of the material.

Only static indentation and rebound testing are discussed in this article. These two methods account for virtually all routine hardness testing in the metalworking industry. Static indentation hardness testing is the more widely used of the two methods, although rebound testing is extensively employed, particularly for hardness measurements on large workpieces or for applications in which visible or sharp impressions in the test surface cannot be tolerated.

BRINELL HARDNESS TESTING

The Brinell hardness test is basically simple, and consists of applying a constant load, usually 500 to 3000 kg, on a hardened steel ball-type indenter, 10 mm in diameter, to the flat surface of a workpiece (Fig. 1). The 500-kg load is usually used for testing nonferrous metals such as copper and aluminum alloys, whereas the 3000-kg load is most often used for testing harder met-

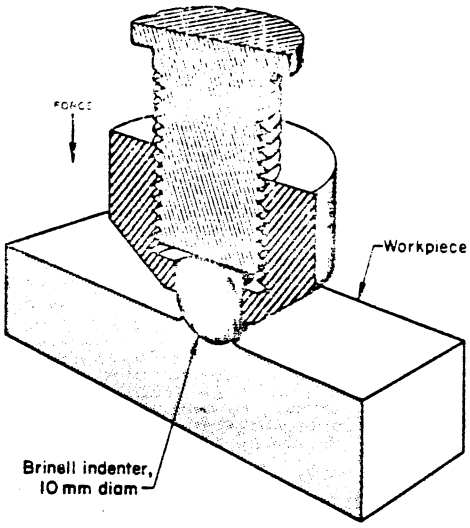

Fig. 1. Sectional view of a Brinell indenter, showing the manner in which the application of force by the indenter causes the metal of the workpiece to flow

als such as steels and cast irons. The load is held for a specified time (10 to 15 s for iron or steel and about 30 s for softer metals), after which the diameter of the recovered indentation is measured in millimetres. This time period is required to ensure that plastic flow of the work metal has stopped.

Hardness is evaluated by taking the mean diameter of the indentation (two readings at right angles to each other) and calculating the Brinell hardness number (HB) by dividing the applied load by the surface area of the indentation according to the following formula:

$$HB = L/(\pi D/2)[D - (D^2 - d^2)^{1/2}]$$

where L is the load, in kilograms; D is the diameter of the ball, in millimetres; and d is the diameter of the indentation, in millimetres.

It is not necessary, however, to make the calculation for each test. Such calculations are available in table form for all diameters of indentations in Section 1 of this Desk Edition.

Highly hardened steel (or other very hard metals) cannot be tested by a hardened steel ball by the Brinell method, because the ball will flatten during penetration and a permanent deformation will take place. This problem is recognized in specifications for the Brinell tests.

Tungsten carbide balls are recommended for Brinell testing materials of hardness from 444 HB up to about 627 HB (indentation of 2.45 mm in diameter). However, higher Brinell values will result when using carbide balls instead of steel balls, because of the difference in elastic properties.

Surface Preparation. The degree of accuracy that can be attained by the Brinell hardness test can be greatly influenced by the surface smoothness of the workpiece being tested.

The surface of the workpiece on which the Brinell indentation is to be made must be filed, ground, machined or polished with emery paper (3/0 emery paper is suitable) so that the identation diameter is clearly enough defined to permit its measurement. There should be no interference from tool marks.

Indentation Measurement. The diameter of the indentation is measured by a microscope to the nearest 0.05 mm (0.002 in.). This microscope contains a scale, and usually a built-in light to facilitate easy reading.

The indentations produced in Brinell hardness tests may exhibit different surface characteristics. These have been carefully studied and analyzed. In some instances there is a ridge around the indentation extending above the original surface of the workpiece. In other instances the edge of the indentation is below the original surface. Sometimes there is no difference at all. The first phenomenon is called a "ridging" type of indentation and the second a "sinking" type. Cold worked metals generally have the former type of indentation, and annealed metals the latter type.

Brinell Hardness Testers. Several types of testers that exert the prescribed force on the indenter are in general use. The one most commonly used is the hydraulic, manually operated type shown in Fig. 2.

The workpiece is placed on the anvil and raised, by means of the elevating screw, to a position

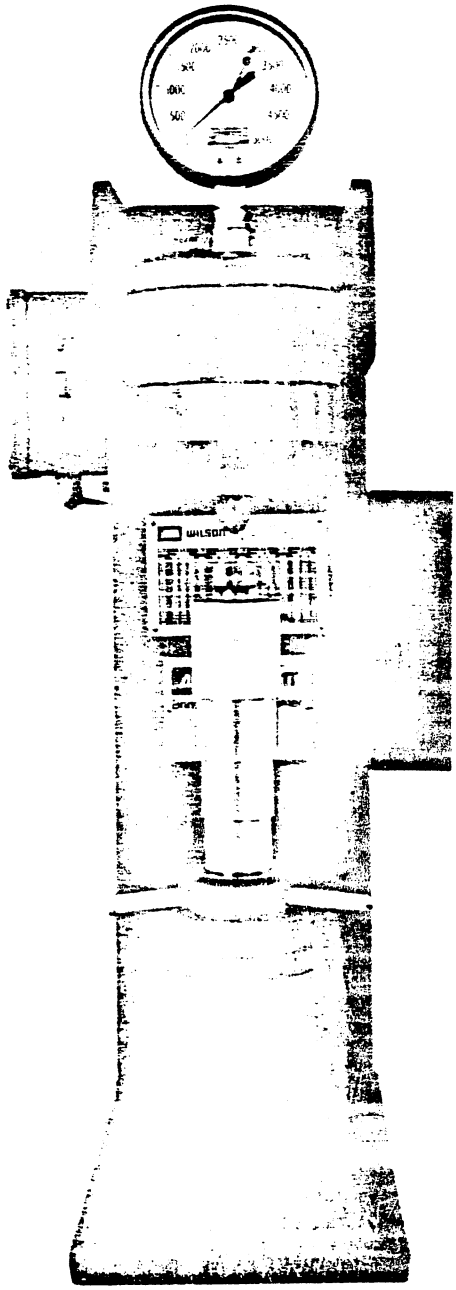

Fig. 2. Brinell hardness tester

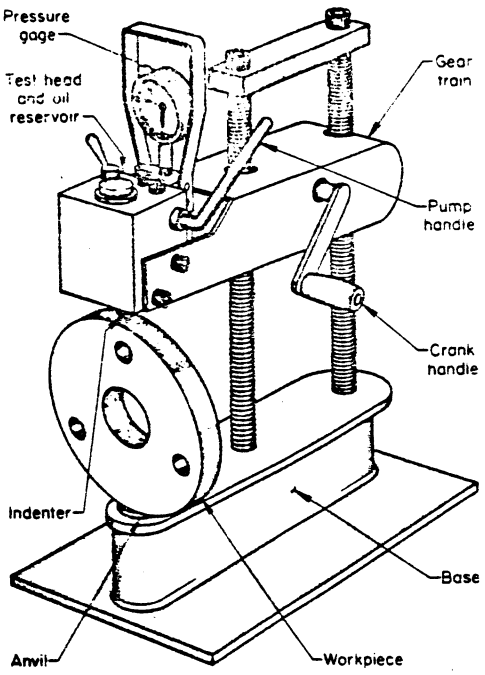

Fig. 3. Hydraulic, manually operated portable Brinell hardness tester

near the indenter. Fingertip rotation of the control knob allows a selected force (in kilograms), indicated on the gage, to be applied. This force is held for a pre-established length of time and then released. The specimen is removed and the indentation measured. The entire cycle, including indenting and measurement, requires approximately one minute.

For production testing, speed direct-reading Brinell-type testers also are available.

Portable Brinell Hardness Testers. Conventional Brinell hardness testers described above have limited use, for two reasons: (*a*) the workpieces to be tested must be brought to the testers, and (*b*) size and design of the workpieces must be such that they can be placed between the anvil and the indenter.

Some of the problems posed by the above limitations can often be solved by use of a portable hardness tester (Fig. 3). A hardness tester of the general design shown in Fig. 3 weighs no more than about 25 lb; thus, it can be easily transported to the workpieces.

Spacing of Indentations. To ensure accurate results, indentations should not be made too close to the edge of the workpiece being tested. Lack of sufficient supporting material on one side of the workpiece will cause the resulting indentation to be large and unsymmetrical. It is generally agreed that the error in a Brinell hardness number is negligible if the distance from the center of the indentation is not less than $2\frac{1}{2}$ times (and preferably 3 times) the diameter of the indentation from any edge of the workpiece.

Similarly, indentations should not be made too close to one another. If indentations are too close together, the work metal may be cold worked by the first indentation, or there may not be sufficient supporting material for the second indentation. The latter condition would produce too large an indentation, whereas the former may produce too small an indentation. To prevent this, the distance between centers of adjacent indentations should be at least three times the diameter of the indentation.

General Precautions. To avoid misapplication of Brinell hardness testing, the fundamentals and limitations of the test must be clearly understood. Further, to avoid inaccuracies, some general rules should be followed. Such rules include the following:

1. Indentations should not be made on a curved surface having a radius of less than 1 in.
2. Spacing of indentations should be correct, as outlined above under "Spacing of Indentations."
3. The load should be applied steadily to avoid overloading caused by inertia of the weights.
4. The load should be applied in such a way that the direction of loading and the test surface are perpendicular to each other within 2°.
5. The thickness of the workpiece being tested should be such that no bulge or mark showing the effect of the load appears on the side of the workpiece opposite the indentation. In any event, the thickness of the specimen shall be at least ten times the depth of indentation.
6. The surface finish of the workpiece being tested should be such that the indentation diameter is clearly outlined.

Limitations. The Brinell hardness test has three principal limitations:

1. Size and shape of the workpiece must be capable of accommodating the relatively large indentations.
2. Because of the relatively large indentations, the workpiece may not be usable after testing.
3. The limit of hardness range—about 11 HB with the 500-kg load to 627 HB with the 3000-kg load—is generally considered the practical range.

ROCKWELL HARDNESS TESTING

Rockwell hardness testing is the most widely used method for determining hardness. There are several reasons for this distinction: (*a*) the Rockwell test is simple to perform and does not require highly skilled operators; (*b*) by use of different loads and indenters, Rockwell hardness testing can be used for determining hardness of most metals and alloys, ranging from the softest bearing materials to the hardest steels; (*c*) a reading can be taken in a matter of seconds with conventional manual operation and in even less time with automated setups; and (*d*) no optical measurements are required (all readings are direct).

Rockwell hardness testing differs from Brinell hardness testing in that the hardness is determined by the depth of indentation made by a constant load impressed upon an indenter. Although a number of different indenters are used for Rockwell hardness testing, the most common type is a diamond ground to a 120° cone with a spherical apex having a 0.2-mm radius, which is known as a Brale indenter (see Fig. 4).

As shown in Fig. 5, the Rockwell hardness test consists of measuring the additional depth to which an indenter is forced by a heavy (major) load (Fig. 5b) beyond the depth of a previously applied light (minor) load (Fig. 5a). Application of the minor load eliminates backlash in the load train and causes the indenter to break through slight surface roughness and to crush particles of foreign matter, thus contributing to much greater accuracy in the test. The basic principle involving minor and major loads illustrated in Fig. 5 applies to steel-ball indenters as well as to diamond indenters.

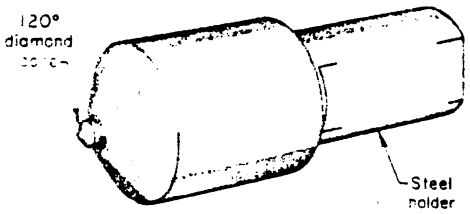

Fig. 4. Diamond-cone Brale indenter used in Rockwell hardness testing (shown at about 2×)

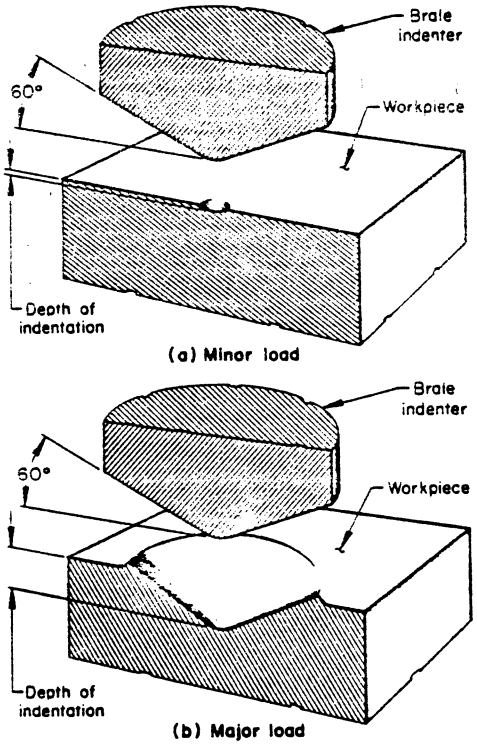

The hardness value is based on the difference in depths of indentation produced by the minor and major loads.

Fig. 5. Indentation in a workpiece made by application of (a) the minor load, and (b) the major load, on a diamond Brale indenter in Rockwell hardness testing

The minor load is applied first, and a reference or "set" position is established on the measuring device of the Rockwell hardness tester. Then the major load is applied at a prescribed, controlled rate. Without moving the workpiece being tested, the major load is removed and the Rockwell hardness number is automatically indicated on the dial gage. The entire operation takes from 5 to 10 s.

Diamond indenters are used mainly for testing materials such as hardened steels and cemented carbides. Steel-ball indenters, available with diameters of $\frac{1}{16}$, $\frac{1}{8}$, $\frac{1}{4}$ and $\frac{1}{2}$ in., are used for testing materials such as soft steel, copper alloys, aluminum alloys and bearing metals.

There are two basic types of Rockwell hardness testers—regular and superficial. Both have similar basic mechanical principles and significant components. A schematic view of a regular Rockwell hardness tester is shown in Fig. 6.

Regular Rockwell Hardness Testing. In regular Rockwell hardness testing the minor load is always 10 kg. The major load, however, can be 60, 100 or 150 kg. No Rockwell hardness value is expressed by a number alone. A letter has been assigned to each combination of load and indenter, as shown in Table 1. Each number is suffixed by first the letter H (for hardness), then the letter R (for Rockwell), and finally the letter that indicates the scale used. For example, a value of 60 on the Rockwell C scale is expressed as 60 HRC, and so on. Regardless of the scale used, the "set" position is the same; however, when the diamond Brale indenter is used, the readings are taken from the black divisions on the dial gage. When testing with any of the ball indenters, the readings are taken from the red divisions.

One Rockwell number represents an indentation of 0.002 mm (0.00008 in.). Therefore, a reading of 60 HRC indicates indentation from minor to major load of (100 − 60) × 0.002 mm = 0.080 mm or 0.0032 in. A reading of 80 HRB indicates an indentation of (130 − 80) × 0.002 mm = 0.100 mm or 0.004 in.

Superficial Rockwell hardness testing employs a minor load of 3 kg, but the major load can be 15, 30 or 45 kg.

Just as in regular Rockwell testing, the indenter may be either a diamond or a steel ball, depending mainly on the nature of the metal being tested. Regardless of load, the letter N designates use of the superficial Brale, and the letters T, W, X and Y designate use of steel-ball indenters. Scale and load combinations are presented in Table 1. Superficial Rockwell hardness values are always expressed with the number suffixed by a number and a letter that show the load/indenter combination. For example, if a load of 30 kg is used with a diamond indenter and a reading of 80 is obtained, the result is reported as 80 HR30N (where H means hardness, R means Rockwell, 30 means a load of 30 kg, and N indicates use of a diamond indenter).

All tests are started from the "set" position. One Rockwell superficial hardness number represents an indentation of 0.001 mm or 0.00004 in. Therefore, a reading of 80 HR30N indicates indentation from minor to major load of (100 − 80) × 0.001 mm = 0.020 mm or 0.0008 in.

Dials on the superficial hardness testers contain only one set of divisions, which is used with all types of superficial indenters.

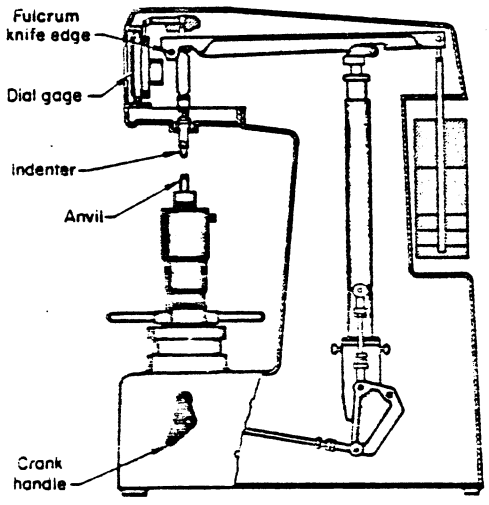

Fig. 6. Principal components of a regular (normal) Rockwell hardness tester. Superficial Rockwell testers are similarly constructed.

Table 1. Rockwell-hardness-scale designations for combinations of type of indenter and major load

Scale designation	Indenter Type	Indenter Diam., in.	Major load, kg	Dial figure
Regular Rockwell tester				
B	Ball	1/16	100	Red
C	Brale	...	150	Black
A	Brale	...	60	Black
D	Brale	...	100	Black
E	Ball	1/8	100	Red
F	Ball	1/16	60	Red
G	Ball	1/16	150	Red
H	Ball	1/8	60	Red
K	Ball	1/8	150	Red
L	Ball	1/4	60	Red
M	Ball	1/4	100	Red
P	Ball	1/4	150	Red
R	Ball	1/2	60	Red
S	Ball	1/2	100	Red
V	Ball	1/2	150	Red
Superficial Rockwell tester				
15N	N Brale	...	15	
30N	N Brale	...	30	
45N	N Brale	...	45	
15T	Ball	1/16	15	
30T	Ball	1/16	30	
45T	Ball	1/16	45	
15W	Ball	1/8	15	
30W	Ball	1/8	30	
45W	Ball	1/8	45	
15X	Ball	1/4	15	
30X	Ball	1/4	30	
45X	Ball	1/4	45	
15Y	Ball	1/2	15	
30Y	Ball	1/2	30	
45Y	Ball	1/2	45	

Table 2. Typical applications of regular Rockwell hardness scales

Scale(a)	Typical applications
B	Copper alloys, soft steels, aluminum alloys, malleable iron
C	Steel, hard cast irons, pearlitic malleable iron, titanium, deep case-hardened steel and other materials harder than 100 HRB
A	Cemented carbides, thin steel and shallow case-hardened steel
D	Thin steel and medium case-hardened steel and pearlitic malleable iron
E	Cast iron, aluminum and magnesium alloys, bearing metals
F	Annealed copper alloys, thin soft sheet metals
G	Phosphor bronze, beryllium copper, malleable irons. Upper limit is 92 HRG, to avoid flattening of ball.
H	Aluminum, zinc, lead
K,L,M,P, R,S,V	Bearing metals and other very soft or thin materials. Use smallest ball and heaviest load that do not give anvil effect.

(a) The N scales of a superficial hardness tester are used for materials similar to those tested on the Rockwell C, A and D scales, but of thinner gage or case depth. The T scales are used for materials similar to those tested on the Rockwell B, F and G scales but of thinner gage. When minute indentations are required, a superficial hardness tester should be used. The W, X and Y scales are used for very soft materials.

Selection of Rockwell Scale

Where no specification exists or there is doubt about the suitability of a specified scale, an analysis should be made of those factors that influence the selection of the proper scale. These influencing factors are found in the following four broad categories:

1. Type of work metal
2. Thickness of work metal
3. Width of area to be tested
4. Scale limitations.

Influence of Type of Work Metal. The types of work metal normally tested using the different regular Rockwell hardness scales are given in Table 2. This information also can be helpful when one of the superficial Rockwell scales may be required. For example, note that the C, A and D scales—all with diamond indenters—are used on hard materials such as steel and tungsten carbide. Any material in this hardness category would be tested with a diamond indenter. The choice to be made is whether the C, A, D, or the 45N, 30N, or 15N scale is applicable. Whatever the choice, the number of possible scales has been reduced to six. The next step is to find a scale, either regular or superficial, that will guarantee accuracy, sensitivity and repeatability of testing.

Influence of Thickness of Work Metal. The metal immediately surrounding the indentation in a Rockwell hardness test is cold worked. The depth of material affected during testing is on the order of ten times the depth of the indentation. Therefore, unless the thickness of the metal being tested is at least ten times the depth of the indentation, an accurate Rockwell hardness test cannot be expected.

The depth of indentation for any Rockwell hardness test can easily be computed; in practice, however, computation is not necessary, because tables of minimum thicknesses are available (for example, see Table 3). The values for minimum thickness do follow the 10-to-1 ratio in some ranges, but they are actually based on experimental data accumulated on various thicknesses of low-carbon steels and of steel strip that has been hardened and tempered.

To use the values in Table 3, assume that it is necessary to check the hardness of a strip of steel 0.014 in. thick, of an approximate hardness of 63 HRC. According to Table 3, material having a hardness of 63 HRC must be approximately 0.028 in. thick for an accurate test using the C scale. Therefore, this steel strip should not be tested on the C scale. At this point, check the approximate converted hardness on the other Rockwell scales equivalent to 63 HRC. These values—taken from a conversion table—are: 83 HRA, 70 HR45N, 80 HR30N and 91 HR15N. Referring again to Table 3 for hardened 0.014-in.-thick material, there are only three Rockwell scales to choose from—45N, 30N and 15N. The 45N scale is not suitable because the material should be at least 74 HR45N. On the 30N scale, 0.014-in.-thick material must be at least 80 HR30N, and the material at hand is 80 HR30N. On the 15N scale, the material must be at least 76 HR15N, and this material is 91.5 HR15N. Therefore, either the 30N or 15N scale may be used. After all limiting factors have been eliminated, and a choice exists between two or more scales, the scale applying the heavier load should be used. The heavier load will produce a larger indentation, covering a greater portion of the material, and a Rockwell hardness number more representative of the material as a whole will be obtained. In addition, the heavier the load, the greater the sensitivity of the scale. Checking any conversion table and comparing the 15N scale to the 30N scale will show that in the hard-steel range a difference in hardness of one point on the 30N scale represents a difference of only 0.5 point on the 15N scale. Therefore, smaller differences in hardness can be detected when using the 30N scale.

Table 3. Minimum work-metal hardness values for testing various thicknesses of metals with regular and superficial Rockwell hardness testers(a)

Metal thickness, in.	Minimum hardness for superficial hardness testing: Diamond Brale indenter 15N (15 kg)	30N (30 kg)	45N (45 kg)	Ball indenter, 1/16 in. 15T (15 kg)	30T (30 kg)	45T (45 kg)	Minimum hardness for regular hardness testing: Diamond Brale indenter A (60 kg)	D (100 kg)	C (150 kg)	Ball indenter, 1/16 in. F (60 kg)	B (100 kg)	G (150 kg)
0.005	...	...	...	93	...	...	...	...	...	...	...	...
0.006	92	...	...	...	...	...	...	...	...	...	...	...
0.008	90	...	...	...	...	...	...	...	...	...	...	...
0.010	88	...	...	90	87	...	...	...	...	...	...	...
0.012	83	82	77	...	...	...	...	...	...	...	...	...
0.014	76	80	74	...	...	...	...	...	...	...	...	...
0.015	...	...	...	78	77	77	...	...	...	...	...	...
0.016	68	74	72	...	...	...	86	...	...	...	...	...
0.018	(b)	66	68	...	...	...	84	...	...	...	...	...
0.020	(b)	57	63	(b)	58	62	82	77	...	100	...	...
0.022	(b)	47	58	...	...	...	78	75	69	...	...	...
0.024	(b)	(b)	51	...	...	...	76	72	67	...	...	...
0.025	...	...	...	(b)	(b)	26	...	...	...	92	92	90
0.026	(b)	(b)	37	...	...	...	71	68	65	...	...	...
0.028	(b)	(b)	20	...	...	...	67	63	62	...	...	...
0.030	(b)	(b)	(b)	(b)	(b)	(b)	60	58	57	67	68	69
0.032	(b)	(b)	(b)	...	...	...	(b)	51	52	...	...	...
0.034	(b)	(b)	(b)	...	...	...	(b)	43	45	...	...	...
0.035	...	...	...	(b)	(b)	(b)	...	...	...	(b)	44	46
0.036	(b)	(b)	(b)	...	...	...	(b)	(b)	37	...	...	...
0.038	(b)	(b)	(b)	...	...	...	(b)	(b)	28	...	...	...
0.040	(b)	(b)	(b)	(b)	(b)	(b)	(b)	(b)	20	(b)	20	22

(a) These values are approximate only and are intended primarily as a guide; see text for example of use. Materials thinner than shown may be tested on a Tukon microhardness tester. The thickness of the workpiece should be at least 1 1/2 times the diagonal of the indentation when using a Vickers indenter, and at least 1/2 times the long diagonal when using a Knoop indenter. (b) No minimum hardness for metal of equal or greater thickness.

The above approach would also apply in determining which scale should be used to measure the hardness of [illegible] approximate depth and hardness.

Influence of Test-Area Width. In addition to the limitation of indentation depth for a workpiece of given thickness and hardness, there is a limiting factor on the minimum width of material. If the indentation is placed too close to the edge of a workpiece, the edge will deform outward and the Rockwell hardness number will be decreased accordingly.

Experience has shown that the distance from the center of the indentation to the edge of the workpiece must be at least $2\frac{1}{2}$ times the diameter of the indentation to ensure an accurate test. Therefore, the width of a narrow test area must be at least five indentation diameters when the indentation is placed in the center.

Limitations of Rockwell Scales. The potential range of each Rockwell scale can be determined readily from the dial-gage divisions on the tester: the black scale (for diamond indenter) on all regular hardness-tester dial gages is numbered from 0 to 100, with 100 corresponding to the "set" position; the red scale (for ball indenters) is numbered from 0 to 130, with 130 being the "set" position. On the superficial hardness tester, the dial gage has only one set of divisions, numbered from 0 to 100.

Use of the diamond indenter when readings fall below 20 is not recommended, since there is loss of sensitivity when indenting this far down the conical section of the indenter. Brale indenters are not calibrated below values of 20, and if used on soft materials there is no assurance that there will be the usual degree of agreement in results when replacing the indenters. Another scale should be used—for example, the B scale.

Support for Workpiece. A fundamental requirement of the Rockwell hardness test is that the surface of the workpiece being tested be approximately normal to the indenter and that the workpiece must not move or slip in the slightest degree as the major load is applied. The depth of indentation is measured by the movement of the plunger rod holding the indenter; therefore, any slipping or moving of the workpiece will be followed by the plunger rod and the motion transferred to the dial gage, causing an error to be introduced into the hardness test. As one point of hardness represents a depth of only 0.00008 in., a movement of only 0.001 in. could cause an error of over 10 Rockwell numbers. The support must be of sufficient rigidity to prevent its permanent deformation in use.

Figure 7 shows five types of anvils that, collectively, can accommodate a fairly broad range of workpiece shapes.

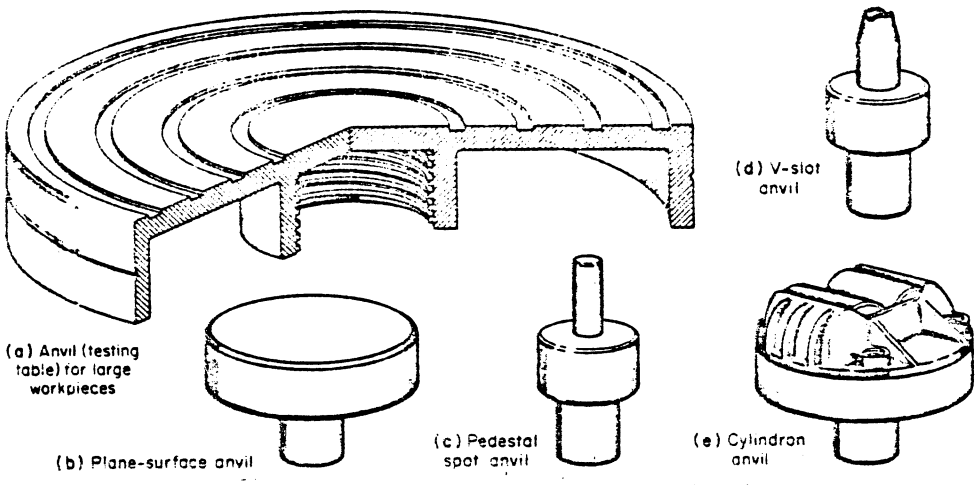

Fig. 7. Several commonly used types of anvils that are designed to support various shapes of workpieces during hardness testing in a Rockwell tester

VICKERS HARDNESS TESTING

The Vickers hardness test follows the Brinell principle, in that an indenter of definite shape is pressed into the material to be tested, the load removed, the diagonals of the resulting indentation measured, and the hardness number calculated by dividing the load by the surface area of indentation.

The indenter is made of diamond, and is in the form of a square-base pyramid having an angle of 136° between faces (Fig. 8). This indenter thus has angle across corners, or so-called edge angle, of 148° 6′ 42.5″. The facets are highly polished and free from surface imperfections, and the point is sharp. The loads applied vary from 1 to 120 kg; the standard loads are 5, 10, 20, 30, 50, 100 and 120 kg. For most hardness testing, 50 kg is maximum.

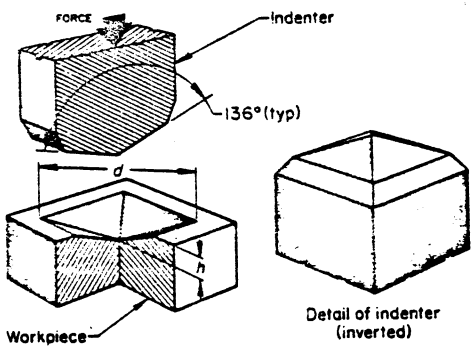

Fig. 8. Schematic representation of the square-base pyramidal diamond indenter used in a Vickers hardness tester, and of the resulting indentation in the workpiece

With the Vickers indenter, the depth of indentation is about one-seventh of the diagonal length of the indentation. For certain types of investigation, there are advantages to such a shape. The Vickers hardness number (HV) is the ratio of the load applied to the indenter to the surface area of the indentation. By formula:

$$HV = 2P \sin(\theta/2)/d^2$$

where P is the applied load, in kilograms, d is the mean diagonal of the indentation, in millimetres; and θ is the angle between opposite faces of the diamond indenter (136°).

Equipment for determining the Vickers hardness number should be designed to apply the load without impact, and friction should be reduced to a minimum. The actual load on the indenter should be correct to less than 1% and the load should be applied slowly, because the Vickers is a static test. Some standards require that the full load be maintained for 10 to 15 s.

To obtain the greatest accuracy in hardness testing, the applied load should be as large as possible, consistent with the dimensions of the workpiece. Loads of more than 50 kg are likely to fracture the diamond, especially when used on hard materials.

The accuracy of the micrometer microscope should be checked against a stage micrometer, which consists of ruled lines, usually 0.1 mm apart, that have been checked against certified length standards. The average length of the two diagonals is used in determining the hardness value.

The corners of the indentation provide indicators of the length of the diagonals. The area must be calculated from the average of readings of both diagonals. The indentations are usually measured under vertical illumination with a magnification of about 125 diameters.

The included angle of the diamond indenter should be 136° with a tolerance of less than ±0.50°, which is readily obtainable with modern diamond-grinding equipment. This would mean an error of less than 1% in the hardness number. The indenters must be carefully controlled during manufacture so that in use the indentations produced will be symmetrical. Tables are available for converting the values of the diagonals of indentation in millimetres to the Vickers hardness number.

Several types of hardness testers have proved acceptable for making the Vickers test in accordance with the above requirements. One type is illustrated in Fig. 9. This hardness tester, which has a mainframe section that carries the stage and a starting handle having a 20-to-1 ratio, applies the load through a thrust rod to a tube, which is free to reciprocate vertically, and which carries the Vickers indenter at its lower end. Attached to the mainframe is a smaller frame that contains the control mechanism. The plunger reciprocates vertically under the influence of a rotating cam, its purpose being to apply and release the test load. The cam is mounted on a drum, and when the starting handle has been depressed, the cam is rotated by a weight attached by a flexible wire, the speed of rotation being controlled by a piston and an oil-filled dashpot. The rate of displacement of the oil is regulated by an adjustable control valve. The plunger carries a rubber pad at its upper end, which engages with a cone mounted in the beam, thereby ensuring a very slow and diminishing rate of application for the last portion of the loading cycle. Because the cam both lowers and raises the plunger, errors due to inertia and premature load removal are eliminated.

The microscope is usually mounted on a hinged bracket and may be moved to position over the

indentation after the workpiece has been lowered sufficiently to clear the microscope. A knife-edge type of micrometer ocular is provided, and the indentations are read to knife-edges. The readings are taken from a digital counter mounted on the microscope. Tables for converting digital readings to Vickers hardness numbers are supplied. The micrometer ocular may be rotated through 90° so that each diagonal may be measured.

In use, the workpiece is placed on the stage, which is raised by a handwheel on the side of the hardness tester until the workpiece nearly touches the diamond indenter. The load is applied by tripping the starting handle. The time taken in the application and duration of the load may be adjusted by the oil control valve in the dashpot within a range of 10 to 30 s minimum.

If the workpiece has not been elevated sufficiently for the testing load to be applied satisfactorily, a warning is given by an automatically actuated buzzer. A foot pedal will ready the hardness tester for the next test after a test cycle is completed. The stage may be fitted with a V-block for supporting cylindrical work.

If routine hardness testing is to be carried out, a sliding table may be attached to the stage and the microscope may be mounted on an auxiliary bracket on the right-hand side of the tester so that hardness testing may be continuous without the need for winding the stage up or down.

SCLEROSCOPE HARDNESS TESTING

The Scleroscope hardness test is essentially a dynamic indentation hardness test, wherein a diamond-tipped hammer is dropped from a fixed height onto the surface of the material being tested. The height of rebound of the hammer is a measure of the hardness of the metal. The Scleroscope scale consists of units that are determined by dividing the average rebound of the hammer from a quenched (to maximum hardness) and untempered water-hardening tool steel into 100 units. The scale is continued above 100 to permit testing of materials having hardnesses greater than that of fully hardened tool steel.

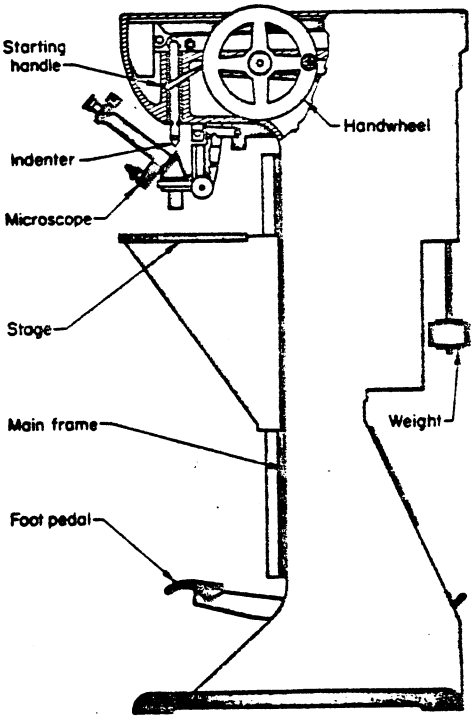

Fig. 9. Principal components of one type of Vickers hardness tester

Testers. Two types of Scleroscope hardness testers are shown in Fig. 10. The Model C Scleroscope consists of a vertically disposed barrel containing a precision-bore glass tube. A base-mounted version of a Model C Scleroscope is shown in Fig. 10(a). The scale is graduated from 0 to 140. It is set behind and is visible through the glass tube. Hardness is read from the vertical scale, usually with the aid of the reading glass attached to the tester. A pneumatic actuating head, affixed to the top of the barrel, is manually operated by a rubber bulb and tube. The hammer drops and rebounds with the glass tube.

The Model D Scleroscope hardness tester (Fig. 10b) is a dial-reading tester. The tester consists of a vertically disposed barrel that contains a clutch to arrest the hammer at maximum height of rebound. This is made possible because of the short rebound height. The hammer is longer and heavier than the hammer in the Model C Scleroscope and develops the same striking energy although dropping a shorter distance.

Both models of the Scleroscope hardness tester may be mounted on various types of bases. The C-frame base, which rests on three points and is for bench use in hardness testing small workpieces, has a capacity about 3 in. high by $2^1/_2$ in. deep. A swing arm and post is also for bench use, but has height and reach capacities of 9 and 14 in., respectively. Another type of base is used for mounting the Scleroscope hardness tester on rolls and other cylindrical objects having a minimum diameter of $2^1/_2$ in., or on flat, horizontal surfaces having a minimum dimension of 3 by 5 in. The Model C Scleroscope hardness tester is commonly used unmounted. However, when the hardness tester is unmounted, the workpiece should have a minimum weight of 5 lb. The Model D Scleroscope hardness tester should not be used unmounted.

Workpiece Surface-Finish Requirements. As with other metallurgical hardness testers, certain surface-finish requirements on the workpiece must be met for Scleroscope hardness testing to make an accurate hardness determination. An excessively coarse surface finish will yield erratic readings. Hence, when necessary, the surface of the workpiece should be filed, machined, ground or polished to permit accurate, consistent readings to be obtained.

Limitations on Workpiece and Case Thickness. Case-hardened steels having cases as thin as 0.010 in. can be accurately hardness tested provided the core hardness is no less than 30 Scleroscope. Softer cores require a minimum case thickness of 0.015 in. for accurate results.

Thin strip or sheet may be tested, with some limitations, but only when the Scleroscope hardness tester is mounted in the clamping stand. Ideally, the sheet should be flat and without undulation. If the sheet material is bowed, the concave side should be placed up to preclude any possibility of erroneous readings due to spring effect. The minimum thicknesses of sheet in various categories that may be hardness tested are as follows:

Hardened steel	0.005 in.
Cold finished steel strip	0.010
Annealed brass strip	0.015
Half-hard brass strip	0.010

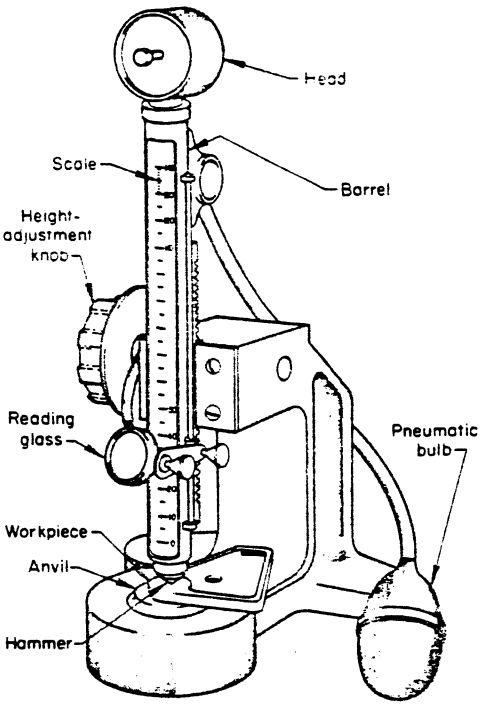

(a) Model C (vertical scale) Scleroscope hardness tester

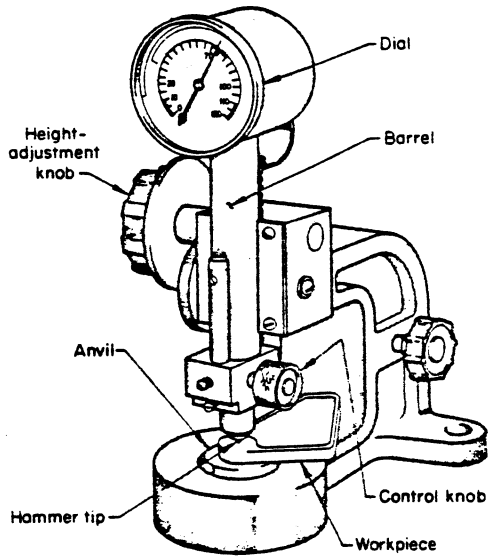

(b) Model D (dial reading) Scleroscope hardness tester

Fig. 10. Principal components of two types of base-mounted Scleroscope hardness testers

Test Procedure. To perform a hardness test with either the Model C or the Model D Scleroscope hardness tester, the tester should be held or set in a vertical position, with the bottom of the barrel in firm contact with the workpiece. The hammer is raised to the elevated position and then allowed to fall and strike the surface of the workpiece. The height of rebound is then measured, which indicates the hardness. When using the Model C Scleroscope hardness tester, the hammer is raised to the elevated position by squeezing the pneumatic bulb. The hammer is released by again squeezing the bulb. When using the Model D Scleroscope hardness tester, the hammer is raised to the elevated position by turning the knurled control knob clockwise until a definite stop is reached. The hammer is allowed to

strike the workpiece by releasing the control knob. The reading is recorded on the dial.

Spacing of Indentations. Indentations should be at least 0.50 mm (0.020 in.) apart and only one at the same spot. Flat workpieces with parallel surfaces may be hardness tested within ¼ in. (6 mm) of the edge when properly clamped.

Taking the Readings. Experience is necessary to interpret the hardness readings accurately on a Model C Scleroscope hardness tester. Thin materials or those weighing less than 5 lb must be securely clamped to absorb the inertia of the hammer. The sound of the impact is an indication of the effectiveness of the clamping: a dull thud indicates that the workpiece has been clamped solid, whereas a hollow ringing sound indicates that the workpiece is not tightly clamped or is warped and not properly supported. Five hardness determinations should be made and their average taken as representative of the hardness of a particular workpiece.

Advantages of the Scleroscope hardness test are summarized as follows:

1. Tests can be made very rapidly—over 1000 tests per hour are possible.
2. Operation is simple, and does not require highly skilled technicians.
3. The Model C Scleroscope tester is portable and may be used unmounted for hardness testing workpieces of unlimited size—rolls, large dies and machine-tool ways.
4. The Scleroscope hardness test is a nonmarring test; no crater is left, and only in the most unusual instances would the tiny hammer mark be objectionable on a finished workpiece.
5. A single scale accommodates the entire hardness range from the softest to the hardest metals.

Limitations of the Scleroscope hardness test are summarized as follows:

1. The hardness tester must be in a vertical position or the free fall of the hammer will be impeded and result in erratic readings.
2. Scleroscope hardness tests are more sensitive to variations in surface conditions than some other hardness tests.
3. Because readings taken with the Model C Scleroscope hardness tester are those observed from the maximum rebound of the hammer on the first bounce, even the most experienced operators may disagree among themselves by one or two points in the reading.

MICROHARDNESS TESTING

The term "microhardness" usually refers to indentation hardness tests made with loads not exceeding 1 kg (1000 g). Such hardness tests have been made with a load as light as 1 g, although the majority of microhardness tests are made with loads of 100 to 500 g. In general, the term is related to the size of the indentation rather than to the load applied.

Fields of Application. Microhardness testing is capable of providing information regarding the hardness characteristics of materials that cannot be obtained with hardness tests such as the Brinell, Rockwell or Scleroscope.

Because of the required degree of precision for both equipment and operation, microhardness testing is usually, although not necessarily, performed in a laboratory. Such a laboratory, however, is often a process-control laboratory and may

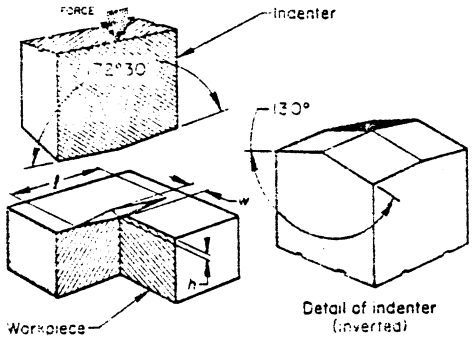

Fig. 11. Schematic representation of a pyramidal Knoop indenter, and of the resulting indentation in the workpiece

be located close to production operations. Microhardness testing is recognized as a valuable method for controlling numerous production operations in addition to its use in research applications. Specific fields of application of microhardness testing include:

1. Measuring hardness of precision workpieces that are too small to be measured by the more common hardness-testing methods
2. Measuring hardness of product forms such as foil or wire that are too thin or too small in diameter to be measured by the more convenient methods
3. Monitoring of carburizing or nitriding operations, which is usually accomplished by hardness surveys taken on cross sections of test pieces that accompanied the workpieces through production operations
4. Measuring hardness of individual microconstituents
5. Measuring hardness close to edges, thus detecting undesirable surface conditions such as grinding burn and decarburization
6. Measuring hardness of surface layers such as plating or bonded layers.

Indenters. Microhardness testing is peformed with either the Knoop or the Vickers indenter. The Knoop indenter is the more widely used in the United States; the Vickers indenter is the more widely used in Europe.

Knoop indentation testing is performed with a diamond ground to pyramidal form that produces a diamond-shape indentation having an approximate ratio between long and short diagonals of 7 to 1 (Fig. 11). The pyramidal shape employed has an included longitudinal angle of 172° 30′ and an included transverse angle of 130°. The depth of indentation is about one thirtieth of its length. Because of the shape of the indenter, indentations of accurately measurable lengths are obtained with light loads.

The Knoop hardness number (HK) is the ratio of the load applied to the indenter to the unrecovered projected area of indentation. By formula:

$$HK = P/A = P/Cl^2$$

where P is the applied load, in kilograms; A is the unrecovered projected area of indentation, in square millimetres; l is the measured length of the long diagonal, in millimetres; and C is 0.07028, a constant of the indenter relating projected area of the indentation to the square of the length of the long diagonal.

For details of the Vickers indenter, the reader is referred to Fig. 8.

Figure 12 presents a comparison of the indentations made by the Knoop and Vickers indenters. Each has some advantages over the other. For example, the Vickers indenter penetrates about twice as far into the workpiece as does the Knoop indenter, and the diagonal of the Vickers indentation is about one-third of the total length of the Knoop indentation. Therefore, the Vickers indenter is less sensitive to minute differences in surface conditions than is the Knoop indenter. However, the Vickers indentation, because of the shorter diagonal, is more sensitive to errors in measurement than is the Knoop indentation.

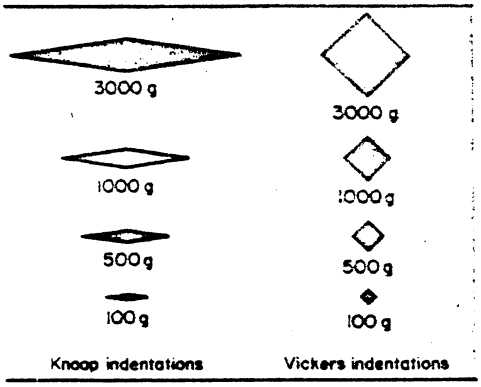

Fig. 12. Comparison of indentations made by Knoop and Vickers indenters in the same work metal and at the same loads

Microhardness Testers. Several types of microhardness testers are available. The most accurate operate through the direct application of load by dead weight, or by weights and lever.

The Tukon tester is widely used for microhardness testing. Several different designs of this microhardness tester are available; they vary mainly in load range, but all can accommodate both Knoop and Vickers indenters.

The Tukon microhardness tester shown in Fig. 13 has a load range of 1 to 1000 g. Loads are applied by dead weight. The microscope is furnished with three objective lenses having magnifications of about 150, 300 and 600 diameters.

Sources of tester error include inaccuracy in loading, vibration, rate of load application, duration of contact period, and impact. To limit the shock that can occur when the operator removes the load (this generally has an adverse effect on indentations made with loads below 500 g), an automatic test cycle is built into the Tukon microhardness tester. With this automatic test cycle, the load is applied at a constant rate, maintained in the work for 18 s, and smoothly removed. Thus, the operator does not need to touch the tester while the load is being applied and removed. The design of microhardness testers will vary from one type to another, but it is essential to remove the applied load without touching the tester if clear-cut indentations are to be obtained.

A movable stage to support the workpiece is an essential component of a microhardness tester. In many applications the indentation must be in a selected area, usually limited to a few thousandths of a square millimetre. In testing with the type of Tukon microhardness tester shown in Fig. 13, first the required area is located by looking through the microscope and moving the me-

chanical stage until the desired location is centered within the optical field of view. The stage is then inserted under the indenter, and the automatic indentation cycle is initiated by tripping the handle. After the cycle is completed, signaled by a telltale light, the stage is again indexed back under the objective for indentation measurement.

Optical equipment used in microhardness testers for measuring the indentation must focus on both ends of the indentation at the same time, as well as be rigid and free from vibration. Lighting is also important. Complete specifications of measurement, including the mode of illumination, are necessary in microhardness-testing techniques. Polarized light, for instance, results in larger measurements than does unpolarized light. Apparently, this is caused by the reversal of the diffraction pattern; that is, the indentation appears brighter than the background. When test data are recorded, it is recommended that both the magnification and the type of illumination used be reported.

Measuring the Indentation. In measuring the indentation, the proper illumination to obtain optimum resolution is essential, and the appropriate objective lens should be selected. In operation, the ends of the indentation diagonals should be brought into sharp focus. With the Knoop indenter, one leg of the long diagonal should not be more than 20% longer than the other. If this is not apparent or if the ends of the diagonal are not in focus, the surface of the workpiece should be checked to make sure it is normal to the axis of the indenter. With the Vickers indenter, both diagonals should be measured and the average used for calculating the Vickers hardness number (HV).

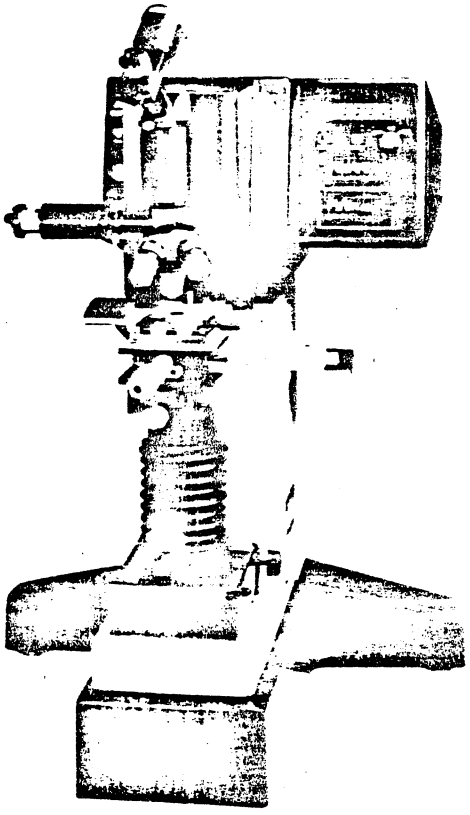

Fig. 13. Principal components of a Tukon microhardness tester

Indentation in a particle of chromium-vanadium carbide (white constituent) showed a value of 1930 HK, whereas the indentation in the matrix (darker constituent) was 801 HK. Both indentations were made with a 50-g load. (Specimen was polished, and etched in Villela's reagent; shown at 1000×.)

Fig. 14. Comparison of Knoop indentations in two microconstituents of quenched-and-tempered D2 tool steel

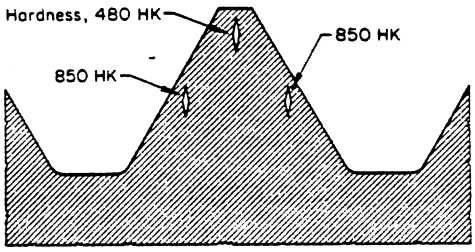

Fig. 15. Cross section of a tap tooth showing hardness variations caused by overheating during grinding

Preparing and Holding the Specimen. Regardless of whether the metal being tested for microhardness is an actual workpiece or a representative specimen, surface finish is of prime importance.

To permit accurate measurement of the length of the Knoop indentation or diagonals of the Vickers indentation, the indentation must be clearly defined. In general, as the test load decreases, the surface-finish requirements become more stringent. When the load is 100 g or less, a metallographic finish is recommended.

Specific Applications of Microhardness Testing

Microhardness testing is used extensively in research and for controlling the quality of manufactured products, as well as for solving shop problems.

Testing of small workpieces is an important use of microhardness testing. Many manufactured products, notably in the instrument and electronics industries, are too small to be tested for hardness by the more conventional methods. Many such workpieces can be tested without impairing their usefulness, generally by means of various types of holding and clamping fixtures.

Microhardness testing is also applied to product forms that cannot be tested by other means. Thin foils and small-diameter wires are typical examples.

Monitoring of Surface-Hardening Operations. Microhardness testing is the best method in present use for accurately determining case depth and certain case conditions of carburized or nitrided workpieces, using the hardness-survey procedure. In most instances this is accomplished by use of test coupons that have accompanied the actual workpieces through the heat treating operation. The coupons are then sectioned and usually mounted for testing. To ensure accurate readings close to the edge of the cross section, the 100-g load is most often used, although a 500-g load is sometimes preferred. If the 100-g load is used, a metallographic finish is essential.

Readings are taken at pre-established intervals (commonly, 0.004 or 0.005 in.), usually beginning at least 0.001 in. from the edge of the workpiece.

Measuring Hardness of Microconstituents. A great deal can be learned about metals and their potential properties (for example, their resistance to wear) by knowing the actual hardnesses of their various microconstituents. Notable examples are the highly alloyed tool steels. Figure 14 shows a micrograph of polished and etched D2 tool steel. Knoop indentations taken on the matrix (darker constituent) and on the particles of complex alloy carbide (white) show an obvious variation in size. In this instance the tests were made with a load of 50 g. The indentation on the matrix was 801 HK, whereas the carbide showed a value of 1930 HK. Actual Rockwell hardness on the C scale was 64 HRC (822 HK by conversion). Therefore, the Rockwell C scale did not register the true conditions.

Shop problems are often solved with the help of microhardness testing. Some of the most notable examples involve cutting edges of tools.

Cutting tools made from high speed steels, even though they have been correctly heat treated, are frequently damaged in grinding. Taps are among the most vulnerable, because the crests of teeth are thin and thus are likely to become overheated during grinding.

In one instance, taps were failing prematurely from dulling of the tap teeth. Hardness measurements taken at various locations (where it was possible to measure) on the taps showed consistent values of 65 HRC, which was entirely acceptable. However, when one of the taps was sectioned and a tooth area was examined with a microhardness tester, results were quite different. Measurements taken at various locations with a Knoop indenter and a 100-g load showed readings of about 850 HK (by conversion, about 65 HRC) in the center of the tooth and to within 0.003 to 0.005 in. of the edge (see Fig. 15). At the very edge of the tooth crest, however, readings were as low as 480 HK (see Fig. 15), which converts to approximately 46 HRC. Variation in size of the indentations can be clearly seen in Fig. 15. Obviously, the softened condition was a result of abusive grinding practice and rendered the tap useless.

SELECTED REFERENCES

Hardness Testing, by E. R. Petty: in *Techniques of Metals Research*, Vol 5, Part 2, edited by R. F. Bunshah, Wiley-Interscience, 1971, p 157

Hardness Measurements of Metals and Alloys, 2nd Ed., by H. O'Neil: Chapman and Hall, London, 1967

The Hardness of Metals, by B. Tabor: Oxford University Press, London, 1951

The Science of Hardness Testing and Its Research Applications, edited by J. H. Westbrook and H. Conrad: ASM, Metals Park, OH, 1973

Tension Testing

By George E. Dieter, University of Maryland

THE TENSION TEST is the test most commonly used to evaluate the mechanical properties of materials (Ref 1). Its chief use is the determination of properties related to the elastic design of machines and structures. In addition, the tension test gives information on a material's plasticity and fracture. The chief advantages of the tension test are that the stress state is well established, that the test has been carefully standardized (Ref 2) and that the test is relatively easy and inexpensive to carry out. This article will not detail this test technique, because it is well covered by standard methods (Ref 2); instead, the interpretation and limitations of the test results will be discussed.

ENGINEERING STRESS-STRAIN CURVE

In the conventional engineering tension test, stress is defined by the applied load divided by the original cross-sectional area of the specimen. Engineering strain, e, is the change in length divided by the initial length:

$$e = \frac{L - L_0}{L_0} = \frac{\Delta L}{L_0} \qquad \text{(Eq 1)}$$

In the elastic region of the stress-strain curve (Fig. 1), stress is linearly related to strain, $\sigma = Ee$, where E is the elastic modulus. As long as the specimen is loaded within the elastic region, the strain is totally recoverable and the specimen will return to its original length when the load is relaxed to zero. However, when the load exceeds a value corresponding to the yield stress, the specimen undergoes gross plastic deformation and is permanently deformed when the load returns to zero. The stress to produce continued plastic deformation increases with increasing strain—the metal strain hardens. To a good engineering approximation, the volume remains constant during plastic deformation, $AL = A_0L_0$, and, as the specimen elongates, it decreases uniformly in cross-sectional area along its gage length. Initially the strain hardening more than compensates for this decrease in area, and the engineering stress continues to rise with increasing strain. Eventually a point is reached where the decrease in area is greater than the increase in deformation load arising from strain hardening. This condition will be reached first at some point in the specimen that is slightly weaker than the rest. All further plastic deformation is concentrated in this region, and the specimen begins to neck or thin down locally. Because the cross-sectional area is now decreasing far more rapidly than the deformation load is being increased by strain hardening, the engineering stress continues to decrease until fracture occurs.

The maximum in the engineering stress-strain curve corresponds to the ultimate tensile strength, σ_u. The strain at maximum load, up to which point the cross-sectional area decreases uniformly along the gage length as the specimen elongates, is the uniform elongation, e_u. For stretching-type forming operations, such as stretch forming of aircraft components or forming of automobile fenders, local necking determines the formability limit, and in such applications uniform elongation can be an important measure of ductility. In many metals, the engineering stress-strain curve is relatively flat in the vicinity of necking, and it may not be possible to establish the maximum load without ambiguity. In these cases, the method suggested by Nelson and Winlock (Ref 3) is useful.

DUCTILITY

The conventional measures of ductility that are obtained from the tension test are the engineering strain at fracture, e_f (usually expressed as a percentage elongation), and the reduction of area at fracture, RA (also usually expressed as a percentage):

$$e_f = \frac{L_f - L_0}{L_0} \qquad \text{(Eq 2)}$$

$$RA = \frac{A_0 - A_f}{A_0} \qquad \text{(Eq 3)}$$

Because an appreciable fraction of the deformation will be concentrated in the necked region of the specimen, the value of e_f will depend on the gage length L_0 over which the measurement was taken. The smaller the gage length, the greater the contribution from the neck and the higher the value of e_f.

To eliminate this difficulty and to provide a measure of ductility that correlates with forming operations in which the gage length is very short, it is possible to determine the zero-gage-length elongation, e_0. From the constancy-of-volume relationship for plastic deformation, $AL = A_0L_0$:

$$\frac{L}{L_0} = \frac{A_0}{A} = \frac{1}{1 - RA}$$

$$e_0 = \frac{L - L_0}{L_0} = \frac{A_0}{A} - 1$$

$$= \frac{1}{1 - RA} - 1 = \frac{RA}{1 - RA} \qquad \text{(Eq 4)}$$

Thus, the zero-gage-length elongation may be determined directly from the reduction of area at fracture or from the change in length of grid marks near the actual fracture. The data presented in Table 1 show how basing a comparison of the formability of aluminum alloys on the elongation in a 2-in. (50.8-mm) gage length would lead to erroneous conclusions for forming operations where local ductility determines the forming limit (Ref 4).

Table 1. Comparison of several measures of ductility for two aluminum alloys (Ref 4)

Alloy	e_0	$e_{2.0}$	e_u
24S-O (2024-O)	1.22	0.18	0.16
24S-T (2024-T)	0.64	0.18	0.15
75S-O (7075-O)	1.55	0.16	0.11
75S-T (7075-T)	0.44	0.11	0.09

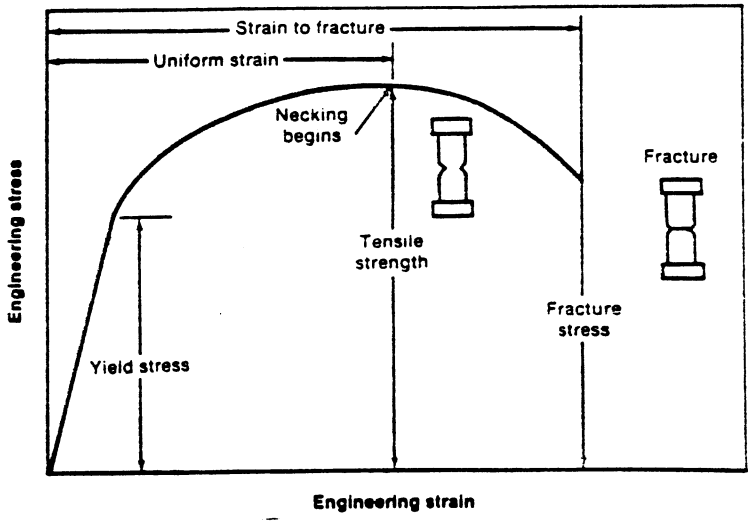

Fig. 1. Engineering stress-strain curve

TRUE-STRESS/TRUE-STRAIN CURVE

The necking phenomenon which occurs in the tension test clouds the usefulness of the engineering stress-strain curve beyond the maximum load. The falloff in stress which occurs beyond P_{max} is artificial and occurs only because the stress continues to be calculated on the basis of the original cross-sectional area, A_0, when in fact the area at the necked region is now much smaller than A_0. If the *true stress*, based on the actual cross-sectional area of the specimen, is used, the stress-strain curve increases continuously up to fracture. Then, if strain is expressed as *true strain*, we have a plot called the true-stress/true-strain curve (Fig. 2).

Note that this curve continues to rise beyond necking all the way to fracture. However, once necking occurs, the constraints produced by the nondeforming region outside the neck produce a state of triaxial stress in the neck. Thus, the average stress required to cause flow from maximum load to fracture is higher than would be required if only a uniaxial stress were present. Bridgman (Ref 5) has made a mathematical analysis of the stresses in the neck that permits correction of the true-stress/true-strain curve for the

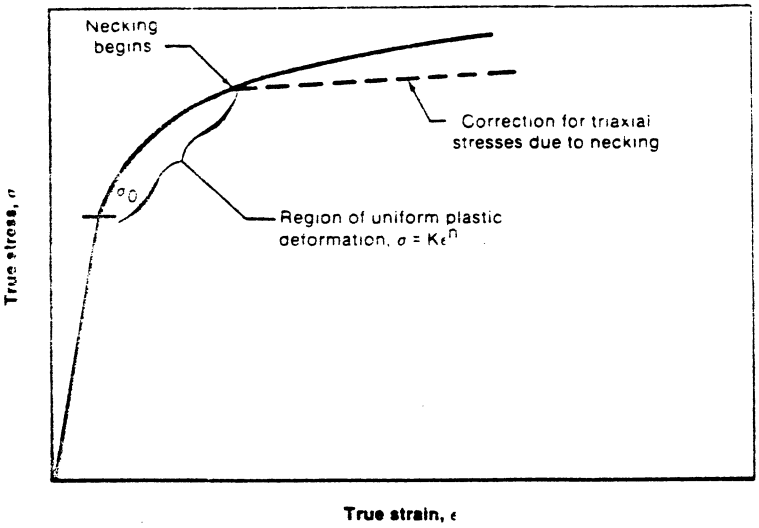

Fig. 2. True-stress/true-strain curve (flow curve)

existence of triaxial stresses. More recent studies have utilized finite-element analysis (Ref 6).

The region from yielding to necking is one of uniform plastic deformation in which the specimen gage length increases and the diameter decreases uniformly along the gage length. In this region the true-stress/true-strain curves for many ductile metals can be expressed by a power-law relation:

$$\sigma = K\epsilon^n \qquad \text{(Eq 5)}$$

where K is the strength coefficient, defined by the value of true stress at $\epsilon = 1.0$, and n is the strain-hardening exponent. Equation 5 is valid if a plot of σ versus ϵ is a straight line on log-log coordinates. The strain-hardening exponent is the slope of this line. Thus

$$n = \frac{d(\log \sigma)}{d(\log \epsilon)} = \frac{d(\ln \sigma)}{d(\ln \epsilon)} = \frac{\epsilon}{\sigma}\frac{d\sigma}{d\epsilon} \qquad \text{(Eq 6)}$$

The strain-hardening exponent may have values from n = 0 (a perfectly plastic solid) to n = 1 (an elastic solid). Values of n for most metals are between 0.05 and 0.50.

An increase in strain rate increases the stress to produce plastic deformation (the flow stress). The effect is modest for cold working, but is quite significant for hot working. The dependence of flow stress on strain rate, at constant strain and temperature, is given by

$$\sigma = C(\dot{\epsilon})^m|_{\epsilon,T} \qquad \text{(Eq 7)}$$

where m is the strain-rate sensitivity. The exponent m can be evaluated from the slope of a plot of log σ versus log $\dot{\epsilon}$, or it can be obtained from rate-change tests in which the change in flow stress caused by a step change in $\dot{\epsilon}$ is measured:

$$m = \left(\frac{d \log \sigma}{d \log \dot{\epsilon}}\right) \approx \left(\frac{\Delta \log \sigma}{\Delta \log \dot{\epsilon}}\right)_{\epsilon,T}$$

$$= \frac{\log \sigma_2 - \log \sigma_1}{\log \dot{\epsilon}_2 - \log \dot{\epsilon}_1} = \frac{\log \frac{\sigma_2}{\sigma_1}}{\log \frac{\dot{\epsilon}_2}{\dot{\epsilon}_1}} \qquad \text{(Eq 8)}$$

ANALYSIS OF TENSILE INSTABILITY

The development of a necked region in a specimen loaded in uniaxial tension represents a plastic instability. Because this disturbs the simple analysis of the tension test and limits the engineering usefulness of the test, it has become the subject of considerable study (Ref 7 to 9). A practical application of the ideas presented below is given in the work of Ghosh (Ref 10), who developed a numerical analysis for predicting the shape of the engineering strain-stress curve beyond maximum load as a function of strain hardening, strain-rate hardening, and plastic anisotropy properties of the metal.

Consider a tensile specimen loaded to a value P. At any point a distance L along the specimen, the cross-sectional area is A and $P = \sigma A$. Since P does not vary along the length of the specimen, and $\sigma = f(\epsilon, \dot{\epsilon})$,

$$\frac{dP}{dL} = 0 = A\left\{\left(\frac{d\sigma}{d\epsilon}\right)_{\dot{\epsilon}}\frac{d\epsilon}{dL} + \left(\frac{d\sigma}{d\dot{\epsilon}}\right)_{\epsilon}\frac{d\dot{\epsilon}}{dL}\right\} + \sigma\frac{dA}{dL} \qquad \text{(Eq 9)}$$

Because the volume of the specimen remains constant, the true strain can be written as

$$d\epsilon = \frac{dL}{L} = -\frac{dA}{A} \qquad \text{(Eq 10)}$$

and

$$\frac{d\epsilon}{dL} = -\frac{1}{A}\frac{dA}{dL} \qquad \text{(Eq 11)}$$

Also, from Eq 10, we can express the strain-rate $\dot{\epsilon}$ by

$$d\dot{\epsilon} = \frac{d\epsilon}{dt} = -\frac{1}{A}\frac{dA}{dt} = -\frac{\dot{A}}{A} \qquad \text{(Eq 12)}$$

so that

$$\frac{d\dot{\epsilon}}{dL} = -\frac{1}{A}\frac{d\dot{A}}{dL} + \frac{\dot{A}}{A^2}\frac{dA}{dL} \qquad \text{(Eq 13)}$$

The material parameters which are important to the necking process are the dimensionless work-hardening coefficient:

$$\gamma = \frac{1}{\sigma}\frac{d\sigma}{d\epsilon} \qquad \text{(Eq 14)}$$

and the strain-rate sensitivity:

$$m = \left(\frac{d \ln \sigma}{d \ln \dot{\epsilon}}\right)_{\epsilon} = \frac{\dot{\epsilon}}{\sigma}\left(\frac{d\sigma}{d\dot{\epsilon}}\right)_{\epsilon} \qquad \text{(Eq 15)}$$

When Eq 12 and 13 are substituted into Eq 9, and the definitions for γ and m are added through Eq 14 and 15, the result is

$$\frac{dA}{dL}(\sigma - m\sigma - \gamma\sigma) = -\frac{d\dot{A}}{dL}\frac{m\sigma A}{\dot{A}} \qquad \text{(Eq 16)}$$

A final rearrangement gives

$$\frac{\frac{1}{\dot{A}}\frac{d\dot{A}}{dL}}{\frac{1}{A}\frac{dA}{dL}} = \frac{\frac{d}{dL}(\ln \dot{A})}{\frac{d}{dL}(\ln A)} = \frac{m + \gamma - 1}{m} \qquad \text{(Eq 17)}$$

This equation describes the rate of change of area with length, and gives the criterion for the onset of necking.

Any real tension specimen will have variations in cross-sectional area along its length. These can arise from an intentional taper, from machining errors or from heterogeneities of structure which lead to weaker cross sections. Deformation becomes unstable when the smallest cross section of the specimen shrinks faster than the rest. This occurs when $d\dot{A}/dA > 0$. Deformation will be uniform and stable when $d\dot{A}/dA < 0$. Since $\dot{A}/A$ is negative in tension, stable deformation in tension occurs when $d\dot{A}/dA \geq 0$. Therefore, from Eq 17, the condition for stable, uniform tensile deformation is

$$\gamma + m \geq 1 \qquad \text{(Eq 18)}$$

Necking is involved with the interplay between the applied stress and the flow resistance of the material. As the specimen elongates under a given load the area decreases and the stress increases. If necking is not to occur, the material's strength must increase through strain hardening (γ) and strain-rate hardening (m).

For room-temperature deformation, $m \rightarrow 0$ and the instability criterion reduces to $\gamma \geq 1$. Thus, stable tensile deformation occurs for

$$\frac{d\sigma}{d\epsilon} \geq \sigma \qquad \text{(Eq 19)}$$

If the true-stress/true-strain curve is given by $\sigma = K\epsilon^n$, then

$$\frac{d\sigma}{d\epsilon} = nK\epsilon^{n-1} = \sigma = K\epsilon^n$$

and necking occurs when

$$\epsilon = n \qquad \text{(Eq 20)}$$

Because n in tension rarely exceeds 0.5, we can see that the available uniform strain in the tension test is limited.

ELONGATION MEASUREMENTS IN TENSION TESTING

The measured elongation depends on the gage length or the dimensions of the cross section of the specimen. This is because the total extension consists of two components, the uniform extension up to the point of necking and the localized extension after necking (Fig. 3). The extent of uniform extension will depend on the metallurgical condition of the material (through n) and the

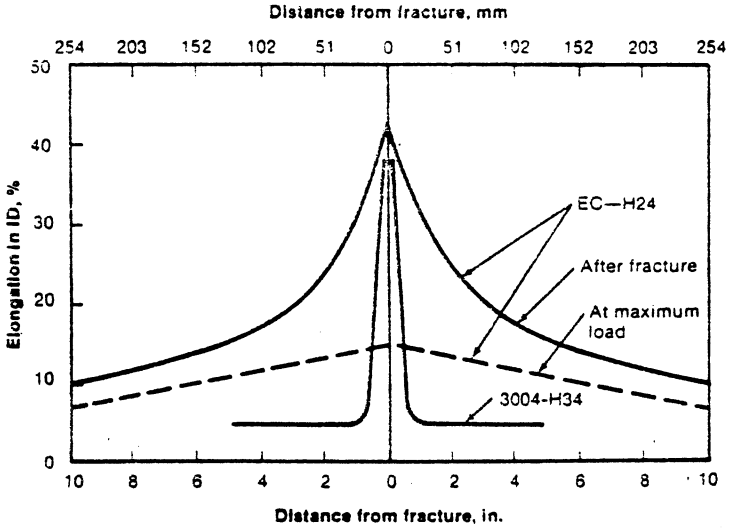

Fig. 3. Local elongation measured at positions away from fracture in tension specimens for two aluminum alloys (Ref 11)

effect of specimen size and shape on the development of a neck.

However,

$$L_f - L_0 = a + e_u L_0 \qquad \text{(Eq 21)}$$

where a is the local necking extension and $e_u L_0$ is the uniform extension. We then have

$$e_f = \frac{L_f - L_0}{L_0} = \frac{a}{L_0} + e_u \qquad \text{(Eq 22)}$$

which clearly indicates that the total elongation is a function of the gage length. Numerous attempts to rationalize the strain distribution in the tension test (Ref 12) have been made, dating back to 1850. Following Barba's law (Ref 13), which states that geometrically similar specimens develop geometrically similar necks, it is usually assumed that the local extension at the neck is proportional to the linear dimension of the cross-sectional area, $a = \beta\sqrt{A_0}$, so that the elongation equation becomes

$$e_f = \frac{\beta\sqrt{A_0}}{L_0} + e_u \qquad \text{(Eq 23)}$$

This equation for elongation, which is usually attributed to Unwin (Ref 14), clearly shows the rationale for the use of fixed ratios of gage length to diameter or gage length to square root of cross-sectional area in specifying tensile-specimen dimensions. It also reinforces the importance of stating the gage length over which the measurement was made when reporting elongation values. In the United States, the standard tensile specimen is 0.505 in. (12.83 mm) in diameter and 2 in. (50.8 mm) in gage length, so $1/D \simeq 4$. However, the testing standards in other countries specify different gage lengths for the measurement of elongation (Table 2).

To compare the ductilities of different metals by elongation measurements, the gage length should be adjusted as a function of the cross-sectional area of the test specimen. However, when flat specimens are cut from sheet or plate primarily to determine whether quality of individual lots meets specifications, it is usual to use fixed gage lengths, because of the lower cost of preparing and testing a large number of such specimens.

Table 2. Dimensional relationships for specimens used in different countries for measurement of elongation

Type of specimen	Dimensional relationship	United Kingdom Before 1962	United Kingdom Current	United States (ASTM)	Germany
Sheet	$L_0/\sqrt{A_0}$	4.0	5.65	4.5	11.3
Round bar	L_0/D_0	3.54	5.0	4.0	10.0

The effect of specimen geometry on total elongation is of particular concern in testing of sheet-metal specimens. Various proposals concerning the effect of ratio of width to thickness can be found in the literature (Ref 15). However, the correlation is more meaningful in terms of specimen cross-sectional area. A study of the effect of specimen geometry on elongation of sheet specimens (Ref 16) showed that, although Unwin's equation was obeyed (within considerable scatter), a simpler equation due to Templin (Ref 17) was possibly in better agreement with the results:

$$e_f = C(A)^b \qquad \text{(Eq 24)}$$

Analysis of the results showed that the exponent b in Templin's equation depends on both uniform strain and localized fracture strain. Thus it will vary with processing and heat-to-heat differences in the metal, and it cannot be considered to be a real constant of the metal. A general trend was shown to exist between the exponent b in Templin's equation and the logarithm of the ratio of the zero-gage-length (fracture-strain) elongations to the infinite-gage-length (uniform-strain) elongations.

Although (even after 100 years of study) opinions differ in detail concerning the effect of specimen geometry on elongation, there is general agreement concerning the validity and importance of one factor—the ratio $\sqrt{A/L}$. Even here it appears to be better validated for round bars than for rectangular specimens. However, if sufficient data on the influence of specimen size on elongation are not available, the elongation of a specimen of arbitrary size can be estimated by using the concept that a constant elongation is obtained if $\sqrt{A/L}$ is maintained constant, as suggested by Eq 23. Then, at a constant value of elongation, $\sqrt{A_1/L_1} = \sqrt{A_2/L_2}$, where A and L are the areas and gage lengths of two different specimens, 1 and 2, of the same metal. To predict the elongation in length L_2 on a specimen with area A_2 from measurements on a specimen with area A_1, it is only necessary to adjust the gage length of specimen 1 to conform to $L_1 = L_2\sqrt{A_1/A_2}$. As an example, suppose that sheet 1/8 in. (3.2 mm) thick is available and it is desired to predict the elongation in 2 in. (50.8 mm) in identical material 0.080 in. (2.03 mm) thick. Using sheet specimens 1/2 in. (12.7 mm) wide, we would predict that a test specimen with $L = 2\sqrt{0.125/0.080} = 2.5$ in. (63.5 mm) from the 1/8-in. (3.2-mm) sheet would give the same elongation as a 2-in. (50.8 mm) gage length in sheet 0.080 in. (2.0 mm) thick. The usefulness of this procedure is shown in Fig. 4, where solid lines

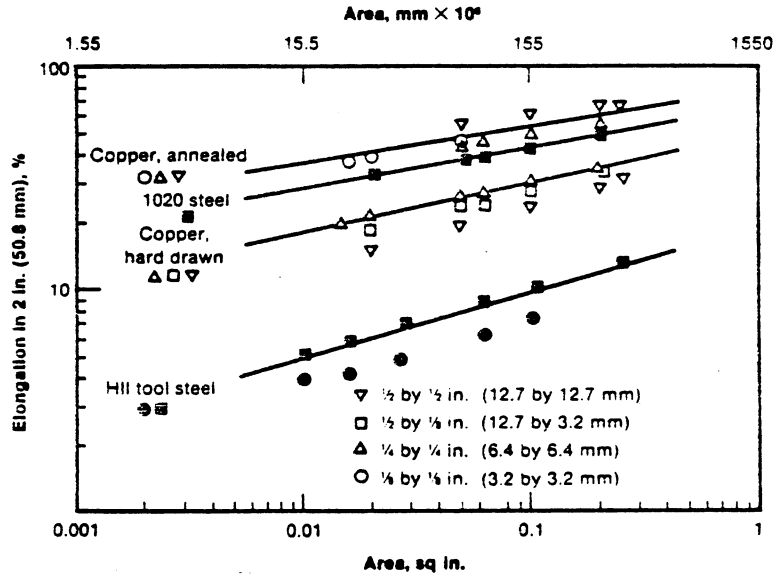

Fig. 4. Calculated variation of elongation in 2 in. (50.8 mm) with specimen cross-sectional area (Ref 16)

are experimental and points indicate predicted elongations for specimens of different areas.

The above discussion indicates that the measures of ductility that are available with the tension test leave a great deal to be desired in providing quantitative values. The main difficulty arises from the necking of the specimen. The occurrence of uniform and localized deformation makes the percentage elongation at fracture of little value as a quantitative measure of ductility, although it is usually required in metallurgical specifications. Reduction of area is a better measure of ductility, but its quantitative use is made difficult by the poorly defined triaxial stress state that is introduced by the formation of a neck.

PLANE-STRAIN TENSION TEST

A special type of tension-test specimen has been designed (Ref 18) to give maximum plastic constraint so as to emphasize the differences in fracture behavior of nominally ductile materials (Fig. 5). The deep grooves in the specimen restrict the deformation to the grooved region. The ratio B/L is large enough so that approximately plane-strain conditions are achieved in the test section (Ref 19). Thus, strain occurs in the thickness and length directions but not in the width direction. The true strain is given by

$$\epsilon = \ln h_0/h \qquad \text{(Eq 25)}$$

where h_0 is the initial thickness of the reduced section and h is the thickness at any time after deformation has begun. However, the ratio L/h is large enough so that there is no notch effect, and thus a specimen designed to the specification in Fig. 5 is an unnotched plane-strain specimen. Thus, the true stress can be determined directly from the load divided by the area (h × B).

The ability of the plane-strain tension test to distinguish between material ductilities is shown in Table 3.

The plane-strain tension specimen described in Fig. 5 has the disadvantage that it may not be practical to machine such a specimen in a thin sheet. Also, since all deformation is confined to the notch region, it may be difficult to make axial-strain measurements in those limited confines. A special clip-on fixture allows a regular sheet specimen to be converted to a plane-strain specimen (Ref 20).

This plane-strain tension specimen is 38 mm wide and 200 mm long. The specimen contains two circular edge notches with a 19-mm radius. A special fixture containing four knife edges is clamped to the surface of the specimen. The knife edges run parallel to the tensile axis of the specimen and fall just inside the reduced cross section. These knife edges prevent any deformation in the width direction. As a result, necking and failure occur perpendicular to the tensile axis.

SUMMARY

The tension test is a "benchmark test" or "reference test" that provides much basic information about the mechanical state of a material. This test provides information on the flow of a material and its ductility.

The flow resistance is evaluated on the basis of yield stress. The yield stress is variously determined by the first deviation from linear elastic behavior, or more precisely by the stress corresponding to the intersection with the stress-strain curve at an offset strain of 0.002 (the 0.2% offset yield strength). If the stress-strain curve can be expressed by Eq 5, then the yield stress corresponding to a particular cold reduction, expressed as reduction of area, RA, is given by the following equation (Ref 21):

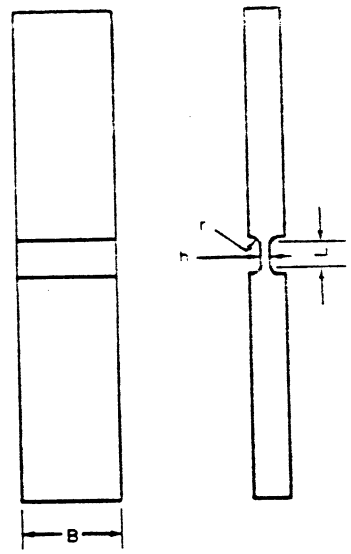

B = 1 in.; L = 1/4 in.; h = 0.080 in.; r = 1/16 in.

Fig. 5. Plane-strain tension specimen

$$\sigma_y = K \ln \left(\frac{1}{1 - RA} \right)^n \qquad \text{(Eq 26)}$$

This shows that a high strain-hardening exponent n leads to higher flow stress. In addition, with high n values the deformation is spread out and local points of weakness, which can lead to thinning or fracture, are minimized. At elevated temperatures, strain-rate sensitivity becomes important, and strain hardening becomes less important.

Elongation and reduction of area in the tension test cannot be calculated from each other because the occurrence of necking prevents the constant-volume relationship ($A_0L_0 = A_1L_1$) from being invoked over a distance containing the necked region. While elongation and reduction of area usually vary in the same way—for example, as a function of test temperature or alloy content—this is not always the case. Generally speaking, elongation and reduction of area measure different types of material behavior. Elongation measurements in the tension test are chiefly influenced by uniform elongation (except when the gage length is very short) and thus depend on the strain-hardening capacity of the material. Reduction of area is more a measure of the deformation required to produce fracture. It is the most structure-sensitive ductility parameter.

Table 3. Fracture strains for various steels (Ref 18)

Steel	Fracture strain (ϵ_f) Tension test(a)	Plane-strain tension test
ABS-2	1.04	0.75
A302-B	0.98	0.72
HY-80	1.22	0.86
18Ni (180 ksi)	1.00	0.42
18Ni (250 ksi)	0.89	0.15

(a) Standard 0.252-in.-diam specimen.

REFERENCES

1. *Mechanical Metallurgy*, 2nd Ed., by G. E. Dieter: McGraw-Hill, New York, 1976, Chapter 9
2. "Standard Methods of Tension Testing of Metallic Materials": ASTM Designation E8, Annual Book of ASTM Standards (see current index for tension tests of various product forms)
3. P. G. Nelson and W. Winlock: *ASTM Bull.*, Vol 156, Jan 1949, p 53
4. *Measurement of Ductility in Sheet Metals*, by J. R. Low and T. A. Prater: ASTM STP 87, 1948
5. P. W. Bridgman: *Trans. ASM*, Vol 32, 1944, p 553
6. A. S. Argon, J. Im and A. Needleman: *Met. Trans.*, Vol 6A, 1975, p 815
7. E. W. Hart: *Acta Met.*, Vol 15, 1976, p 351
8. *The Inhomogeneity of Plastic Deformation*, by A. S. Argon: American Society for Metals, Metals Park, OH, 1973, Chapter 7
9. J. W. Hutchinson and K. W. Neale: *Acta Met.*, Vol 25, 1977, p 839
10. A. K. Ghosh: *Met. Trans. A*, Vol 8A, 1977, p 1221
11. G. W. Stickley and D. J. Brownhill: *Proc. ASTM*, Vol 65, 1965, p 597
12. T. C. Hsu, G. S. Littlejohn and B. W. Marchbank: *Proc. ASTM*, Vol 65, 1965, p 874
13. M. J. Barba: *Mem. Soc. Ing. Civils*, Part I, 1880, p 682
14. W. C. Unwin: *Proc. Inst. Civil Eng.*, Vol 155, Aug 1903, p 170
15. "The Influence of Sheet Thickness on Tensile Properties of Sheet Metal," by A. Rudnick and R. L. Carlson: DMIC Memo 5, Battelle Memorial Institute, Columbus, OH, Jan 23 1959
16. E. G. Kula and N. N. Fahey: *Mat. Res. Std.*, Vol 1, Aug 1961, p 631
17. R. L. Templin: *Proc. ASTM*, Vol 26, 1926, p 378
18. D. P. Clausing: *Int. J. Fracture Mechanics*, Vol 6, 1970, p 71
19. J. P. Elington: *J. Mech. Phys. Solids*, Vol 6, 1958, p 276
20. H. Sang and Y. Nishikawa: *J. Metals*, Feb 1983, p 30
21. L. A. Erasmus: *Metallurgia and Metal Forming*, Apr 1975, p 94

Compression Testing

THE CONCEPTS of uniaxial tensile and compressive loading are quite similar. In both cases, a strain is produced parallel to the applied load that has the same sign as the applied load, and two transverse strains are produced that are opposite in sign to the applied load. Below the proportional limit, the strain in the load direction, in both cases, can be calculated using a single value of Young's modulus. Similarly, the transverse strain can be calculated using a second material constant, Poisson's ratio (ν):

$$\epsilon_{transverse} = \nu\epsilon_{axial}$$

Compression testing is an extremely valuable testing procedure which is often overlooked because it is not properly understood. One of the main advantages of the compression test is that tests can be performed with a minimum of material, and thus mechanical properties can be obtained from specimens that are too small for tension testing. Compression tests are also very helpful for predicting the bulk formability of materials (behavior in forging, extrusion, rolling, etc.).

In compression testing, the material does not neck as in tension, but undergoes barreling; failure occurs by different mechanisms and therefore there is no UTS (ultimate tensile strength). In general, ductile materials do not fail in compression but tend to flow in response to the imposed loads. Brittle cylindrical specimens loaded in

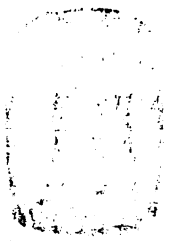

Compression test of gray cast iron, grade 40, illustrating brittle fracture. The compression strength of this specimen is 110.517 ksi (762 MPa), which is approximately three times its tensile strength of 40 ksi (276 MPa).

Fig. 6. Brittle compression

compression fail in shear on a plane inclined to the load, and therefore actually break into two or more pieces (Fig. 6). In this case, an ultimate (compressive) stress can be defined.

In comparison with tension testing, several difficulties are encountered in conducting compression tests and interpretation of the experimental data. For example, maintaining complete axiality of the applied load is important. In tension testing, self-aligning grips make this relatively simple to accomplish. In compression testing, if the specimen is tall in relation to its diameter, this can present a major difficulty. Nonaxiality of the load induces a bending load in the specimen, in addition to the axial load, that potentially will cause buckling. Alignment of the loading platens to impose strict uniaxial loading is easier if the specimen contact area is large, but this in turn introduces other difficulties.

Frictional forces exist at the specimen/platen interface that tend to restrict the increase in diameter of the specimen as it decreases in height. These forces are directly related to the coefficient of friction, μ, and thus care must be given to minimizing μ. P is the compressive load. Due to these frictional forces, loading on the specimen is not uniaxial. The effect of these frictional forces is two fold; (*a*) an analysis indicates that the magnitude of the applied stress is increased over what it would be if the specimen were loaded uniaxially (i.e., the situation if μ equals 0), and (*b*) diametral expansion is hindered near the platens, but not in material well removed from the platen, so that the specimen becomes barrel shaped (Fig. 7). Because of the increased magnitude of

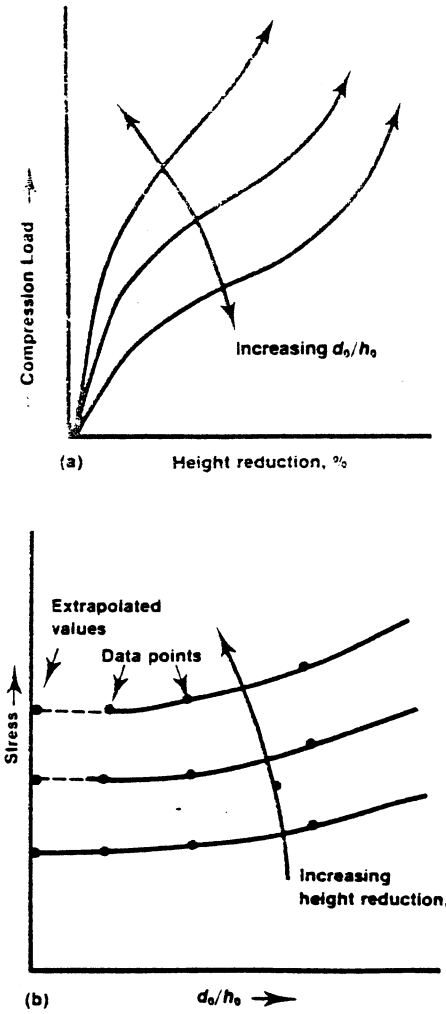

(a) Curves illustrating the relationship of compression load to height reduction for various d_0/h_0 ratios. (b) Replot of curves for extrapolation to $d_0/h_0 = 0$. d_0 is initial diameter; h_0 is initial height.

Fig. 8. Load-deflection curves

the applied stress, deformation at midheight is plastic, whereas it is still elastic near the specimen/platen interface. The ratio of the elastically strained material to the plastically strained material increases as the specimen height decreases, so that barreling increases during the course of a test. The unfortunate consequence of barreling is that specimens selected for easy axial alignment are the same specimens that show extensive barreling and for which the internal stresses in the material have a large biaxial component. Therefore, some compromise must be made in selecting specimen dimensions. A height-to-diameter ratio of about 3 to 1 often is selected to minimize buckling that occurs due to bending loads generated by nonaxial alignment of the load.

Because of the increasing contact area and the elastically strained material near the platen, the load-deflection curve bends upward as the specimen decreases in height (Fig. 8). A dramatic increase in load occurs if the elastically strained regions of Fig. 7 overlap.

Due to the presence of frictional forces, the pressure distribution across the specimen is not uniform, as shown in Fig. 9. The pressure distribution is given by:

$$p = \sigma_0 \exp[(2\mu/h)(r - x)]$$

where p is pressure, σ_0 is yield stress, μ is coefficient of friction, r is cylinder radius, x is distance from center of cylinder to data point on x-axis, and h is cylinder height.

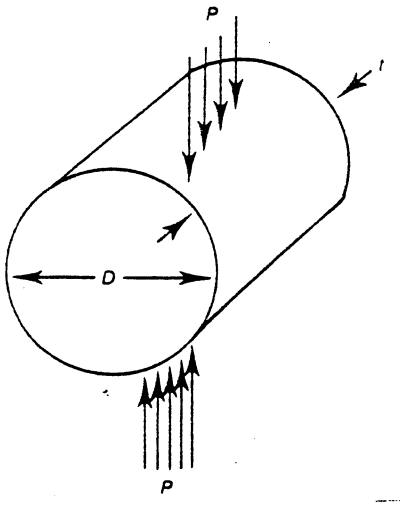

Fig. 9. Line-loaded compression disk

Figure 9 also shows how the pressure distribution changes as the height decreases and as the coefficient of friction changes. The load needed to deform the cylinder can be estimated by multiplying the average pressure on the specimen by the contact area. Figure 9 indicates that the load required to deform materials increases dramatically as the diameter-to-height ratio becomes greater and also increases with a rise in the coefficient of friction. Without overload protection on the load cell, precautions must be taken so that the large loads required to cause plastic flow do not damage the load cell by exceeding its capacity, especially at the large plastic strains characteristic of forming processes.

Coefficients of friction are kept as low as possible to minimize barreling and the development of large loads by providing lubrication at the platen/specimen interface. Two possibilities are the use of lubricating oil and oil grooves in the specimen or platen, or thin Teflon (trademark of DuPont) sheet between the platen and specimen.

An alternative procedure to minimize friction effects and the attendant barreling phenomenon is sequential loading of the specimen—that is, to load until plastic deformation just starts, unload, determine the change in dimensions and relubricate, then reload again until plastic flow initiates.

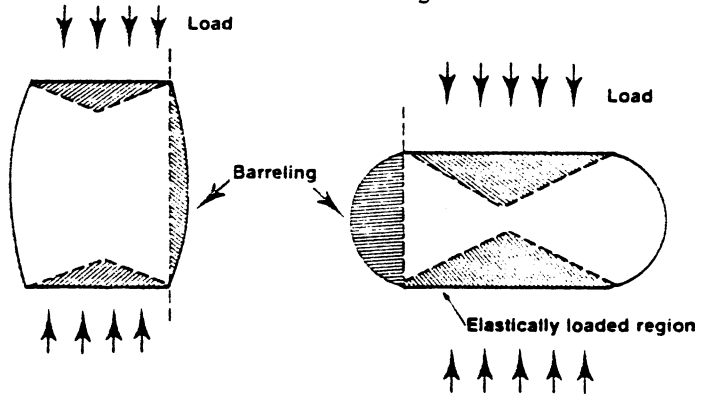

Fig. 7. Elastically loaded region and barreling in a compression specimen for two different height-to-width ratios

This locus of points is then connected to provide a constructed stress-strain curve (Fig. 8).

A tedious but accurate way to determine a true uniaxial compression stress-strain curve is to use a series of specimens having varying l/D ratios. The stress at a given height reduction is then determined for each l/D ratio, plotted as a function of l/D ratio, and extrapolated to an l/D ratio of 0. This might be done at only one value of offset (i.e., corresponding to 0.2% strain) to provide a true flow stress, or a complete curve could be constructed. This procedure is illustrated in Fig. 8 and described in detail in Cook and Clarke (Ref 1).

ASTM STANDARDIZED TESTS

ASTM Method E9 gives the standard procedures for room-temperature compression testing; for elevated-temperature testing, ASTM E209 provides the standard recommended practice. For the high-temperature tests, ASTM E209 specifies that a lubricant, such as molybdenum disulfide or graphite, should be used.

LINE-LOADED COMPRESSION TESTING

For the line-loaded test, a flat disk is loaded, as in Fig. 9. If the disk is of brittle material so that fracture occurs before plastic flow initiates, the thickness of the disk does not affect the calculated stress to cause fracture. The tensile stress at fracture for this case is calculated by:

$$s = \frac{2P}{\pi Dt}$$

where s is maximum tensile stress, P is applied load, D is specimen diameter, and t is specimen thickness. This test is known as the "Brazilian test" and is routinely applied to determine the tensile strength of rocks. More detailed information can be found in Jaeger and Cook (Ref 2).

PLANE-STRAIN COMPRESSION TESTING

The common forming operations—rolling, swaging and forging—are forming operations in which there is little or no change in dimension in one direction. For example, in rolling, a decrease in thickness is converted into an increase in length with little increase in width. Such a state of strain is then two dimensional: it is planar strain. Plane-strain deformation is referred to when the development of a local neck is discussed, and in that case the plane-strain deformation occurred due to an internal state of strain in the body. Two loading situations that develop plane-strain deformation are illustrated here; one in which the plane-strain deformation is developed due to external constraint on the flowing material, and a second, in which the constraint is developed internally in the material.

In Fig 10(a), metal can flow in the x and z directions due to the applied stress in the z direction, but cannot flow in the y direction because of the die wall. In Fig. 10(b), the load P causes flow in the z and y directions, but flow occurs in the x direction if the x dimension or the width-to-thickness ratio of the sheet is large. This is because the material not under the die has no load imposed on it and, therefore, has no tendency to spread in either the x or y direction. Therefore, this unloaded material restrains flow of the material in the x direction (but not the y direction) under the die. There is net flow in the y direction, because the unloaded material is simply pushed out by the expanding material under the die. Plane-strain conditions are realized when the width-to-thickness ratio is about 10 to 1. Because of frictional forces under the die, the b/t ratio should be held to between 2 to 1 and 4 to 1. If large decreases in thickness are obtained in the test, sequential loading with a change in die dimension is necessary to maintain this ratio. In any event, it is again possible to construct a stress-strain curve.

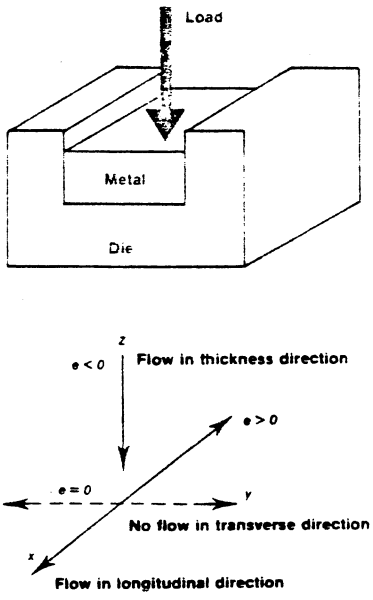

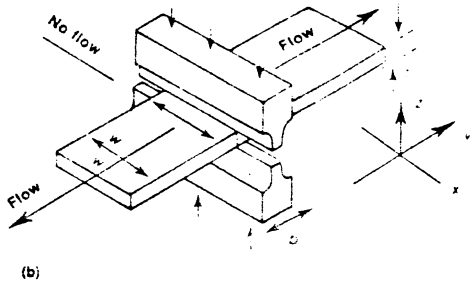

(a) Plane-strain compression of a block in a die. (b) Indenting dies for plane-strain compression testing. Source: *Mechanical Treatment of Metals*, by R. N. Parkins, American Elsevier, New York, 1968, p 22.

Fig. 10. Plane-strain compression

Because the strains are large, true stresses and strains frequently are calculated rather than the nominal stresses and strains. The stress and strain developed in the plane-strain compression test are then given by:

$$\sigma_T = \frac{\text{load}}{\text{area}} = \frac{P}{(w)(b)}$$

and

$$\epsilon_T = \ln \frac{t}{t_0}$$

Although not derived here, the mean stresses and the strain in the load direction in plane-strain deformation are related to the stress and strain developed in a uniaxial compression test of a cylinder by:

$$\sigma_{\text{plane strain}} = 1.15\sigma_{\text{uniaxial compression}}$$

and

$$\epsilon_{\text{plane strain}} = 1.15\epsilon_{\text{uniaxial compression}}$$

Therefore, stresses and strains measured in the plane-strain compression test must be divided by the factor 1.15 if an equivalent curve for uniaxially loaded material is to be constructed or if the data are to be compared with data obtained in a uniaxial test.

UPSET TESTING

Bulk forming processes, such as forging, extrusion and rolling, are also evaluated for formability by upset testing. In the simplest form of this test, a short cylinder is flattened (upset) into a pancake shape. The bulging at the edges pro-

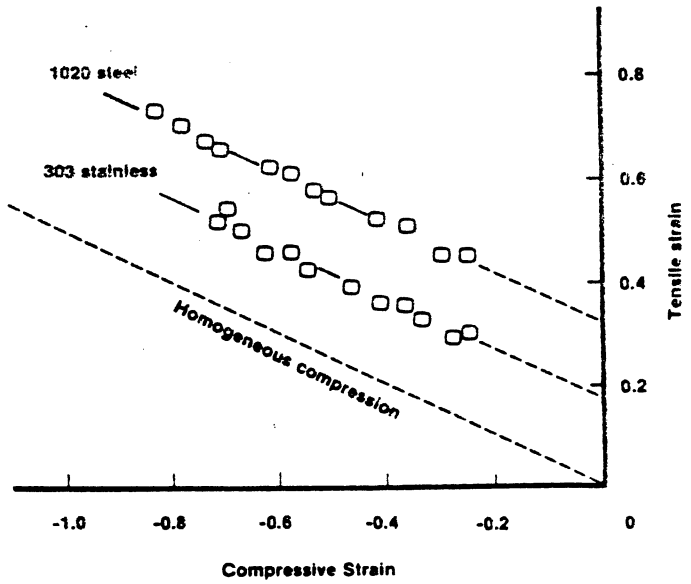

Fig. 11. Fracture-locus lines

duces tensile stresses that cause fractures. Workability is evaluated by determining the largest deformation that can be achieved without producing edge cracking. More typical, however, is use of the hot upset test over a range of temperatures to establish the working temperature that minimizes fracture.

A precision upset test has been developed to determine the three-dimensional analog of the forming-limit diagram. If grid lines are electroetched on the surfaces of small cylinders, then the compressive axial strain (ϵ_z) and the tensile hoop strain (ϵ_θ) at which fracture occurs can be determined. By varying the length-to-diameter ratios (L/D) of the cylinders and the lubrication at the cylinder ends, a wide range of stress states can be developed. By observing the strain in the upset cylinder at which surface fracture just occurs for each of the stress states, a fracture-locus line can be established (Fig. 11). For any combination of strains below the fracture-locus line, fracture has not yet occurred and the condition is safe. When the strain path crosses the fracture line, surface fracture has occurred. This helpful procedure in predicting the bulk formability of metals is discussed by Kuhn (Ref 3) and by Hosford and Caddell (Ref 4).

REFERENCES

1. Cook and Clarke: *J. Inst. Met.*, Vol 71, 1945, p 371
2. *Fundamentals of Rock Mechanics*, 3rd Ed., by J. C. Jaeger and N. G. W. Cook: Chapman and Hall, London, 1979, p 169
3. H. A. Kuhn: in *Formability Topics—Metallic Materials*, ASTM STP 647, 1978, p 206
4. *Metal Forming: Mechanics and Metallurgy*, by W. F. Hosford and R. M. Caddell: Prentice Hall, Englewood Cliffs, NJ, 1983, p 247

Fracture Testing

THE MOST IMPORTANT fracture tests can be grouped into two categories: impact tests and fracture-toughness tests. However, the variety of service circumstances—different types of materials, differing crack morphologies, differing environments and loading rates, effects of size—have spawned a large number of fracture tests, some highly specialized. The most common impact tests are the Charpy test and the Izod test. Both are used primarily for low- and medium-strength materials (typically steels). These materials may break at stresses either above or below yield, depending on the circumstances (temperature, size of crack, etc.). Fracture-toughness tests are intended primarily for medium- and high-strength materials that may break at below-yield stresses, if a crack or other sharp flaw—often quite small—is present. Fracture-toughness tests are based on the theoretical developments of fracture mechanics and give results that can be directly used in calculations relating the size of cracks to applied loads and stresses. In fracture-toughness tests, unlike in impact tests, loads are normally applied relatively slowly—at about the same rate as in an ordinary tension test—and temperature need not be of concern. Although fracture-toughness tests can be conducted in a tension-test machine, the specimen looks quite different. Generally, it is a plate containing a crack grown from a machined notch, rather than the smooth round bar used in tension testing.

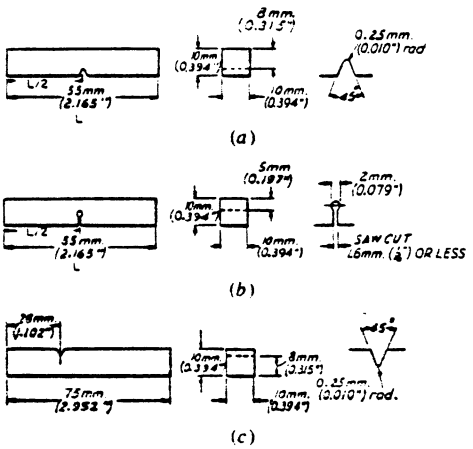

(a) Simple beam V-notch Charpy specimen. (b) Simple beam keyhole-notch Charpy specimen. (c) Cantilever beam notched Izod specimen. Source: Notched Bar Impact Testing of Metallic Materials, E23-81, ASTM, Philadelphia, 1981.

Fig. 1. Notched-bar impact-test specimens

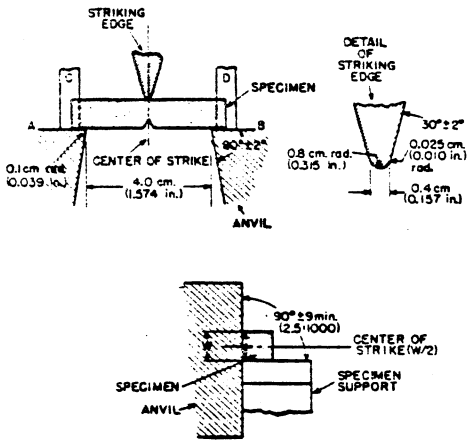

Fig. 2. Setup and specimen for Charpy impact testing

Impact Testing

IMPACT TESTS feature a high but generally indeterminate rate of loading, typically generated by a swinging pendulum or falling weight. The results are not directly related to the stresses and deformations normally calculated during the course of engineering analysis and design, although the results may relate to the temperatures experienced in service. In general, impact-test results have significance based on empirical correlations with service experience, or as a means of comparing materials. The Charpy test is most commonly used to evaluate the effects of metallurgical processes on dynamic mechanical properties. Another test, the Izod impact test, employs a cantilevered specimen hit by a swinging pendulum.

CHARPY TESTS

Specimens used for Charpy tests come in several different configurations. Two examples are the V-notch test specimen, containing a shallow 45° machined notch as a stress concentrator, and the Charpy keyhole specimen, with a stress raiser that looks something like a keyhole (Fig. 1a and b). The V-notch test is the more common of the two tests.

Charpy tests have the virtue of being simple and inexpensive. Furthermore, the specimen is small—also one of the limitations of the test—and Charpy testing machines are widely available. The principal application is for delineating the transition-temperature region in low- and medium-strength steels; in the common test sequence, a series of nominally identical specimens is broken at different temperatures. (Occasionally this test is used for materials other than low- and medium-strength steel.) Material specifications often include required levels of Charpy test performance, but the results of the test have limited fundamental significance. Results only have meaning in terms of correlations with ductile or brittle behavior under service conditions based on actual experience. However, because Charpy tests have been employed for so many years, a good deal of this experience is available in the form of general rules that can be exploited by designers.

Figure 2 illustrates the Charpy bar supported at its ends and struck on the surface opposite the notch so that the loading is three-point bending. The source of the blow is a heavy, swinging pendulum, as can be seen in Fig. 3, with a range of 25 to 240 ft · lb (35 to 325 J) of energy at impact. The weight and height of the pendulum striking head may be modified to produce various foot-pounds (joules) of energy. Testing-machine and specimen details, along with test procedures, are standardized, as described in ASTM E23.

Machining of specimens should be controlled to provide specimen uniformity. The orientation of the bars, with respect to the rolling direction, often has considerable effect on impact behavior.

In its simplest form, a Charpy test is conducted by inserting a specimen into the machine, cocking the pendulum and releasing it to fracture the test bar. Typically, a series of tests is performed at different temperatures. Charpy machines should be periodically checked against standardized specimens to determine their accuracy.

A dial on the machine indicates the energy absorbed in fracturing the specimen (Fig. 3). The test is scaled so that specimens made of virtually any material will be broken by the impact. A small proportion of the initial potential energy of the pendulum is absorbed in overcoming air resis-

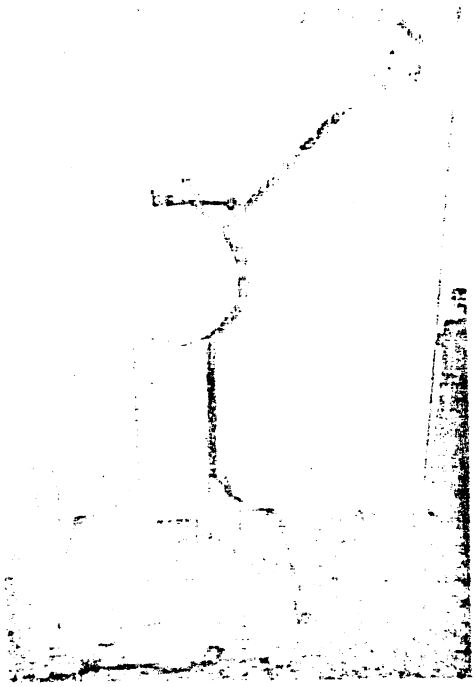

Photographed at American Society for Metals, Metals Park, OH.

Fig. 3. Standard impact-testing machine

tance; this amount, usually $^1/_2$ to 1 ft · lb (0.7 to 1.5 J), can be determined by operating the machine without a specimen in place. Note that the commonly used machine is entirely manual in operation, with no instrumentation beyond the dial. The dial simply gages the height of the pendulum after it has swung through the specimen. The pendulum carries a great deal of energy even after fracturing a specimen and must be treated with respect; safety measures should always be taken. Injury may result if a guard shield is not in place during the pendulum swing. The shield is intended to prevent bodily access during test motion.

In addition to data on energy absorbed, two other quantities are commonly determined for each impact-test specimen. First, the percentage of fibrous fracture area visible on the cross section of the broken specimen is compared with the percentage of cleavage area. Second, the lateral contraction of the broken bar at the root of the notch is measured.

Figure 4 shows a series of fracture surfaces from Charpy V-notch tests at different temperatures. The fracture surface is entirely fibrous in appearance above the transition-temperature region, indicating ductile behavior; it is entirely cleavage below. In the transition region, small decreases in temperature increase the percentage of cleavage fracture. As Fig. 4 shows, the texture difference between fibrous and cleavage regions makes identification straightforward for specimens (such as annealed low-carbon steel) which fail by cleavage at low temperatures. The percentages can be estimated visually or, if more precision is needed, the fracture surfaces can be photographed and further analyzed. Note that in the transition region, cleavage takes place in the center of the specimen, with fibrous fracture near the outer surfaces of the bar. This is a result of the differing states of stress in the interior and near the surface. The inner material is constrained against plastic deformation and more likely to fracture by cleavage.

Notch-root contraction, measured as indicated in Fig. 5, is also a direct indication of fracture behavior—in this case, of the amount of plastic deformation accompanying the fracture. The contraction is usually easiest to measure with a micrometer caliper. The thickness of the unbroken specimen at the notch root should be measured *before* the test.

The energy absorbed and the fracture-surface appearance are the most commonly specified results of the Charpy test. For example, steels for certain applications may be required to have a certain minimum level of energy absorption—

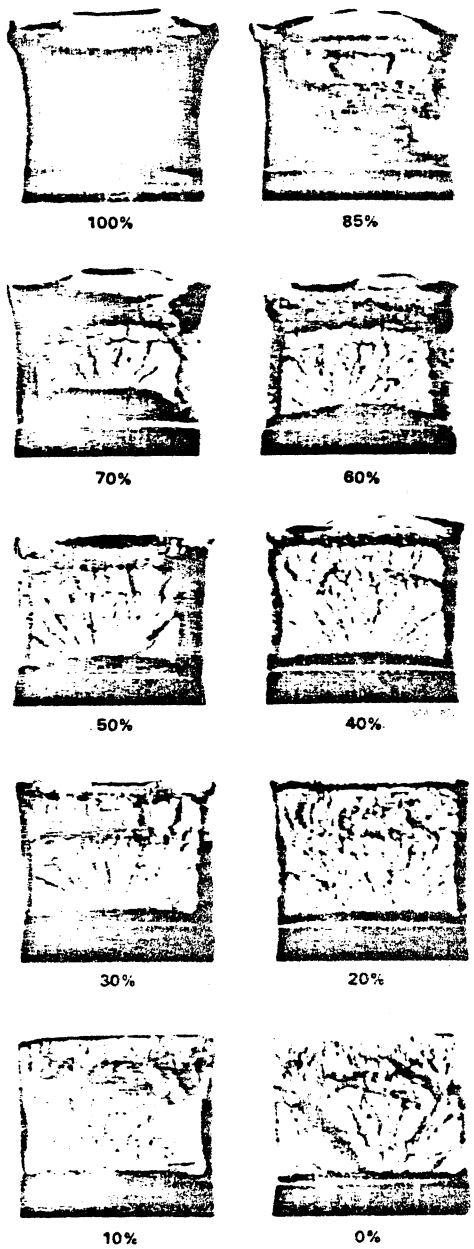

Source: Army Materials and Mechanics Research Center, Watertown Arsenal.

Fig. 4. Series of fractographs of Charpy V-notch specimens of 4340 steel tested at different temperatures, showing the change in appearance and estimated percentages of fibrous fracture

10 or 15 ft · lb (15 or 20 J) are common values—at the lowest expected service temperature. Alternately, some minimum percentage of fibrous fracture (e.g., 50%) may be required. Again, note that such requirements have no intrinsic significance and can only be defined based on correlations with service experience.

The energy absorbed in impact, percentage of fibrous fracture, and notch-root contraction can be plotted against temperature to determine the ductile-to-brittle transition temperature. However, the particular definition of the ductile-to-brittle transition temperature must be clearly specified in the data report.

The standard Charpy impact test yields direct readings only of the energy absorbed. "Instrumented" tests make use of testing machines with auxiliary sensors to acquire other data, typically load data. A specially made striking tup instrumented with strain gages can give a load-time history that allows initiation of the crack from the machined notch to be distinguished from propagation of that crack through the specimen. This is a relatively specialized test that is utilized for specific limited applications. The advantages of the basic Charpy test—small specimen size and low cost—are retained, while allowing fracture-mechanics parameters such as toughness to be estimated under specific circumstances.

THE IZOD TEST

The Izod test is a cantilever-beam test as compared to the simple-beam Charpy test. As shown in Fig. 6, the Izod specimen is held in a fixture with the V-notch facing the striking anvil of the pendulum. The center of the V-notch is in the same plane as, and parallel to, the supporting fixture. The actual fracture test is performed in the same manner as the Charpy test, and data on energy consumed are reported in foot-pounds (joules). The Izod test does not lend itself to variable-temperature testing because of the appreciable time required to place and clamp the specimen, which results in rapid temperature change due to specimen and fixture contact. Izod tests are generally specified for materials tested at room temperature and where the engineering part is designed to operate under cantilever loading.

DYNAMIC TEAR TESTS

Dynamic tear tests and drop-weight tear tests come in several varieties, two of which have been standardized by ASTM. All are similar to the Charpy test in the use of the kinetic energy of a swinging pendulum (or occasionally a falling weight) to break an artificially notched test specimen. In essence, they are larger versions of the Charpy test, with test specimens that are both thicker and wider to represent the fracture behavior of thick-section structural materials. While the Charpy test is used almost exclusively to investigate the transition-temperature behavior of low- and medium-strength steels, dynamic tear (DT) tests can be used as well for high-strength steels and for aluminum and titanium alloys. When such materials are broken in a Charpy machine, the energy absorbed is typically so low, compared to the testing machine's capacity, that little meaningful information can be obtained. The larger DT specimen allows different alloys and heat treatments to be more reliably compared.

Typical DT specimens are shown in Fig. 7. The larger specimen is used only where full-

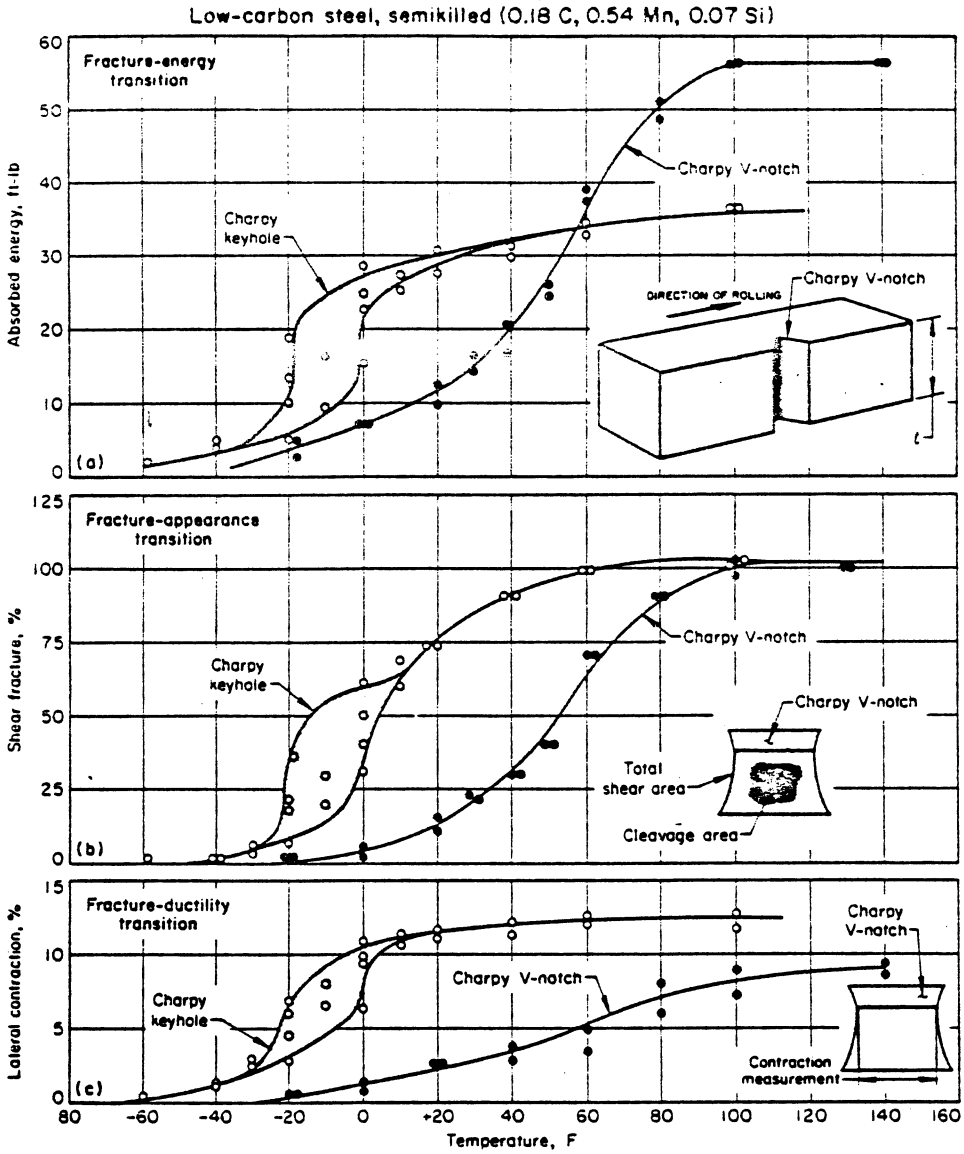

Tests determined by (a) fracture energy, (b) fracture appearance and (c) fracture ductility. The drawings of the Charpy V-notch specimens at lower right in the graphs indicate: (a) orientation of the specimen notch with plate thickness, t, and direction of rolling; (b) location of the total fibrous area and cleavage area on the fracture surface; and (c) location of the contraction measurement in this series of tests. Percentage of fibrous fracture and lateral contraction were based on the original dimensions of the specimen.

Fig. 5. Characteristics of the transition-temperature range of Charpy V-notch and Charpy keyhole tests of low-carbon steel plate

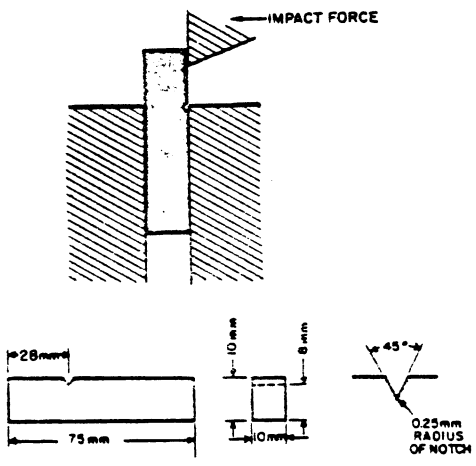

Fig. 6. Setup and specimen for Izod impact testing

thickness tests representative of actual structures must be undertaken.

As in a Charpy test, the basic information obtained from a DT test is the energy absorbed in breaking the specimen, although fracture-surface appearance and the extent of plastic deformation near the fracture can also be useful.

The two varieties of ASTM standard dynamic tear or drop-weight tests have the designations E436 (Drop-Weight Tear Tests for Ferritic Steels) and E604 (Dynamic Tear Energy of Metallic Materials). As the names imply, the purposes are quite different, even though the general features are similar.

The E436 drop-weight tear test uses a specimen, normally of the actual thickness of the steel plate being investigated, with an easily produced, pressed notch (see ASTM E436 for details). The test is used only for steels, and indicates the transition temperature between ductile and brittle behavior. To this end, specimens are

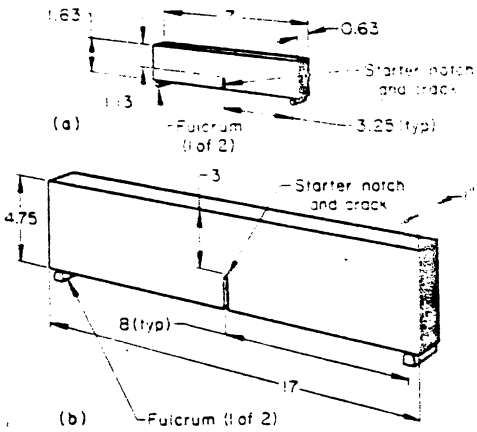

In the specimens, a crack with a sharp tip is produced by making a brittle electron beam weld or by pressing with a knife edge. With either method of providing the crack tip, and with either size of specimen, maximum-constraint conditions are attained. Dimensions are in inches.

Fig. 7. Two sizes of the standard specimen for the Naval Research Laboratory standardized dynamic tear test

tested at increasing (or decreasing) temperatures until the crack propagates as a fully developed fibrous fracture away from the notch (it makes no difference if the crack initiates by a cleavage mechanism). This is determined by visual examination of the fractured specimen; no quantitative data need be gathered. Thus, the test is simple and inexpensive. It is used primarily for quality control purposes on structural steels—notably, for pipeline applications.

The ASTM E604 test differs, as the name "Dynamic Tear Energy of Metallic Materials" implies, in two fundamental ways:

1. The energy absorbed in fracturing the specimen is measured.
2. The test can be used on materials other than steels.

The standard dimensions of the specimen are less than for either of the specimens shown in Fig. 7; the notch is machined, and the specimen is always $^3/_8$ in. (15.9 mm) thick. Tests can be conducted at a fixed temperature to compare several materials, or over a range of temperatures to investigate transition-temperature effects. Considerable effort has gone into correlating DT test results with plane-strain fracture-toughness values, because the more sophisticated testing procedures required for the latter are more costly and time consuming. In some cases, the DT test can be used to estimate plane-strain toughness.

DROP WEIGHT TEST

As the name implies, in a drop weight test (DWT) the specimen is broken by a falling weight rather than by a pendulum (Fig. 8). However, the essential difference between this test and those described earlier is that it provides the operational definition of an important parameter termed the nil-ductility temperature (NDT). The NDT is the highest temperature at which a particular steel is likely to fracture in brittle fashion by cleavage. Above this temperature, the fracture will be accompanied by some macroscopic plastic flow associated with fibrous fracture and a microvoid-coalescence process on the microscale. The DWT

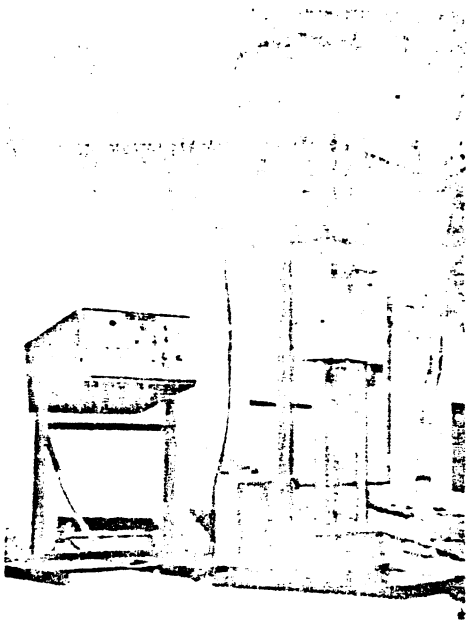

Fig. 8. Drop weight test equipment

procedure does not, however, require interpretation of the fracture appearance, nor must any quantitative data be gathered beyond the temperature of the specimen. As the definition of the term NDT implies, the test is used only for low- and medium-strength steels that show a cleavage-fibrous transition as the temperature is increased.

The DWT also has been standardized by ASTM (E208). The specimen is a flat plate with a hard-surfacing weld bead deposited on one side, as shown in Fig. 9. The brittle weld is notched to act as a crack-starter. The fixture for DWT tests holds the specimen with the notched weld facing downward so that the falling weight will load the specimen in bending. The weld is thus on the tensile surface, and the specimen is backed up so that it can bend only a limited amount (approximately 5°). Well below the NDT, a DWT will produce complete fracture (Fig. 9). Well above the NDT, the specimen will bend elastically and plastically but will not break. The NDT, as defined by this test, is the temperature at which a crack starting at the notched hard-surfacing weld propagates to one or both edges of the tensile surface of the specimen. To conduct a DWT series, specimens are tested over a range of temperatures; the operationally defined NDT is the highest of these temperatures at which the specimen "breaks," according to this definition. The NDT is a widely applied parameter for structural steels—referenced, for example, in the ASME Boiler and Pressure Vessel Code.

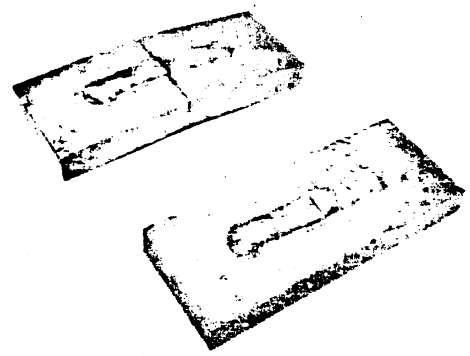

Fig. 9. Fracture appearance of drop weight nil-ductility transition specimens

Fracture-Toughness Testing

By J. H. Underwood, U.S. Army Armament Research and Development Command, and W. W. Gerberich, University of Minnesota

CONCEPTS OF FRACTURE MECHANICS

The concepts of fracture mechanics are basic ideas for developing methods of predicting the load-carrying capabilities of structures and components containing cracks. The concepts deal with basic quantities or parameters of fracture mechanics. These quantities can be discussed in relation to a simple example: a center crack in a plate remotely loaded by a uniform tensile stress (see Fig. 10). When the half-crack length, a, is less than 10% of the total plate width, the relationship among stress-intensity factor, K, applied stress, σ, and half-crack length, a, is very close to the relationship for a crack in an infinitely wide plate, which is:

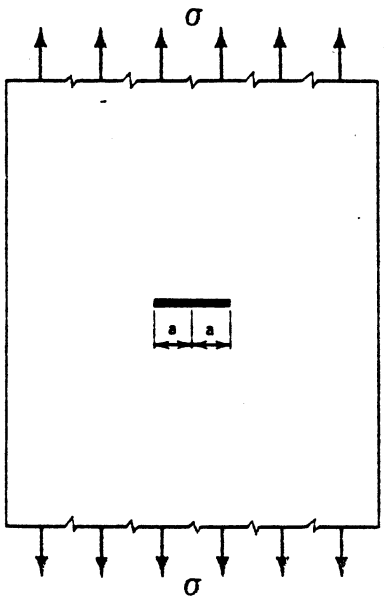

σ is remotely applied uniform tensile stress; a is half-crack length.

Fig. 10. Schematic illustration of a center crack in a wide plate

$$K = \sigma\sqrt{\pi a} \qquad \text{(Eq 1)}$$

The stress applied to the component, the length of the crack, and the stress-intensity factor in the loaded component with a crack are the basic quantities of fracture mechanics. The example in Fig. 10 also provides a simple explanation for the units of stress-intensity factor—i.e., the product of stress and square root of length. But more important is the concept that the stress-intensity factor, K, is a single parameter which includes both the effect of the stress applied to a specimen and the effect of a crack of a given size in a specimen. Still using the example of Fig. 10, if the combination of σ and a in Eq 1 were to exceed a critical value of K, then the fracture strength of the plate would be exceeded and the crack would be expected to propagate by one of the several mechanisms mentioned in this article.

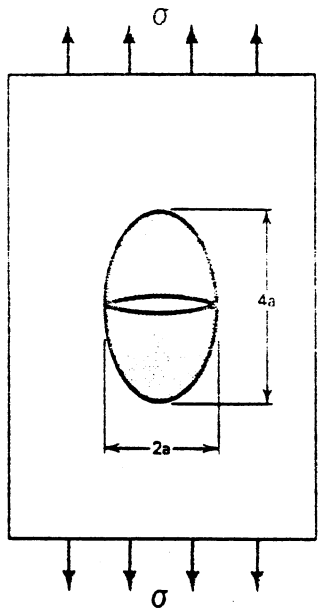

Fig. 11. Schematic illustration of the concept of energy release around a center crack in a loaded plate

Energy-Release Rate

The origins of modern-day fracture mechanics may be traced to Griffith (Ref 1), who established an energy-release-rate criterion for brittle materials. Observations of the fracture strength of glass rods had shown that the longer the rod, the lower the strength. Thus the idea of a distribution of flaw sizes evolved, and it was discovered that the longer the rod, the larger the chance of finding a large natural flaw. This physical insight led to an instability criterion which involved the elastic energy released in a solid at the time a flaw grew catastrophically under an applied stress.

From the theory of elasticity comes the concept that the strain energy contained in an elastic body per unit volume is simply the area under the stress-strain curve, or:

$$U_0 = \frac{\sigma^2}{2E} \qquad \text{(Eq 2)}$$

where σ is the applied stress and E is Young's modulus. However, there is a reduction (that is, a release) of energy in an elastic body containing a flaw or a crack because of the inability of the unloaded crack surfaces to support a load. We shall assume that the volume of material whose energy is released is the area of an elliptical region around the crack (as shown in Fig. 11) times the plate thickness, B; the volume is $\pi(2a)\,(a)B$. This is based on the area of an ellipse being $\pi r_a r_b$, where r_a and r_b are the major and minor radii of the ellipse. Then, the total energy released from the body due to the crack is the energy per unit volume times the volume, which is:

$$U = \pi(2a)(a)B\,\frac{\sigma^2}{2E} = \frac{\pi\sigma^2 a^2 B}{E} \qquad \text{(Eq 3)}$$

In ideally brittle solids, the released energy can be offset only by the surface energy absorbed, which is:

$$W = (2aB)(2\gamma_s) = 4aB\gamma_s \qquad \text{(Eq 4)}$$

where 2aB is the area of the crack and $2\gamma_s$ is twice the surface energy per unit area (because there are two crack surfaces).

Griffith's energy-balance criterion, in the simplest sense, is that crack growth will occur when the amount of energy released due to an increment of crack advance is larger than the amount of energy absorbed:

$$\frac{dU}{da} \geq \frac{dW}{da} \qquad \text{(Eq 5)}$$

Performing the derivatives indicated in Eq 5 and rearranging give the Griffith criterion for crack growth:

$$\sigma\sqrt{\pi a} = \sqrt{2E\gamma_s} \qquad \text{(Eq 6)}$$

Fracture theory was built upon this criterion in the early 1940's by considering that the critical strain-energy-release rate, G_c, required for crack growth was equal to twice an effective surface energy, γ_{eff}:

$$G_c = 2\gamma_{eff} \qquad \text{(Eq 7)}$$

This γ_{eff} is predominantly the plastic energy absorption around the crack tip, with only a small part due to the surface energy of the crack surfaces. Then, with the development of complex variable and numerical techniques to define the stress fields near cracks, this energy view was supplemented by stress concepts—that is, the stress-intensity factor, K, and a critical value of K for crack growth, K_c. Replacing γ_s with γ_{eff} in Eq 6 and noting that the energy and stress concepts are essentially identical (that is, $K = \sqrt{EG}$) give:

$$K_c = \sqrt{EG_c} = \sigma\sqrt{\pi a} \qquad \text{(Eq 8)}$$

which is the crack-growth-criterion equivalent of Eq 1. Thus, K_c is the critical value of K which, when it is exceeded by a combination of applied stress and crack length, will lead to crack growth. For thick-plate plane-strain conditions, this critical value became known as the plane-strain fracture toughness, K_{Ic}, and any combination of applied stress and crack length that exceeds this value could produce unstable crack growth, as indicated schematically in Fig. 12(a) (linear-elastic).

In work with tougher, lower-strength materials, it was later noted that stable slow crack growth could occur even though accompanied by considerable plastic deformation. Such phenomena led to the nonlinear J-integral and R-curve concepts which could be used to predict the onset of stable slow crack growth and final instability under elastic-plastic conditions, as noted in Fig. 12(b). Finally, the fracture-mechanics approach was applied to characterize subcritical-crack-growth phenomena where time-dependent slow crack growth, da/dt, or cyclic crack growth, da/dN, may be induced by special environments or fatigue loading. For combinations of stress and crack length above some environmental threshold, K_{Iscc}, or fatigue threshold, ΔK_{th}, subcritical growth occurs, as indicated in Fig. 12(c).

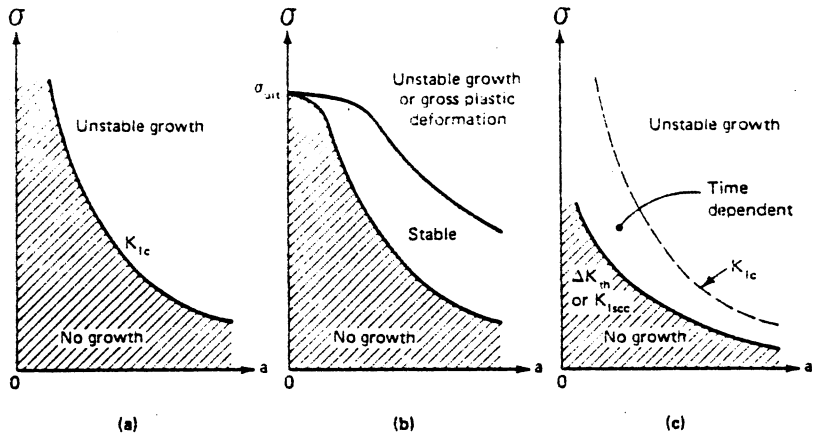

(a) Linear-elastic. (b) Elastic-plastic. (c) Subcritical.

Fig. 12. Relationships between stress and crack length, showing regions and types of crack growth

Assumptions

Additional concepts of fracture mechanics have evolved which are related to the assumptions made in using linear-elastic fracture mechanics. Three assumptions basic to fracture-mechanics analysis are as follows:

1. Cracks exist in the body to be analyzed. Indeed, cracks, or flaws with cracklike behavior, are frequently present in real structural materials.
2. A crack can be represented by a flat, free surface in a linear-elastic, homogeneous, isotropic continuum.
3. A characteristic stress field surrounds any crack in a loaded body. The magnitude of this field, the K value, at the onset of crack extension is a material property which is independent of specimen size and geometry for many conditions of loading and environment.

Stress-Intensity Factor. The second assumption given above makes possible a mathematical description of the stresses in the vicinity of the crack tip. This assumption of a crack in a linear-elastic solid at first appears contradictory to what is known about fracture of metals, because some plastic deformation is always found to accompany fracture. However, when the region of plastic deformation around the crack is small compared with the size of the crack, which often is true with large structures and with high-strength materials, this is a good assumption. Using linear-elastic theory and referring to Fig. 13, the stress at a point P near the crack tip can be expressed as:

$$\sigma_y = \frac{K_I}{\sqrt{2\pi r}} \cos\frac{\theta}{2}\left(1 + \sin\frac{\theta}{2}\sin\frac{3\theta}{2}\right) \qquad \text{(Eq 9)}$$

where σ_y is the stress perpendicular to the crack plane, r is the distance from the crack tip to point P, θ is the angle between the crack plane and the line from point P to the crack tip, and K_I is the applied opening-mode stress-intensity factor. In Eq 9, as the distance from the crack tip, r, approaches zero, the stress, σ_y, approaches infinity. This $1/\sqrt{r}$ singularity cannot actually occur, because plastic deformation relieves elastic stresses very near the crack tip. Nevertheless, in many cases the $1/\sqrt{r}$ singularity provides an adequate over-all description of the stresses near the crack tip and therefore a good description of the conditions for crack growth.

The important implications of Eq 9 are: (*a*) a crack in a loaded component or specimen generates its own intensified stress field near the crack tip, a stress field that differs from another crack-tip stress field only by the scaling factor represented by K; and (*b*) the factor K expresses how much the stress intensifies at the crack tip, and thereby allows the loading and geometry factors that influence crack growth in a specimen to be described on a uniform basis using a single parameter.

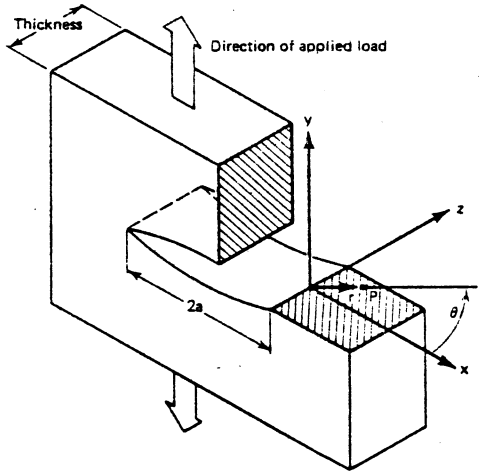

x is the direction perpendicular to the crack tip and in the plane of the crack; y is the direction perpendicular to the plane of the crack; z is the direction parallel to the crack tip; P is a point near the crack tip; r is the distance from the crack tip to point P; θ is the angle between the plane of the crack and a line from point P to the crack tip; a is half-crack length.

Fig. 13. Schematic illustration of a through-thickness crack

The stress-intensity factor, K, can have a simple relation to applied stress and crack length, as in Eq 1. But, more often, the K relation is of greater complexity because of complex loading, various configurations of real structural components, or variations in crack shapes. The K relations for many different types of loading and specimen and crack geometries have been obtained by various experimental and analytical methods. Two handbooks that give a variety of K relations are listed as Ref 2 and 3. These handbooks give K relations for the three basic types of crack-face displacement shown in Fig. 14. Nearly all crack-related fracture processes of practical significance for metals involve mode I, opening-mode deformation, in which the dis-

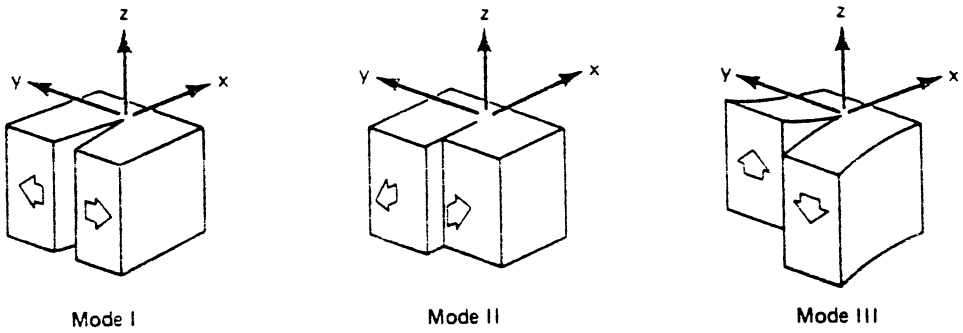

Mode I—opening mode: tension stress in y direction (perpendicular to crack surfaces). Mode II—edge-sliding mode: shear stress in x direction (perpendicular to crack tip). Mode III—screw-sliding mode: shear stress in z direction (parallel to crack tip).

Fig. 14. Modes of crack deformation

placement of the crack faces is in a direction perpendicular to the crack plane. There are cases in which shear deformation by modes II and III accompanies opening-mode deformation, but shear deformation often has little significant effect on the over-all, macroscopic fracture process.

Fracture Toughness. The third assumption given above states that for many test conditions the magnitude of the stress field, K, at the onset of crack extension is a material constant. Tests on precracked specimens of a wide variety of materials have shown that the critical K value at the onset of crack extension approaches a constant value as specimen thickness increases. Figure 15 shows this effect in tests with AISI 4340 steel specimens over a range of thickness (Ref 4). In general, when the specimen thickness and the in-plane dimensions near the crack are large enough relative to the size of the plastic zone, then the value of K at which growth begins is a constant and generally minimum value called the plane-strain fracture-toughness factor, K_{Ic}, of the material. The parameter K_{Ic} is a true material property in the same sense as is the yield strength of a material. The value of K_{Ic} determined for a given material is unaffected by specimen dimensions or type of loading, provided that the specimen dimensions are large enough relative to the plastic zone to ensure plane-strain conditions around the crack tip (strain is zero in the through-thickness or z-direction).

Plane-strain fracture toughness, K_{Ic}, is directly related to the energy required for the onset of crack propagation by the formula:

$$K_{Ic} = \sqrt{\frac{EG_{Ic}}{1 - \nu^2}} \qquad \text{(Eq 10)}$$

where E is the elastic modulus (in MPa or psi), ν is Poisson's ratio (dimensionless), and G_{Ic} is the critical plane-strain energy-release rate for crack extension (in kJ/m^2 or in.·lb/in.^{2}). In simplified concept, G_{Ic} is the critical amount of strain energy that is released from the elastic stress field of the specimen per unit area of new cracked surface for the first small increment of crack extension. The concepts of K_{Ic} and G_{Ic} are essentially interchangeable; K_{Ic} is generally preferred because it is more easily associated with the stress or load applied to a specimen. The value of K_{Ic} for a given material can be measured directly using ASTM Standard Test Method E399 (Ref 5).

Plastic Zone

As mentioned above, under "Stress-Intensity Factor," when the stresses get sufficiently high near the crack tip, plastic deformation must occur. A description of the size of the plastic zone is essential to the understanding of how section size affects the fracture behavior of a specimen or component. The simplest concept is to imagine the point at which σ_y, according to Eq 9, reaches the yield strength of the material. This value of r represents the radius of the plastic zone. This is schematically depicted in Fig. 16; in equation form it is:

$$r_p|_{\theta=0^\circ} = \frac{K_I^2}{2\pi\sigma_{ys}^2} \qquad \text{(Eq 11)}$$

where σ_{ys} is the yield strength. Of course, material at the tip of a crack does not respond simply to the σ_y stress but responds to the complex triaxial state of stress. One yield criterion which has successfully modeled complex states of stress

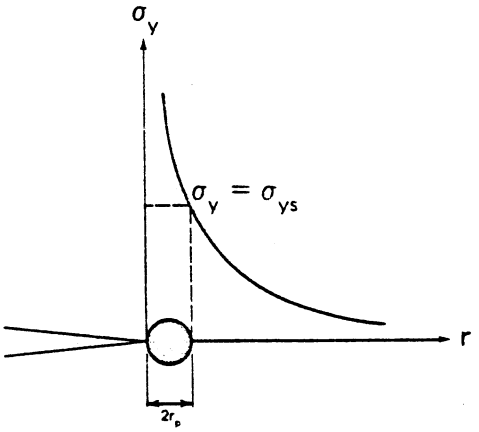

σ_y is the stress perpendicular to the crack plane; σ_{ys} is the yield strength; r is the distance from the crack tip; r_p is the radius of the plastic zone.

Fig. 16. Schematic illustration of plastic zone and stress distribution at a crack tip

in metals is the von Mises or distortional strain energy criterion. Simply stated, yielding is reached under a complex state of stress when the sum of the squares of the principal stress differences is equal to two times the uniaxial tensile yield squared, or:

$$2\sigma_{ys}^2 = (\sigma_1 - \sigma_2)^2 + (\sigma_2 - \sigma_3)^2 + (\sigma_3 - \sigma_1)^2 \qquad \text{(Eq 12)}$$

From linear-elastic theory, all of the values of principal stress may be determined, which for mode I are:

$$\sigma_1 = \frac{K_I}{\sqrt{2\pi r}} \cos\frac{\theta}{2}\left[1 + \sin\frac{\theta}{2}\right] \qquad \text{(Eq 13a)}$$

$$\sigma_2 = \frac{K_I}{\sqrt{2\pi r}} \cos\frac{\theta}{2}\left[1 - \sin\frac{\theta}{2}\right] \qquad \text{(Eq 13b)}$$

$$\sigma_3 = 2\nu\frac{K_I}{\sqrt{2\pi r}} \cos\frac{\theta}{2} \text{ (plane strain)} \qquad \text{(Eq 13c)}$$

$$\sigma_3 = 0 \text{ (plane stress)} \qquad \text{(Eq 13d)}$$

where ν is Poisson's ratio. Combining Eq 12 and 13 gives the elastic-plastic boundary by the inverse method. Although only a first approximation, this approach illustrates the differences between thin-section and thick-section behavior. For plane stress, which would apply to relatively thin

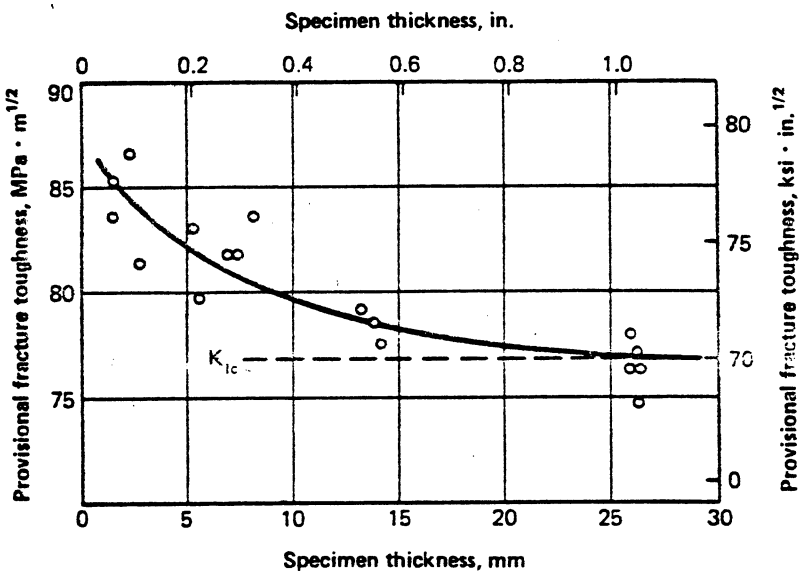

The material was 4340 steel plate that had been hardened and tempered at 400 °C (750 °F) to a yield strength of 1470 MPa (213 ksi).

Fig. 15. Effect of specimen thickness on the critical K value for crack extension in steel specimens (Ref 4)

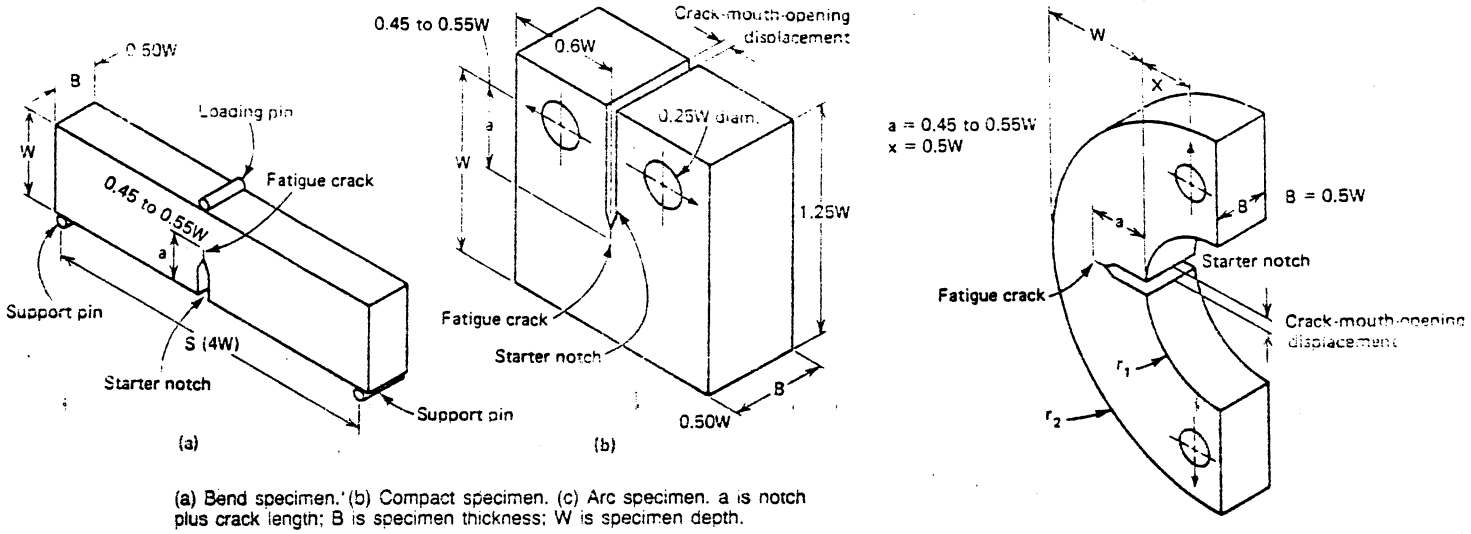

(a) Bend specimen. (b) Compact specimen. (c) Arc specimen. a is notch plus crack length; B is specimen thickness; W is specimen depth.

Fig. 17. Fracture-toughness test specimens

sections having $\sigma_3 = 0$ (stress is zero in the through-thickness direction),

$$r_p \Big|_{\text{plane stress}} = \frac{K_I^2}{2\pi\sigma_{ys}^2}\cos^2\left(\frac{\theta}{2}\right)\left\{1 + 3\sin^2\left(\frac{\theta}{2}\right)\right\}$$

$$\approx \frac{K_I^2}{2\pi\sigma_{ys}^2} \qquad \text{(Eq 14)}$$

which is equivalent to Eq 11 for $\theta = 0°$. However, for thick plates where plane-strain conditions prevail, σ_3 is as given in Eq 13, and now Eq 12 and 13 give:

$$r_p \Big|_{\text{plane strain}} = \frac{K_I^2}{2\pi\sigma_{ys}^2}\cos^2\left(\frac{\theta}{2}\right)\left\{1 + 3\sin^2\left(\frac{\theta}{2}\right) - 4\nu(1-\nu)\right\} \approx \frac{K_I^2}{6\pi^2\sigma_{ys}} \qquad \text{(Eq 15)}$$

For a Poisson's ratio of $\nu = 0.3$, the average plane-strain plastic-zone size is about $^1/_3$ the plane-stress value of Eq 14, considering all values of θ. The important point is that yielding in thick plates is more difficult, the plastic zones are smaller, and hence the energy absorbed around the crack is less.

FRACTURE TEST METHODS

Plane-Strain Fracture Toughness, K_{Ic}

ASTM Method E-399. The first fracture-mechanics test method to become widely accepted in the United States is ASTM Method E399, for measuring plane-strain fracture toughness, K_{Ic}, of metals (Ref 5). Because of this, ASTM E399 is perhaps the most important method to consider in the application of fracture mechanics to selection of structural alloys. In addition, many other test methods use some of the same test specimens and test procedures as those in E399.

Method E399 first appeared in the 1969 ASTM Standards, and the latest revision was in 1981. As discussed previously, ASTM E399 specifies the requirements and procedures for measuring the critical value of the stress-intensity factor, K_{Ic}. The measurement corresponds to at most a 2% extension of a pre-existing fatigue crack in a specimen large enough that plane-strain conditions predominate around the crack. Three types of test specimens which can be used with this method are shown in Fig. 17. They are, in the order in which they were developed for use with E399, the bend specimen, the compact specimen and the arc specimen. These specimens may be taken from plate and other product forms in any of six orientations for various crack-growth directions. These are shown, using the compact specimen as an example, in Fig. 18, which was taken from ASTM E399. For cylindrical products, a similar procedure is used, except that the circumferential and radial (C and R) directions are indicated instead of the long transverse and short transverse (T and S) directions.

The critical dimensions for each of the test specimens are thickness, B, width, W, and overall crack length, a, which includes the machined starter notch and the fatigue precrack. One of the important requirements of this test method is that the specimen thickness, B, and the crack length, a, be at least equal to the quantity $2.5\,(K_{Ic}/\sigma_{ys})^2$, where σ_{ys} is the yield strength of the material. Thus, it is desirable to determine the yield strength and to estimate the K_{Ic} value for any material to be tested by this method before the specimens are prepared. For some materials, often those of lower strength, the dimensions required by the relation $2.5\,(K_{Ic}/\sigma_{ys})^2$ are greater than can be obtained from the available section sizes of material. For such combinations of material and section size, measurement of K_{Ic} is not possible. In these cases, alternative methods of fracture-toughness measurement are necessary, as discussed below, under "Non-Plane-Strain Toughness Tests." When measurement of K_{Ic} *is* possible, the K_{Ic} specimen dimensions should be somewhat greater than the minimum requirements estimated from $2.5\,(K_{Ic}/\sigma_{ys})^2$. For a few materials, notably some aluminum alloys, recent testing (Ref 6) has shown that dimensions about twice as great as those normally required give more consistent K_{Ic} results.

Another important set of requirements for a valid K_{Ic} test involves the fatigue-precracking process. The test results will be valid only if the length of the fatigue crack and the straightness and flatness of the crack are within the prescribed limits. Furthermore, the maximum cyclic load used in producing the fatigue crack must be held below a designated limit to restrict the size of the plastic zone ahead of the fatigue crack.

Once the test specimen has been precracked, the procedure of the K_{Ic} test itself is quite similar to the load-versus-displacement procedure of a standard tension test. The displacement used in the K_{Ic} test is the opening displacement of the notch surfaces at the notch mouth and in the direction perpendicular to the plane of the notch and crack. This displacement is called the crack-mouth-opening displacement (see Fig. 17). A calibrated displacement gage and autographic load-versus-displacement recording equipment are needed to measure and record the test data. Special fixtures with loading pins which are free to rotate during the test are required. This ensures that the same free-rotation loading condition used for the stress and K analysis of the specimens is also present during the test. A load-versus-displacement plot for a high-strength aluminum alloy, which is generally representative of the plots from many steel and aluminum alloys, is shown in Fig. 19 (Ref 7).

Interpretation of the load-versus-displacement plot and calculation of K_{Ic} are described in detail for the various specimen types in ASTM E399. The procedures are described briefly here for the compact specimen. The provisional value of the load at which onset of crack propagation occurs,

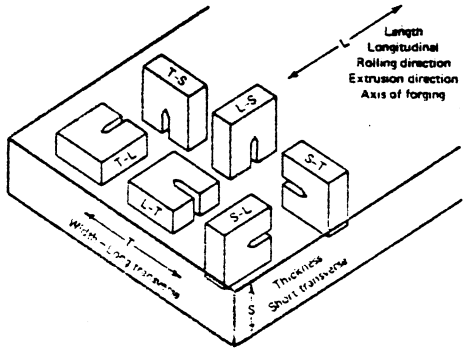

First letter designates the direction perpendicular to the crack plane; second letter designates the direction parallel to the direction of crack growth.

Fig. 18. Orientations of crack plane and direction for fracture specimens taken from rectangular product forms such as plate (from ASTM Method E399)

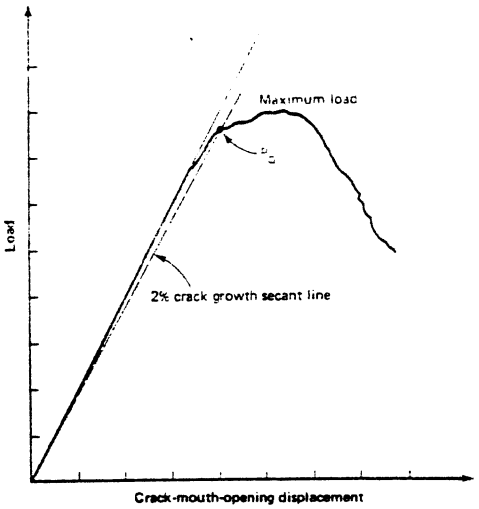

Fig. 19. Load vs crack-mouth-opening displacement typical of high-strength aluminum alloys (Ref 7)

P_Q, is obtained from the test record. The P_Q value is either the maximum load during the test or, more commonly and as shown in Fig. 19, the load corresponding to 2% crack growth as determined by the intersection of a secant line and the plot. The provisional value of the stress-intensity factor, K_Q, is determined by means of equations such as the following, for compact specimens in which K_Q is in units of $MPa \cdot m^{1/2}$ ($psi \cdot in.^{1/2}$):

$$K_Q = (P_Q/BW^{1/2}) \cdot f(a/W) \qquad \text{(Eq 16)}$$

where

$$f(a/W) = \frac{[2 + a/W][0.886 + 4.64a/W - 13.32(a/W)^2 + 14.72(a/W)^3 - 5.6(a/W)^4]}{(1 - a/W)^{3/2}}$$

and where P_Q is load, in MN (lbf); B is specimen thickness, in m (in.); W is specimen width, in m (in.); and a is crack length, in m (in.). It is important to note that, for the compact specimen, the crack length is measured from the centerline of the loading-pin holes. Equation 16 is considered to be accurate within 0.5% over a wide range of crack lengths, for $0.2 \leq a/W < 1$, so it can be used for a variety of fracture-mechanics tests and analyses as well as in the range of interest for K_{Ic} tests, $0.45 \leq a/W \leq 0.55$.

A K_Q value calculated from Eq 16 must meet several criteria in order to be a valid measurement of K_{Ic}. The first, mentioned earlier, is that the specimen thickness and over-all crack length must be equal to or greater than $2.5 (K_{Ic}/\sigma_{ys})^2$. Also, the maximum load supported by the specimen prior to complete fracture must not be more than 10% greater than P_Q. This further ensures that P_Q corresponds to the load at which crack extension takes place rather than the load at which excessive plastic deformation occurs around the crack. The fatigue-crack portion of the fracture surface is examined and measured as designated in the test method, in regard to straightness of the crack front and other criteria.

Because of the complexity of the calculations and the requirements for validity, some of the laboratories in which these tests are run have developed computer programs which compute K_Q values and indicate their validity based on appropriate input data. The complexity of the K_{Ic} test method cannot be denied. Nevertheless, this method has been applied to a wide variety of metallic materials in the past ten years, and very similar methods have been adopted by many other standards organizations around the world. In spite of its complexity, ASTM Method E399 is the preferred standard for measurement of plane-strain fracture toughness, K_{Ic}.

New K_{Ic} Tests. A number of test specimens and methods have been proposed as new K_{Ic} procedures. Three new procedures are described here — two that are related primarily to new specimen geometries and a third that is primarily a new method with existing specimen geometries. These procedures are now being generally used to some extent and are in various stages of consideration by ASTM as K_{Ic} test methods.

A test specimen that is much like the compact specimen, but that is round rather than rectangular in shape, has been used in the United States since 1975. Recently, a round compact specimen and its associated K solution have been added to ASTM Method E399 (Ref 8) and is referred to as the disk specimen. The specimen geometry is sketched in Fig. 20. The K solution is similar both in form and in value (within ±6%) to that of the rectangular compact specimen in the K_{Ic} testing range. The advantage of the disk specimen is that it can be less costly to fabricate because turning operations are often faster than milling. In addition, when round cores are cut from structures or product forms for use in K_{Ic} tests, the disk specimen has a clear advantage.

Another test specimen which has been proposed for use in K_{Ic} measurements is the short rod specimen (Ref 9). The specimen geometry is shown in Fig. 21. The significant advantage in the proposed use of this specimen is that, due to the triangular shape of the area to be cracked, a crack initiates and grows stably during a single application of a relatively low load. This could make possible K_{Ic} tests without the necessity of a fatigue precrack. However, because cracks which have been produced by a single application of load may be sufficiently different from cracks produced by fatigue loading, the resulting K values may not be consistent with those obtained on fatigue-precracked specimens. Further evaluation is needed to determine whether the short rod specimens qualify for plane-strain fracture toughness testing or for screening tests.

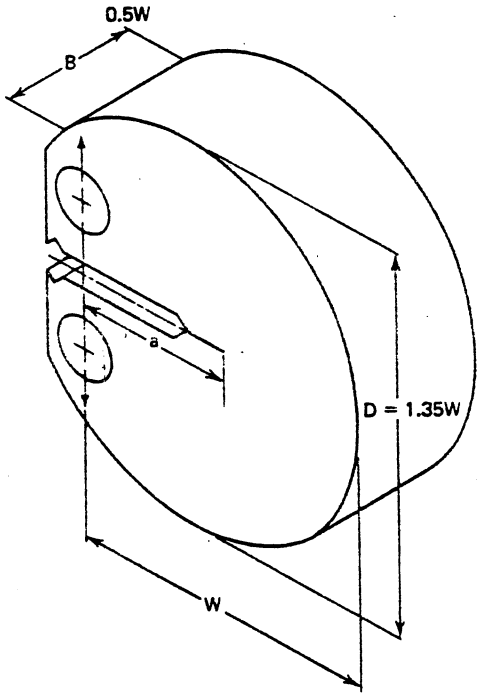

Fig. 20. A round compact K_{Ic} test specimen (the disk specimen)

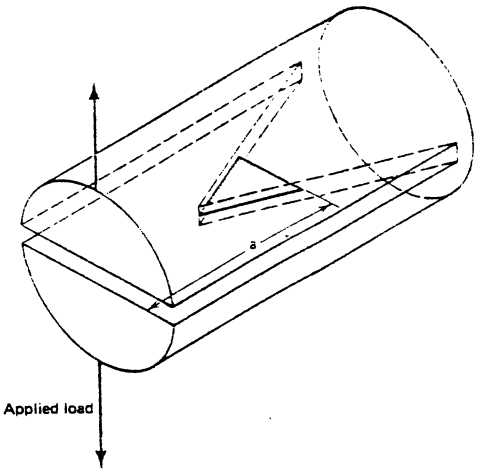

a is notch plus crack length; shaded area indicates crack growth.

Fig. 21. Proposed short rod fracture-toughness specimen

For many years, various laboratories have performed K_{Ic}-type tests at significantly higher loading rates than those specified in E399. Reference 10 describes one example of high-loading-rate K_{Ic} tests on specimens of an alloy steel. A K_{Ic} test procedure based on E399 but at much higher loading rates is being considered by ASTM. Interlaboratory tests have been completed using a pressure-vessel steel tested in closed-loop machines at loading rates in the range of 10^4 $MPa \cdot m^{1/2}/s$; this is about a factor of 10^2 faster than the essentially static loading rate of E399. Compact specimens (Fig. 17b) and many guidelines presented in E399 are generally used in obtaining fracture-toughness data by dynamic K_{Ic} tests. The primary application of dynamic K_{Ic} tests is with the low-to-medium-strength steels, which are known to show loading-rate effects on mechanical properties, particularly yield strength. Problems with the development of the dynamic K_{Ic} test method are related to uncertainties in the yield strength of materials at high loading rates and uncertainties in load measurement at high loading rates.

Non-Plane-Strain Toughness Tests

R-Curve Determination. A consensus R-curve test method is described in ASTM Recommended Practice E561 (Ref 11), first published in 1974 and last revised in 1981. Method E561 describes the determination of the crack-growth resistance of a material under relatively thin-sheet plane-stress conditions which result in a significant amount of plastic deformation at the crack tip. The practice describes the use of center-cracked tensile specimens of the same general type shown in Fig. 10, and compact-type specimens similar to those in Fig. 17(b) except generally much thinner. The basic procedures of the R-curve

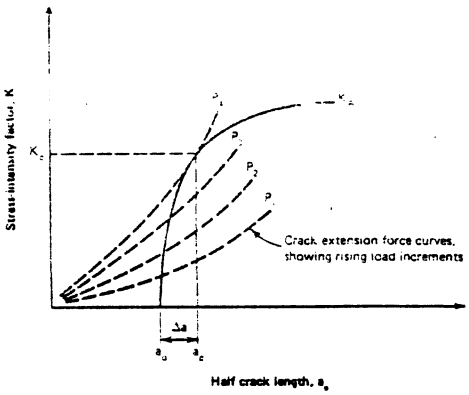

Fig. 22. Typical R-curve test results and analysis (from ASTM Practice E561)

method can be well described by referring to a sketch of typical measurements and calculations from the method using a center-cracked sheet specimen as the example. This sketch, shown in Fig. 22, has coordinates of stress-intensity factor, K, and crack length, a. The solid curve in Fig. 22, marked K_R, is a plot of K applied to the specimen versus the measured crack extension, Δa, produced by the applied K; thus the K_R curve represents the measured crack-extension *resistance* of the material for the particular specimen thickness of the test. The dashed curves are calculations of crack-extension *force* which is available to cause extension of the crack at a given load level. When the applied load is sufficiently high (curve P_4), the crack-extension force exceeds the crack-extension resistance of the material and the crack will grow. Moreover, since the slope of the crack-extension force curve is larger than that of the K_R curve, the crack will become unstable and grow to failure unless the load is decreased. The K value at this point, K_c, is the plane-stress fracture toughness, at which unstable crack growth occurs for this particular combination of material, thickness and other specimen dimensions. The K_R curve is unique to the material and specimen thickness, whereas K_c values may depend on other specimen dimensions in addition to thickness.

The measured data required to plot the K_R curve—that is, load and crack extension—can often be obtained using the same equipment and procedures as those used in K_{Ic} tests. The calculations required to plot the crack-extension force curves are based on the K solution for the specimen, such as Eq 16; the only special requirement is that an adjustment be added to the actual physical crack length, a_p, to account for the effective extension of the crack due to a crack-tip plastic zone. Thus, the effective crack size is:

$$a_e = a_p + \frac{K^2}{2\pi\sigma_Y} \qquad \text{(Eq 17)}$$

where σ_Y is the effective yield strength—that is, the average of the yield and ultimate strengths of the material. Note that the estimate of plastic-zone size from Eq 14 is used here.

Once a K_R curve is obtained for a given material and thickness, it can be used to predict the load at which unstable crack extension will occur in any other geometry, providing that the K solution is known so that the crack-extension curve can be calculated. The K_R-curve approach accounts for crack-tip plastic deformation as discussed above, with the general limitation that the specimen must remain predominantly elastic. Additional information on R-curve methods and their use is available in Ref 12 as well as in ASTM Practice E561 (Ref 11).

J_{Ic} Fracture Toughness. The development of elastic-plastic fracture-toughness tests based on the J-integral concept followed soon after the analyses and estimation of J by Rice, Paris and Merkle (Ref 13) for specimen geometries commonly used in fracture-toughness testing. ASTM has sponsored two cooperative J_{Ic} testing programs, and, based on results from these programs, a proposed J_{Ic} test method has been described in the literature (Ref 14) and has been published as an ASTM standard (Ref 15).

The J_{Ic} test method can be outlined and described in relation to the sketch of typical results in Fig. 23. Values of J are calculated from load versus load-point-displacement data obtained from bend or compact specimens using generally the same specimens, procedures and equipment as in E399. A key requirement is that the displacement must be at the load point; this is allowed but not required in a K_{Ic} test. With this requirement, the area A under the load-versus-displacement curve is a true measure of the combined elastic-and-plastic-strain-energy input to the specimen. The J value is calculated from:

$$J = \frac{2A}{B(W-a)} \qquad \text{(Eq 18)}$$

which applies directly for the bend specimen and with some modification for the compact specimen. The dimensions B, W and a are as described in Fig. 17. At least four specimens are

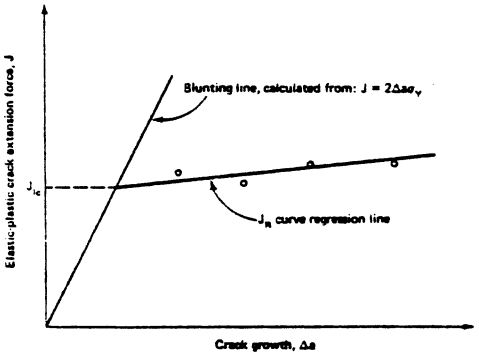

Fig. 23. Typical J_{Ic} test results and analysis (Ref 14)

loaded to produce a range of crack extension, Δa, of about 1 to 2 mm. The value of J calculated from each specimen is plotted versus Δa, and a linear-regression line is fitted to the data. This is the J_R curve as represented by a regression line (see Fig. 23). The blunting line, calculated from $J = 2\Delta a\sigma_Y$, is drawn to represent the amount of apparent crack extension associated with the crack-tip blunting which occurs before actual crack extension occurs. The value of J_{Ic} is determined at the intersection of the J_R curve regression line and the blunting line; so J_{Ic} is a measure of the fracture toughness of the material at the start of actual crack extension from the blunted crack tip.

An important advantage of the J_{Ic} test method is that it can accommodate a significant amount of crack-tip blunting and general plastic deformation in the specimen. If the amount of plastic deformation is small enough, J_{Ic} will be identical to G_{Ic}, and thus J_{Ic} can be converted to an approximately equivalent measure of K_{Ic} (see Eq 10). For large amounts of plastic deformation, a specimen size requirement limits the size of the specimen and, indirectly, the amount of plastic deformation which can be allowed. The specimen size requirement allows a significantly smaller specimen, often ten times smaller, to be tested with the J_{Ic} procedure than with the K_{Ic} procedure. So, although the J_{Ic} test is relatively time consuming due to multiple tests, it can be used over a wider range of material properties and specimen sizes than the K_{Ic} test. In addition, single-specimen J_{Ic} test procedures, such as incremental unloading methods, can reduce both testing time and the required number of specimens in obtaining J_{Ic} test data.

COD Methods. A British test method, "Methods for Crack Opening Displacement (COD) Testing" (Ref 16), is generally similar to the ASTM K_{Ic} method. In this method, a bend specimen is used as in Fig. 17(a), and a load versus crack-mouth-opening-displacement (CMOD) plot is obtained as in Fig. 19. Then, by use of results from experiments and analyses, the displacement at the crack tip, called the crack-tip-opening displacement, or CTOD, is calculated from CMOD. Critical values of CTOD are defined including values corresponding to elastic, plane-strain conditions and values corresponding to significant amounts of plastic deformation. Methods which determine CTOD have the advantage of concentrating on the area in which the actual crack-extension process occurs; however, CTOD methods have the disadvantage of being indirect measurements of the parameter of interest—that is, the opening of the crack faces at the crack tip. Harrison *et al* (Ref 17) have described the British COD method and its application to welded structural components.

Correlation Fracture Tests

Several tests with notched or cracked specimens have been developed for specific engineering applications, in contrast to the tests described above under "Plane-Strain Fracture Toughness, K_{Ic}" and "Non-Plane-Strain Toughness Tests," which were developed to measure directly the fracture-toughness properties of materials. These engineering-application tests have been used extensively for correlation and screening in relation to fracture-toughness tests.

The most long-standing and probably the most widely used test which is used for correlation with fracture toughness is ASTM Method E23, "Notched Bar Impact Testing of Metallic Materials" (Ref 18), commonly known as the Charpy impact test. The Charpy specimen is a three-point bend-type specimen of one size, with B = W = 10 mm and with a length between support points of 40 mm (see Fig. 24). A somewhat similar test and test specimen are described in ASTM Method E604, "Dynamic Tear Energy of Metallic Materials" (Ref 19), which uses a bend specimen with B = 16 mm, W = 38 mm, and a length of 165 mm. Both of these methods measure the energy required to break the notched bend specimen by impact loading with a falling mass. The Charpy impact test, as well as the dynamic tear test, measure the total energy required to initiate and then grow a crack to complete failure of the specimen, whereas K_{Ic} is a measure of K for initial growth of a pre-existing crack. This difference, along with the differences in loading rate and specimen size between Charpy impact and

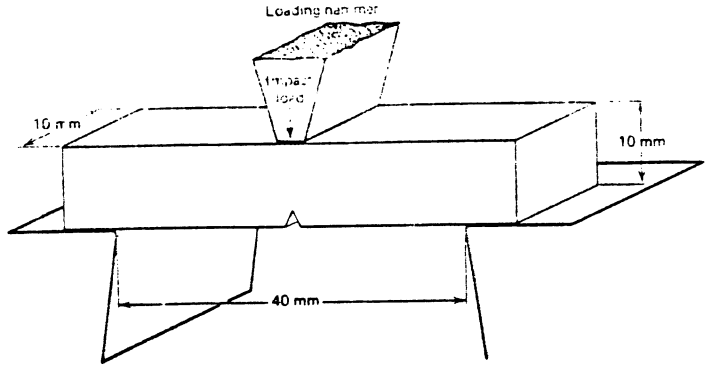

Fig. 24. Schematic illustration of Charpy impact specimen and test arrangement

K_{Ic} tests, limits the correlations between Charpy energy and K_{Ic} to certain materials and to certain ranges of Charpy energy and K_{Ic} values. However, the use of Charpy impact tests to correlate with K_{Ic} has resulted in significant time and cost savings, particularly with medium-to-high strength steels. Many structural components are purchased and inspected to a Charpy energy specification which has been shown to correspond in laboratory testing to a certain required level of K_{Ic}. However, errors could result if the correlation between Charpy energy and K_{Ic} is extended beyond the range of laboratory data for which it was established.

Two tests which are used for correlation with K_{Ic}, generally with high-strength aluminum alloys, are ASTM Method E338, "Sharp-Notch Tension Testing of High-Strength Sheet Materials" (Ref 20), and ASTM Method E602, "Sharp-Notch Tension Testing with Cylindrical Specimens" (Ref 21). Method E338 describes tests on center-notched and edge-notched sheet specimens; Method E602 describes tests on circumferentially notched cylindrical specimens. Both methods require a maximum radius of 0.018 mm (0.0007 in.) at the notch, and this effectively limits these methods to aluminum and magnesium alloys, which are readily machinable. The sharp-notch tensile-strength parameters are used extensively in the aluminum industry to screen materials in respect to their ability to meet corresponding K_{Ic} requirements. The test results are very sensitive to notch sharpness, and thus machining and inspection of the notch must be done carefully to ensure proper correlation.

Two tests that employ the Charpy specimen (Fig. 24) modified by a fatigue precrack ahead of the notch are now being considered by ASTM. They are the proposed "Method for Nominal Crack Strength of Slow-Bend Precracked Charpy Specimens of High-Strength Metallic Materials" and the proposed "Method for Impact Testing of Precracked Charpy Specimens of Metallic Materials." The slow-bend precracked Charpy method uses the maximum load during the test to calculate a nominal crack strength of the specimen which may be correlated with K_{Ic}. The impact-precracked Charpy method uses an instrumented tup on the load hammer to obtain a load-versus-time plot which, if it meets certain criteria, can be used to calculate a maximum K value which is a measure of dynamic fracture toughness. Both of these proposed precracked Charpy test methods measure a maximum stress or K value associated with crack growth from a pre-existing crack; this type of measurement is similar to that of a K_{Ic} test, so the results from these methods should correlate better with K_{Ic} than do the results of other methods. This advantage is offset by the increased difficulty in precracking the specimens and in performing and analyzing the tests.

A review of the correlation fracture tests described above, as well as others, is given in a report of the National Materials Advisory Board (Ref 22).

Sustained-Loading Crack-Growth Tests

The two general types of sustained-loading crack-growth tests are (*a*) determination of K_{Iscc}, the lowest threshold value of K_I at which stress-corrosion cracking occurs, and (*b*) determination of stress-corrosion crack-growth rate, da/dt, resulting from the combination of sustained loading and an aggressive environment. Similar terminology and testing procedures are used for threshold, K_{th}, and crack-growth rate, da/dt, involving internal or external embrittling species such as hydrogen or liquid metals. A standard method for measuring K_{Iscc} is now (1982) being prepared by ASTM Committee E24 on Fracture. The method is based on a large body of research, such as in Ref 23, as well as on the experience and results of an ASTM interlaboratory testing program. Tests were run at 17 laboratories using AISI 4340 steel specimens in 3.5% NaCl for times up to 7000 h. Additional interlaboratory tests on 7075-T7651 aluminum alloy are under way in a cooperative program of ASTM Committees E24 and G1 on Corrosion of Metals.

In determining K_{Iscc}, a group of fatigue-precracked specimens are held at different values of K_I (calculated from load and crack length) in the environment of interest, and the lowest value of K_I at which cracking occurs is K_{Iscc}. Another procedure for determining K_{Iscc} is the rising-load procedure, in which the load on a single precracked specimen is very slowly increased until crack growth occurs, and the associated value of K_I is K_{Iscc}. Rising-load K_{Iscc} tests of an AISI 4340 steel in an H_2S atmosphere are described by Clark in Ref 24.

Measurements of stress-corrosion crack-growth rate, da/dt, are performed at constant load with crack-length measurements taken at various time increments depending on the value of da/dt. Direct measurements of crack length on the specimen surfaces are made if the environment and test plan allow it. Indirect measurement of crack length is often made by measuring specimen displacement—usually the crack-mouth-opening displacement (CMOD)—as shown in Fig. 17. The crack length can then be determined by using the known compliance relations between CMOD and crack length.

Various specimen geometries are used for stress-corrosion-cracking tests. Specimen orientation is designated as it is for fracture-toughness specimens (Fig. 18). The more commonly used specimens are described here. The most frequently used is the compact specimen: it is tension-loaded through pins as in other fracture tests (Fig. 25a), or it is self-loaded using a bolt (Fig. 25b). A double-beam specimen (often called double cantilever beam), with a configuration similar to that of the compact specimen, is used particularly for da/dt tests (see Fig. 25c). Because the crack is liable to grow out of the intended crack plane, side grooves are usually added to the double-beam specimen. Bend specimens also are used, either in three-point bending or in cantilever loading, as shown in Fig. 25(d).

Use of Fracture-Test Results

Measured values of plane-strain fracture toughness, K_{Ic}, and non-plane-strain and correlation measures of fracture toughness, are used in general to calculate the critical crack size in a loaded component which will lead to an abrupt failure. A critical-size crack may be assumed to have been present in the component as fabricated, or may have grown to critical size during service by subcritical crack growth due to fatigue loading or stress-corrosion cracking. Regardless of the cause of the crack, the measured value of toughness is used to calculate the combination of crack size and load which will cause failure.

Measured values of da/dN, K_{Iscc} and da/dt are used to determine the conditions for subcritical crack growth. These test results are used to calculate the crack sizes and loading combinations which will cause cracks to grow from small initial sizes to critical sizes.

Compilations of fracture-mechanics data for specific materials have been included in various handbooks such as the *Damage Tolerant Design Handbook* (Ref 25) and in reports of testing programs such as "Fracture Mechanics Evaluation of B-1 Materials" (Ref 26). Data from such sources may be used in a preliminary assessment

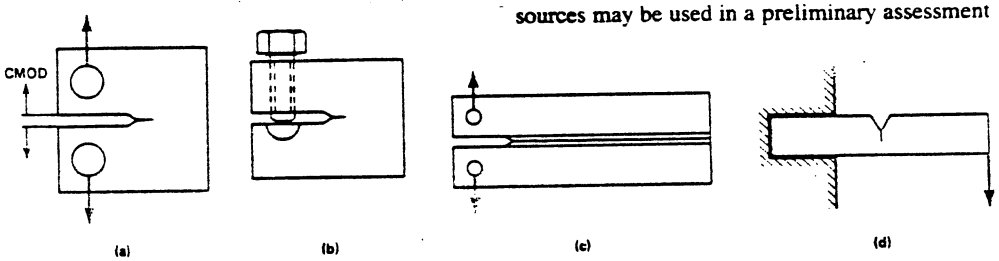

(a) Compact specimen: tension loaded; general use. (b) Modified compact specimen: bolt loaded; K_{Iscc} testing. (c) Double-beam specimen: tension loaded; K_{Iscc} and da/dt testing. (d) Bend specimen: cantilever loaded; K_{Iscc} and da/dt testing.

Fig. 25. Schematic illustration of test specimens and loading used in sustained-load crack-growth testing

of materials and their fracture properties, but when dealing with critical structures, test data should be obtained on specimens that are truly representative of the material in the structures.

REFERENCES

1. The Phenomena of Rupture and Flow in Solids, by A. A. Griffith: *Philosophical Transactions*, Vol 221, 1921, p 163-198

2. *Compendium of Stress Intensity Factors*, by D. P. Rooke and D. J. Cartwright: Hillingdon Press for Her Majesty's Stationery Office, Uxbridge, Middlesex, UK, 1976

3. *The Stress Analysis of Cracks Handbook*, by H. Tada, P. C. Paris and G. R. Irwin: Del Research Corporation, Hellertown, PA, 1973

4. The Influence of Crack Length and Thickness in Plane Strain Fracture Toughness Tests, by M. H. Jones and W. F. Brown, Jr.: in *Review of Developments in Plane Strain Fracture Toughness Testing*, STP 463, American Society for Testing and Materials, Philadelphia, 1970, p 63-101

5. Standard Test Method for Plane-Strain Fracture Toughness of Metallic Materials: E399-81, *1981 Annual Book of ASTM Standards*, Part 10, American Society for Testing and Materials, Philadelphia, 1981, p 588-618

6. Experience in Plane-Strain Fracture Toughness Testing per ASTM Method E399, by J. G. Kaufman: in *Developments in Fracture Mechanics Test Methods Standardization*, edited by W. F. Brown, Jr., and J. G. Kaufman, STP 632, American Society for Testing and Materials, Philadelphia, 1977, p 3-24

7. Fracture Toughness of Plain and Welded 3-In.-Thick Aluminum Plate, by F. G. Nelson and J. G. Kaufman: in *Progress in Flaw Growth and Fracture Toughness Testing*, STP 536, American Society for Testing and Materials, Philadelphia, 1973, p 359-376

8. A Proposed Standard Round Compact Specimen for Plane Strain Fracture Toughness Testing, by J. H. Underwood, J. C. Newman, Jr., and R. R. Seeley: *Journal of Testing and Evaluation*, Vol 8, No. 6, 1980, p 305-313

9. A Simplified Method for Measuring Plane Strain Fracture Toughness, by L. M. Barker: *Engineering Fracture Mechanics*, Vol 9, 1977, p 361-369

10. Fracture Toughness Properties of SA540 Steels for Nuclear Bolting Applications, by R. R. Seeley, W. A. Van Der Sluys and A. L. Lowe, Jr.: *Journal of Pressure Vessel Technology*, Vol 99, 1977, p 419-426

11. Standard Recommended Practice for R-Curve Determination: E561-81, *1981 Annual Book of ASTM Standards*, Part 10, American Society for Testing and Materials, Philadelphia, 1981, p 673-692

12. *Fracture Toughness Evaluation by R-Curve Methods:* STP 527, American Society for Testing and Materials, Philadelphia, 1973

13. Some Further Results of J-Integral Analysis and Estimates, by J. R. Rice, P. C. Paris and J. G. Merkle: in *Progress in Flaw Growth and Fracture Toughness Testing*, STP 536, American Society for Testing and Materials, Philadelphia, 1973, p 231-245

14. A Procedure for the Determination of Ductile Fracture Toughness Values Using J Integral Techniques, by G. A. Clarke, W. R. Andrews, J. A. Begley, J. K. Donald, G. T. Embley, J. D. Landes, D. E. McCabe and J. H. Underwood: *Journal of Testing and Evaluation*, Vol 7, Jan 1979, p 49-56

15. Standard Test for J_{Ic}, A Measure of Fracture Toughness: E813-81, *1981 Annual Book of ASTM Standards*, Part 10, American Society for Testing and Materials, Philadelphia, 1981, p 810-828

16. *Methods for Crack Opening Displacement (COD) Testing*: BS.5762, British Standards Institution, London, 1979

17. The COD Approach and Its Application to Welded Structures, by J. D. Harrison, M. G. Dawes, G. L. Archer and M. S. Kamath: in *Elastic Plastic Fracture*, STP 668, American Society for Testing and Materials, Philadelphia, 1979, p 606-631

18. Standard Methods for Notched Bar Impact Testing of Metallic Materials: E23-81, *1981 Annual Book of ASTM Standards*, Part 10, American Society for Testing and Materials, Philadelphia, 1981, p 273-296

19. Standard Test Method for Dynamic Tear Energy of Metallic Materials: E604-80, *1981 Annual Book of ASTM Standards*, Part 10, American Society for Testing and Materials, Philadelphia, 1981, p 702-710

20. Standard Method of Sharp-Notch Tension Testing of High-Strength Sheet Materials: E338-81, *1981 Annual Book of ASTM Standards*, Part 10, American Society for Testing and Materials, Philadelphia, 1981, p 553-560

21. Standard Method for Sharp-Notch Tension Testing with Cylindrical Specimens: E602-81, *1981 Annual Book of ASTM Standards*, Part 10, American Society for Testing and Materials, Philadelphia, 1981, p 693-701

22. *Rapid Inexpensive Tests for Determining Fracture Toughness:* National Materials Advisory Board, National Academy of Sciences, Washington, 1976

23. *Stress Corrosion—New Approaches*, edited by H. L. Craig, Jr.: STP 610, American Society for Testing and Materials, Philadelphia, 1976

24. Effect of Cold Working on K_{Iscc} in a 4340 Steel, by W. G. Clark, Jr.: in *Flaw Growth and Fracture*, STP 631, American Society for Testing and Materials, Philadelphia, 1977, p 331-344

25. *Damage Tolerant Design Handbook:* Report MCIC-HB-01, Metals and Ceramics Information Center, Battelle Columbus Laboratories, Columbus, OH, 1975

26. Fracture Mechanics Evaluation of B-1 Materials, by R. R. Ferguson and R. C. Berryman: Report AFML-TR-76-137, Rockwell International, B-1 Div., Los Angeles, Contract F33657-70-C-0800, Air Force Materials Laboratory, Wright-Patterson AFB, OH, Oct 1976

Fatigue Testing

A METAL subjected to repetitive loads below the yield stress may fail after a certain number of cycles. A large number of components are subjected to this type of loading (e.g., automotive engines and turbine components), and the design has to obey the constraints of the material strength under these conditions. Failure of materials under cyclic loading is called "fatigue failure," and techniques for measuring susceptibility to fatigue failure are called "fatigue testing." It has been stated (Ref 1) that fatigue accounts for at least 90% of all service failures due to mechanical causes; this shows the importance of the subject. Most fatigue failures start at the surface and progress initially in a slow manner; after the slowly growing crack has reduced the cross-sectional area sufficiently, fracture occurs suddenly. The first portion of the fracture-propagation process yields a fracture surface that usually is significantly different from the second portion. The slowly growing portion produces striations at each cycle, corresponding to each small advance of the crack front. Sometimes these striations are eliminated by subsequent "rubbing" of the surfaces. The second portion of the fracture, corresponding to the rapid propagation of the crack, shows surface features typical of tensile fracture: dimples (in the case of ductile fracture) or cleavage facets (in the case of brittle fracture).

In this article, the more traditional fatigue-testing methods, which provide S-N curves, are described first; the rotating-bending technique with the Moore machine is the best-known test. Next, the methods for analysis and presentation of these data are given. The more modern techniques, in which fatigue-crack growth is monitored as the process proceeds and in which use is made of fracture mechanics, are then presented. Fatigue life is highly susceptible to stress concentrations and to the condition of the surface.

ASTM STANDARDIZED SPECIMENS

ASTM E466 specifies specimens to be used in axial fatigue tests. For bending tests (rotating bending and peak bending), there are no ASTM specifications. The specific dimensions of specimens depend on the objective of the experimental program, on the machine to be used, and on the available material. ASTM does not specify dimensions, but details preparation techniques and reporting techniques. In reporting, a sketch of the specimen, with dimensions, should be given. The surface-roughness and out-of-flatness dimensions should be included. Specimens should not be subjected to any surface treatment. The surface preparation is extremely critical to all fatigue specimens. For axial loading, ASTM E466 states that, regardless of the machining, grinding or polishing method used, the final metal removal should be in a direction approximately parallel to the longitudinal axis of the specimen. Improper preparation methods can greatly bias the results. For instance, Fluck (Ref 2) reports that AISI 3130 steel tested under completely reversed bending at 95 000 psi has a fatigue life of 24 000 cycles when lathe-formed (surface roughness of 105 μin.) and a fatigue life of 234 000 cycles when ground and polished (surface roughness of 2 μin.). Hence, preparation techniques should be carefully developed; if a change in the preparation technique is made, it has to be demonstrated that it does not introduce any bias in the results.

TESTING MACHINES

Rotating-Bending Machines

Rotating-bending fatigue tests of the simple beam type are performed in testing machines such as that illustrated in Fig. 1, sometimes called the R. R. Moore testing machine. In operation, an electric motor rotates a cylindrical specimen, usually at 1800 rpm or higher, while a simple mechanical counter records the number of cycles. Loads are applied to the center of the specimen by a system of bearings and dead weights. A limit switch stops the test when the specimen breaks and the weights descend.

The weights produce a moment that causes the specimen to bend. A strain gage placed on the specimen shows compressive stresses on the top and tensile stresses when the gage is rotated to the bottom. Stresses range from maximum tension to maximum compression during each revolution of the testing machine. Figure 2 shows a typical R. R. Moore machine.

Bending moments can be converted to stress

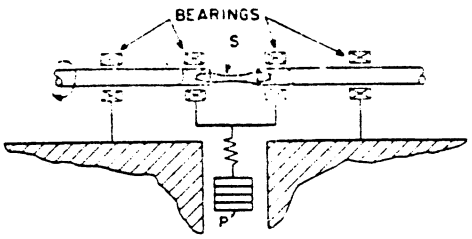

S indicates specimen. P indicates load.

Fig. 1. Loading arrangement for a rotating-beam fatigue-testing machine

by assuming that they are elastic and by employing the flexure formula:

$$\sigma = \frac{MC}{I}$$

For circular specimens, $I = \pi C^4/4$, where C is the specimen radius. The maximum stress at the outer fiber, σ, is proportional to the bending moment, M. This moment is the product of the moment arm and the force. In Fig. 2, it can be seen that the weight is equally distributed between the two sides. Hence, $M = L(P/2)$, where L is the distance from the end of support to the center of application of load.

The specimen is machined from the material to be tested, as shown in Fig. 3, and is fastened into the bearing housing with special cap screws, as shown in Fig. 4. The effective dead weight of the R. R. Moore machine and weighing apparatus (Fig. 2) is 10 lb (4.54 kg), which is deducted from the total weight required and added to the weight pan (Fig. 1) to provide the desired stress:

30.13 lb − 10 lb = 30.13 lb

(18.22 kg − 4.54 kg = 13.68 kg)

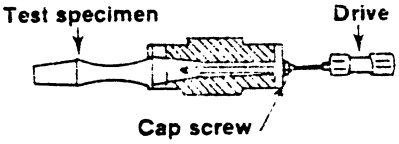

Fig. 4. Cap screw used to fasten the specimen into the bearing housing for a rotating-beam fatigue-testing machine

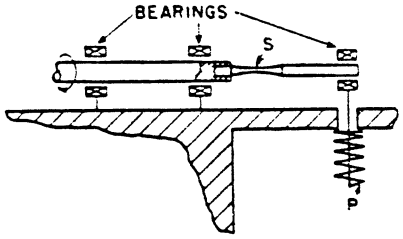

S indicates specimen. P indicates load.

Fig. 5. Loading arrangement for a cantilever-beam fatigue machine for rotating-bending testing

When the drive motor is actuated, a counter records the number of revolutions. If the specimen breaks, the bearing housing descends and actuates a switch that shuts off the drive motor. If the specimen does not break (carbon and low-alloy steels may achieve a million or more cycles), the stress is at or below the endurance limit. Next, the machine is shut off and another specimen is run at a higher stress level. A series of tests is performed to provide sufficient data at varying stress levels.

For cantilever-beam rotating-bending machines of the White-Souther type (Fig. 5), a different bending moment is used in stress calculation. A weight, P, is supported by fixture to a ball-bearing housing at the free end of the specimen. This produces a bending moment, M, that equals P × L, which is the distance of the specimen from the center of the applied load, 3 in. (75 mm). The stress in the outer fiber is

$$S = \frac{PL}{Ic}$$

The weight added to the weight pan is the calculated weight minus the weight of the weighing apparatus.

The cantilever specimen is machined from the material to be tested, as shown in Fig. 6, and is fastened into the bearing housing at one end. The weighing apparatus is assembled, proper weights are applied, and the drive motor is actuated. A series of tests is run and data are plotted to provide an S-N graph.

Plate-Bending Machines

In rotating-bending tests, the mean or average stress is always zero. The effect of mean stress, which is very important in fatigue, is evaluated by cantilever bending machines that are used to test plate materials. In these machines, sometimes called Kraus plate-bending machines, specimens are loaded with constant deflection by means of an eccentric crank (Fig. 7). Stresses can be calculated by assuming that they are elastic. In many cases this is not a good assumption, because, when tested, some soft materials may involve small amounts of plastic stress.

Specimens are usually tapered to provide a constant-stress test area. The approximate stress, S, is given by:

$$S = \frac{ytE}{l^2}$$

where y is the specimen deflection, t is the thickness of the specimen, E is the elastic modulus, and l is the distance from load application to the back of the specimen. Constant-deflection beam-type machines are used to test both strip and plate.

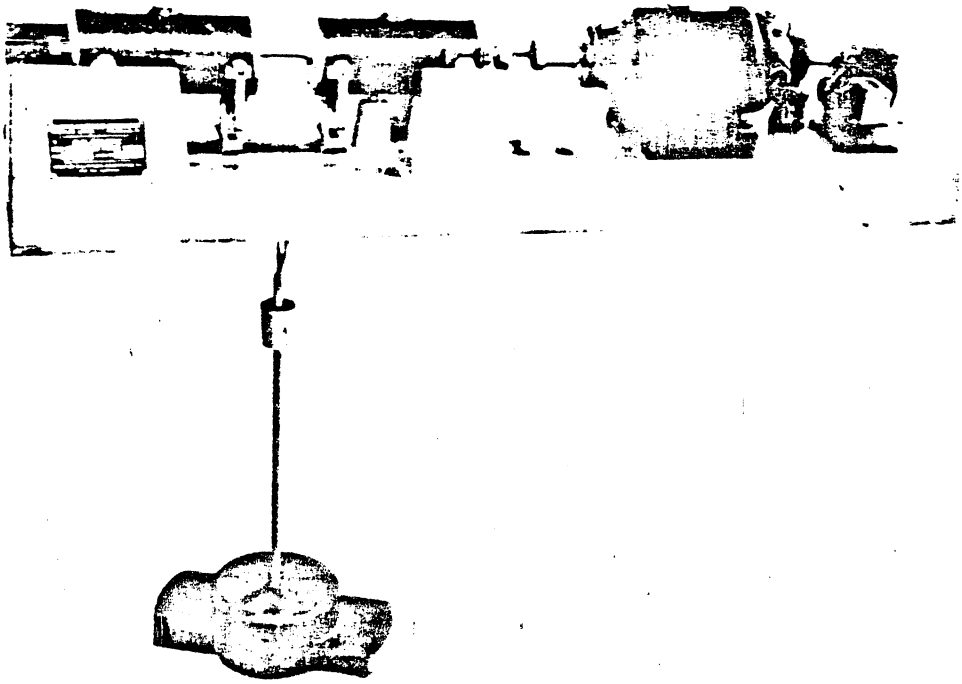

Fig. 2. Typical R. R. Moore machine for rotating-bending fatigue testing

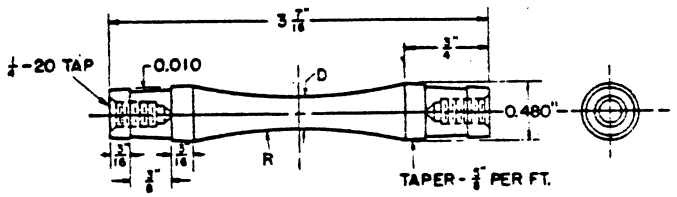

D = 0.200 to 0.400 in., selected on basis of ultimate strength of material.
R = 3.5 to 10 in.

Fig. 3. Simple rotating-beam specimen for fatigue testing

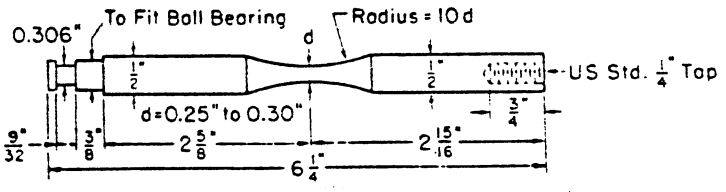

Fig. 6. Rotating cantilever-beam specimen for fatigue testing

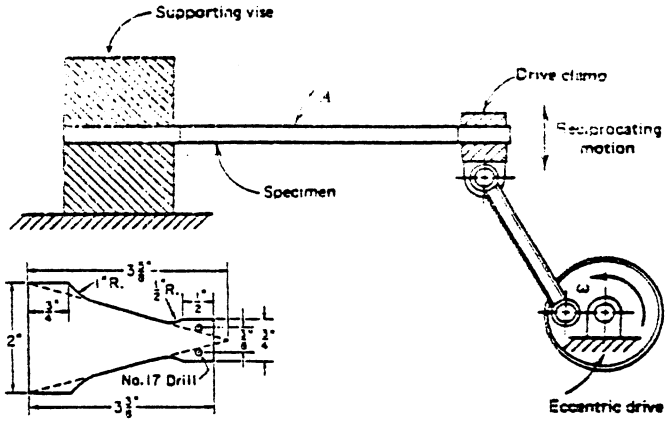

Fig. 7. Reciprocating-bending fatigue-testing machine, and typical specimen (at lower left) for testing of sheet

A typical specimen is shown at lower left in Fig. 7.

Resonant-Testing Machines

Machines for resonant testing are basically spring-mass, vibrating systems. The frame design is based on a resonant, spring-mass system that consists of two masses linked by the specimen and grip string and that oscillates as a dipole. The system is excited by an electromagnet housed in the machine base. The masses and load string are positioned in the vertical frame, which is suspended and guided on leaf springs. The eight springs are arranged in a special configuration to make a unique and compact design without the need for a heavy seismic block.

Mean load is applied by a motor located in the base of the system. The motor drives the four corner gearboxes through two shafts and applies mean loads in both tension and compression. The mean-load force is carried by the box-type structure of springs, and the level either is adjusted by a hand-held controller or is maintained at a level preset by the controller. The magnet air gap is maintained automatically by the action of the gap servomotor driving a wedge beneath the electromagnet. A linear variable displacement transformer (LVDT) constantly monitors the air gap, and control is maintained even when the mean load is changed while the machine is running. A manually operated drive located in the upper mass permits major adjustment of specimen spacing.

The electromagnet excites the dual-mass system at its natural frequency by means of pulse excitation. This feature enables a simple switch to replace the conventional power amplifier, thus providing high reliability at low cost and, in addition, eliminating the need to tune an oscillator to the natural frequency of the system. Closed-loop amplitude control is achieved by controlling the pulse power to the magnet from the error between the actual and demanded load amplitudes, thereby providing fast response to changing load demands. A strain-gaged load cell provides accurate load monitoring and digital indication of peak dynamic load, mean load, and frequency.

STRESS-LIFE DATA

ASTM Specifications for Constant Amplitude Axial Fatigue Tests of Metallic Materials, E466, and Standard 468, Constant Amplitude Fatigue Test Results for Metallic Materials, are recommended sources for fatigue-testing results.

Data Presentation

In laboratory fatigue testing, the specimen is loaded so that stress is cycled between either a maximum and a minimum tensile stress or a maximum tensile stress and a maximum compressive stress. The latter, considered a negative tensile stress, is given an algebraic minus sign and, therefore, is called the minimum stress.

The mean stress, S_m, is the algebraic average of the maximum and minimum stresses in one cycle:

$$S_m = (S_{max} + S_{min})/2$$

In the completely reversed test, the mean stress is zero. The range of stress, ΔS, is the algebraic difference between the maximum and minimum stresses in one cycle:

$$\Delta S = S_{max} - S_{min}$$

The stress amplitude, S_a, is one half the range of stress:

$$S_a = \Delta S/2 = (S_{max} - S_{min})/2$$

During a fatigue test, the stress cycle is usually maintained constant so that applied stress conditions can be written as $S_m \pm S_a$, where S_m is the static or mean stress, and S_a is the alternating stress equal to half the stress range. The positive sign is used to denote a tensile stress; the negative sign denotes a compressive stress. Some of the possible combinations of S_m and S_a are illustrated in Fig. 8. When $S_m = 0$ (Fig. 8a), the maximum tensile stress is equal to the maximum compressive stress. This is called an alternating stress or a completely reversed stress. When $S_m = S_a$ (Fig. 8b), the minimum stress of the cycle is zero. This is called a pulsating or repeated tensile (or compressive) stress. Any other combination is known as a fluctuating stress, which may be a fluctuating tensile stress (Fig. 8c), a fluctuating compressive stress, or a stress that fluctuates between a tensile and a compressive value (Fig. 8d).

Stress ratio is the algebraic ratio of two specified stress values in a stress cycle. Two commonly used stress ratios are the ratio A of the alternating stress amplitude to the mean stress ($A = S_a/S_m$) and the ratio R of the minimum stress to the maximum stress ($R = S_{min}/S_{max}$). If the stresses are fully reversed, the stress ratio, R, is -1; if the stresses are partially reversed, R is a negative number less than 1; if the stress is cycled between a maximum stress and no load, R is zero; and if the stress is cycled between two tensile stresses, R is a positive number less than 1. A stress ratio of 1 indicates no variation in stress, and the test is a sustained-load creep test rather than a fatigue test.

Results of fatigue testing are commonly reported in the form of a stress-life curve, commonly called an S-N curve. Stress is usually plotted vertically on a linear scale and life, N, on the horizontal axis using a logarithmic scale. A typical curve is shown in Fig. 9. Each data point represents a single test. Typically a stress level is selected and the specimen is cycled until it breaks into two pieces or a predetermined number of cycles is reached. Usually, this number is between 10^6 and 10^7. If a specimen does not fail during the test it is called a "runout" and the data points are denoted with an arrow.

Fatigue limit (or endurance limit) is the value of the stress below which a material can presumably endure an infinite number of stress cycles — that is, the stress at which the S-N diagram becomes and appears to remain horizontal. The existence of a fatigue limit only occurs for carbon and low-alloy steels. It is the exception, rather than the rule.

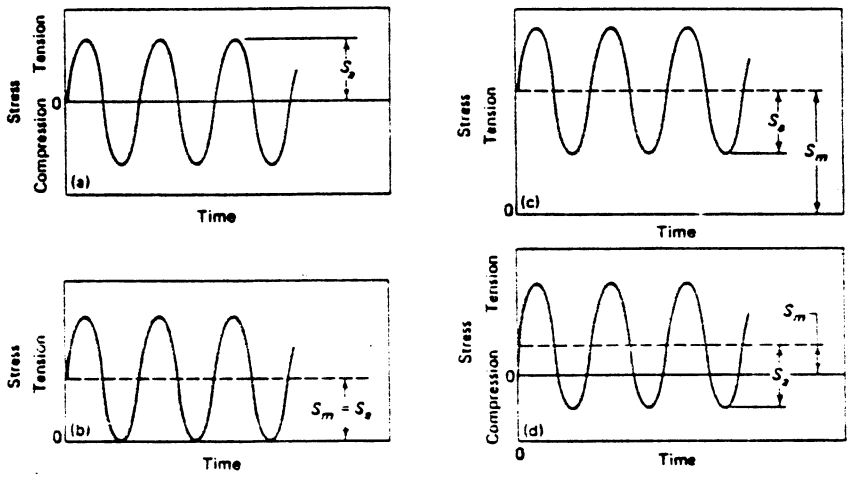

(a) Alternating stress for which $S_m = 0$ and for which R (ratio of minimum stress to maximum stress) $= -1$. (b) Pulsating tensile stress for which $S_m = S_a$, the minimum stress is zero, and $R = 0$. (c) Fluctuating tensile stress for which both the minimum and maximum stresses are tensile stresses, $R = 1/3$. (d) Fluctuating tensile-to-compressive stress for which the maximum stress is a tensile stress, $R = -1/3$.

Fig. 8. Four types of fatigue-test stresses

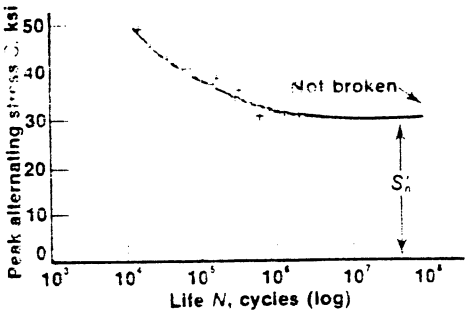

Fig. 9. S-N curve with data plotted on semilog coordinates

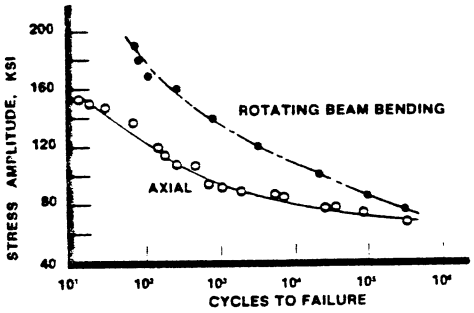

Fig. 10. Fatigue data under axial loading and in rotating bending for 4130 steel

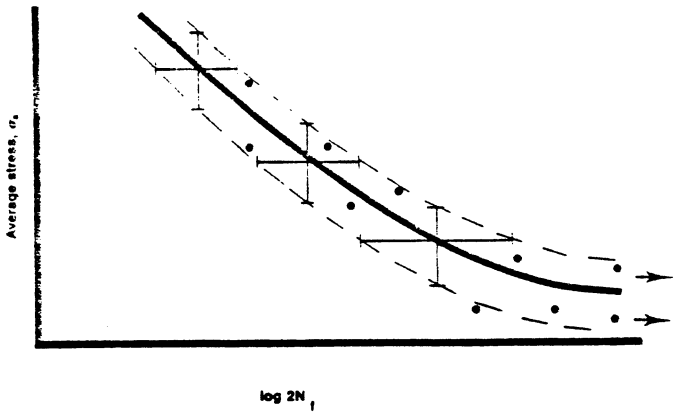

$2N_f$ is reversals to failure. σ_a is the steady-state stress amplitude.

Fig. 11. Scatter band showing S-N curves for fatigue data

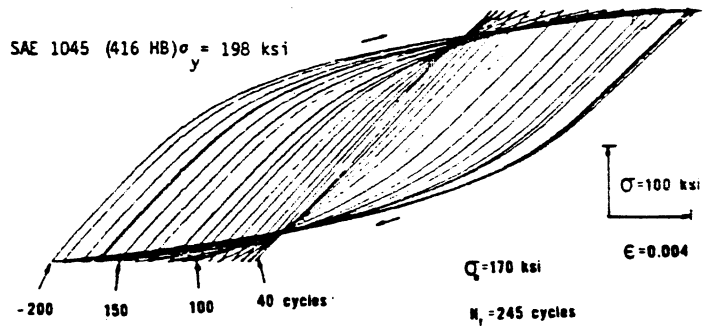

Fig. 12. Cyclic softening of a steel under controlled-stress cycling

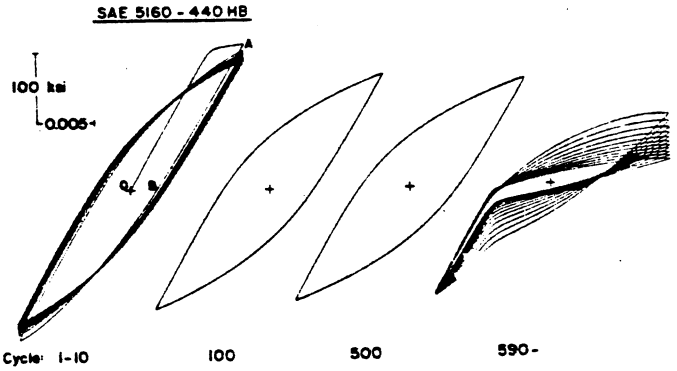

Fig. 13. Cyclic softening of a steel under controlled-strain cycling

Fatigue strength, which should not be confused with fatigue limit, is the stress to which the material can be subjected for a specified number of cycles. Fatigue strength is used for materials, such as most nonferrous metals, that do not exhibit well-defined fatigue limits.

In rotating-beam tests, only the outer fiber is under maximum stress, while in axial tests the entire cross section is under maximum stress. The increased volume of highly stressed material makes failure more likely in axial tests. As a result, data from rotating-bending tests should not be employed for estimating the fatigue lives of structures and components, but only for a rough comparison between two materials. Caution is advised when using the data for design of structures and components. Figure 10 shows S-N curves for both cases; the difference in fatigue life is significant.

Statistical Aspects

In fatigue testing—perhaps more than in other types of mechanical testing—there are always some variations in the material properties. It is not uncommon for two "identical" specimens to have fatigue lives differing by a factor of two. Distributions in fatigue life, as well as fatigue strength, are important, as shown in Fig. 11. Typical S-N curves represent the mean of all test results. Curves often are drawn to display the scatter band of data obtained with multiple tests.

Transient Behavior of Metals

Metals are metastable under application of cyclic loads, and their stress-strain response can be drastically altered when they are subjected to repeated plastic strains. Depending on its initial state (quenched and tempered, normalized, or annealed and softened) and its test condition, a metal may (*a*) cyclically harden, (*b*) cyclically soften, (*c*) remain cyclically stable or (*d*) exhibit mixed behavior (soften or harden, depending on strain amplitude).

The following discussion develops and presents equations similar to those describing the monotonic stress-strain behavior. In addition, properties more appropriate to fatigue analyses—fatigue properties—are defined.

Determination of constant-amplitude fatigue lives of specimens is customarily performed under conditions of controlled stress (as in the rotating-bending or cantilever-bending type of test) or controlled strain. Figure 12 shows the ramifications of controlling stress, providing justification for the use of controlled strain while observing the stress response. As shown, the applied stress amplitude is less than the initial or monotonic yield strength of the steel (as noted by the "linear-elastic" strain response during the first 40 cycles). Because plastic deformation occurs at a microscopic level, however, the macro-level response of the steel is the accrual of ever-increasing amounts of plastic strain. As stress cycling proceeds beyond 40 cycles, a "runaway" process occurs as the steel undergoes cyclic softening.

When the above response is compared to the response of a steel of similar hardness (shown in Fig. 13) under conditions of controlled strain, no instability, as happened under controlled stress, is observed, although the stress limits decrease with increased cycles. These test conditions represent extremes of completely unconstrained or stress-cycling conditions and completely constrained or strain-cycling conditions. In actual engineering structures, stress-strain gradients do exist, and there is usually a certain degree of structural constraint of the material at critical locations. Because this condition is reminiscent of strain control, it is more advantageous to characterize material response under strain-controlled than stress-controlled conditions.

For these reasons, consider the cases illustrated in Fig. 14 and 15, in which total strain is controlled and the stress response is observed. As shown in Fig. 14, if the stress required to enforce the strain increases on subsequent re-

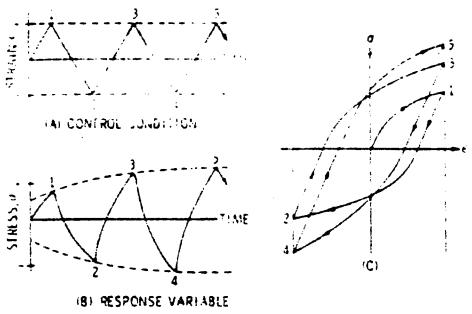

Fig. 14. Cyclic hardening under controlled-strain-amplitude cycling

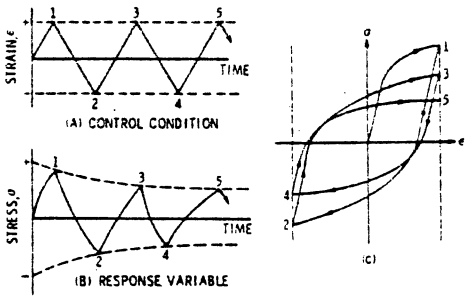

Fig. 15. Cyclic softening under controlled-strain-amplitude cycling

versals, the metal experiences cyclic hardening. The hardness, yield strength and ultimate strength increase. Such behavior is characteristic of annealed pure metals (for example, copper), many aluminum alloys, and as-quenched steels.

As illustrated in Fig. 15, the strain amplitude is controlled, but the stress required to enforce the strain decreases with subsequent reversals. This phenomenon is called cyclic softening and is characteristic of cold worked pure metals and many steels at small strain amplitudes. During cyclic softening, the flow properties (for example, hardness, yield strength and ultimate strength) decrease.

By plotting the stress amplitude versus reversals from controlled-strain test results, cyclic strain hardening and softening can be observed, as illustrated in Fig. 16. Thus, through cyclic hardening and softening, some intermediate strength level is attained that represents a steady-state condition (in which the stress required to enforce the controlled strain does not vary significantly). Some metals are cyclically stable, in which case their monotonic stress-strain behavior adequately describes their cyclic response. The steady-state condition is usually achieved in about 20 to 40% of the total fatigue life in either hardening or softening materials.

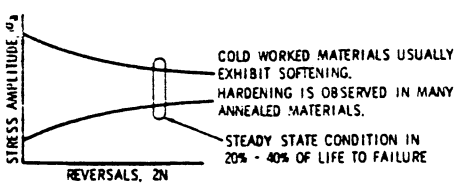

Fig. 16. Steady-state stress response for strain-controlled cycling

Cyclic Stress-Strain Behavior

The cyclic behavior of metals is best described in terms of a stress-strain hysteresis loop, as shown in Fig. 17. For completely reversed, strain-controlled conditions with zero mean strain, the total width of the loop is $\Delta\varepsilon$, or the total strain range:

$$\Delta\varepsilon = 2\varepsilon_a$$

where ε_a is strain amplitude. The total height of the loop is $\Delta\sigma$, or the total stress range:

$$\Delta\sigma = 2\sigma_a$$

where σ_a is stress amplitude.

Because the difference between the total- and elastic-strain amplitudes is the plastic-strain amplitude, the second equation below follows from the first:

$$\frac{\Delta\varepsilon}{2} = \frac{\Delta\varepsilon_e}{2} + \frac{\Delta\varepsilon_p}{2}$$

$$\frac{\Delta\varepsilon_p}{2} = \frac{\Delta\varepsilon}{2} - \frac{\Delta\varepsilon_e}{2} = \frac{\Delta\varepsilon}{2} - \frac{\Delta\sigma}{2E}$$

where E is the modulus of elasticity, ε_e is the elastic-strain amplitude and ε_p is the plastic-strain amplitude.

Changes in stress response of a metal occur rapidly during the first several percent of the total reversals to failure. The metal, under controlled-strain amplitude, eventually attains a steady-state stress response. To construct a cyclic stress-strain curve, the tips of the stabilized hysteresis loops from comparison specimen tests at several controlled-strain amplitudes can be connected.

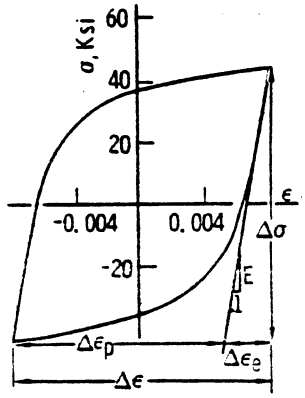

Fig. 17. Steady-state stress-strain hysteresis loop

In the particular example shown in Fig. 18, three companion specimens were tested to failure at three different controlled-strain amplitudes. The steady-state stress response, measured at approximately 50% of the life to failure, is thereby obtained. These stress values are then plotted at the appropriate strain levels to obtain the cyclic stress-strain curve. The cyclic stress-strain curve can be compared directly with the monotonic or tensile stress-strain curve to quantitatively assess cyclically induced changes in mechanical behavior (Fig. 19).

Note that in Fig. 19(a), when a material cyclically softens, the cyclic yield strength is considerably lower than the monotonic yield strength. Using monotonic properties in a cyclic application can result in prediction of fully elastic strains, when in fact considerable plastic strains are present. In T1 steels or an equivalent HSLA steel,

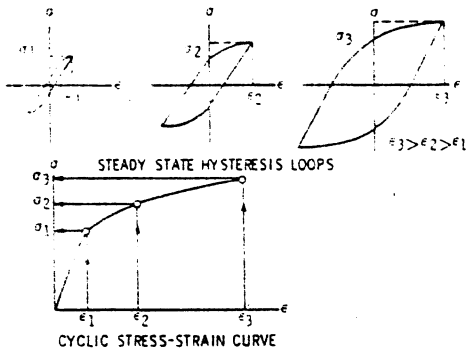

Fig. 18. Construction of cyclic stress-strain curve by joining tips of stabilized hysteresis loops

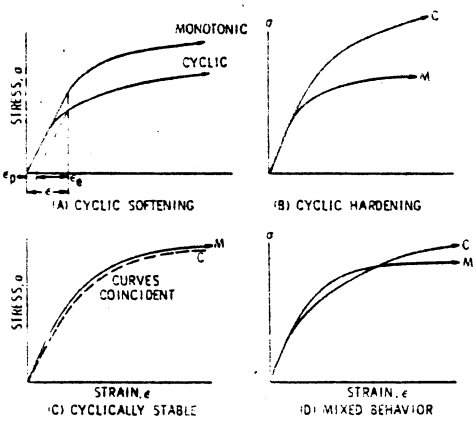

Fig. 19. Various types of cyclic stress-strain curves

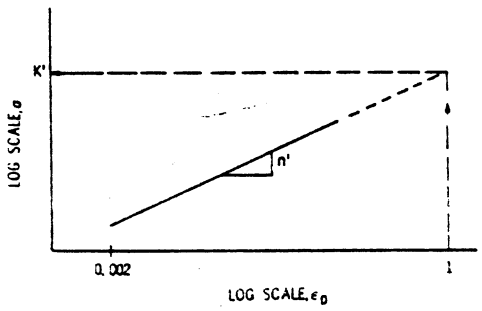

Fig. 20. True stress versus plastic strain for cyclic response (log-log coordinates)

for example, the cyclic yield strength is only about 50% of the monotonic yield strength.

Whereas the steady-state process consumes 20 to 40% of total life in constant-amplitude testing, a single large overload in actual service can produce an immediate change from the monotonic curve to the cyclic. Assembly or even driving of the completed machine "out the door" can cause an instantaneous loss of 50% of the monotonic yield strength.

Using the same approach as with the monotonic stress-strain curve, a plot of true stress versus true strain from constant-strain-amplitude test data of companion specimens on log-log paper results in a straight line (Fig. 20). Again, a power-law function between true stress and plastic strain may be represented as:

$$\sigma_a = K'(\varepsilon_p)^n$$

where σ_s is the steady-state stress amplitude (measured at 50% of life to failure), ε_p is the plastic-strain [illegible], K' is the cyclic-strength coefficient, and n' is the cyclic strain-hardening exponent.

The cyclic stress-strain response of a material is characterized by the following relationship:

$$\varepsilon = \frac{\sigma}{E} + \left(\frac{\sigma}{K'}\right)^{1/n'}$$

The value of n' varies between 0.10 and 0.20, with an average value very close to 0.15. In general, metals with high monotonic strain-hardening exponents ($n > 0.15$) cyclically harden; those with low monotonic strain-hardening exponents ($n < 0.15$) cyclically soften.

STRAIN-LIFE RELATIONSHIPS

The S–log N plot can be linearized with full log coordinates. If true stress amplitudes are used instead of engineering stress, the entire stress-life curve may be linearized, as illustrated in Fig. 21. Thus, stress amplitude can be related to life by:

$$\sigma_a = \sigma_f'(2N_f)^b$$

where $\Delta\sigma$ is σ_a in zero-mean-constant-amplitude test, which is true stress; $2N_f$ is reversals to failure (one cycle is two reversals); σ_f' is the fatigue-strength coefficient; b is the fatigue-strength exponent (Basquin's exponent); and S_f is the fatigue-strength limit applicable to certain steels under very specific loading situations. σ_f and b are fatigue properties of the metal, with σ_f' approximately equal to σ_f for many metals and b varying between approximately −0.05 and −0.12.

Around 1955, Coffin and Manson, who were working independently on the thermal-fatigue problem, established that plastic strain–life data could also be linearized with log-log coordinates (Fig. 22). As with the true stress–life results, the plastic strain–life data can be related by the power-law function:

$$\frac{\Delta\varepsilon_p}{2} = \varepsilon_f'(2N_f)^c$$

where $\Delta\varepsilon_p/2$ is plastic-strain amplitude, $2N_f$ is the reversals to failure, ε_f' is the fatigue-ductility coefficient, and c is the fatigue-ductility exponent. ε_f' and c are also fatigue properties, with ε_f' approximately equal for many metals and c varying between approximately −0.5 and −0.7 for many metals.

It was mentioned previously that total strain has two components: elastic and plastic, or:

$$\varepsilon = \varepsilon_e + \varepsilon_p$$

This can also be expressed as the strain amplitudes from a constant-amplitude, zero-mean-strain controlled test:

$$\frac{\Delta\varepsilon}{2} = \frac{\Delta\varepsilon_e}{2} + \frac{\Delta\varepsilon_p}{2}$$

Therefore:

$$\sigma_a = \sigma_f'(2N_f)^b$$

$$\frac{\Delta\varepsilon_e}{2} = \frac{\sigma_a}{E}$$

Division by E, the modulus of elasticity, obtains:

$$\frac{\Delta\varepsilon_e}{2} = \frac{\sigma_f'}{E}(2N_f)^b$$

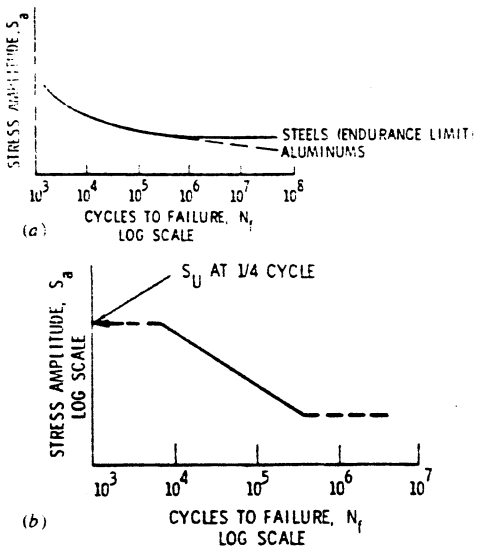

(a) Stress versus log cycles to failure. (b) Log stress versus log cycles to failure.

Fig. 21. Stress-life curves

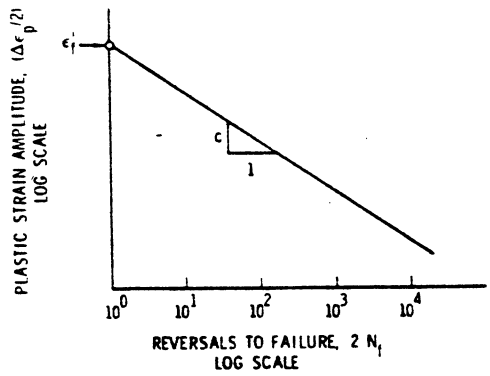

Fig. 22. Log plastic strain versus log reversals to failure

or, with elastic and plastic combined:

$$\frac{\Delta\varepsilon}{2} = \frac{\sigma_f'}{E}(2N_f)^b + \varepsilon_f'(2N_f)^c$$

(Elastic) (Plastic)

This equation is the foundation for the strain-based approach to fatigue and is called the strain-life relationship.

The two straight lines, one for the elastic strain and one for the plastic strain, also can be plotted, as in Fig. 23. Several conclusions may be drawn from the total strain–life curve in Fig. 23. At short lives, less than $2N_t$ (the transition fatigue

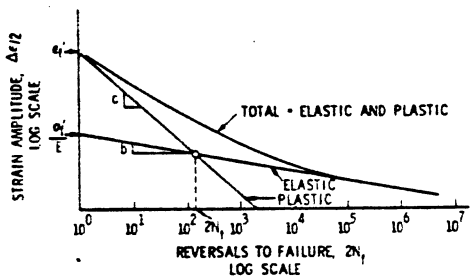

Fig. 23. Log strain versus log reversals to failure

life where $\Delta\varepsilon_p/2 = \Delta\varepsilon_e/2$), plastic strain predominates and ductility controls performance. At longer lives, greater than $2N_t$, the elastic strain is more dominant than the plastic, and strength controls performance. An "ideal material" is one with both high ductility and high strength. Unfortunately, strength and ductility are usually a trade-off; the optimum compromise must be tailored to the expected load or strain environment being considered in a real history for a fatigue analysis. By equating the elastic and plastic components of total strain, the transition fatigue life can be calculated as:

$$2N_t = \left(\frac{\varepsilon_f' E}{\sigma_f'}\right)^{1/(b-c)}$$

FATIGUE-CRACK-GROWTH-RATE TEST METHODS

By J. H. Underwood, U.S. Army Armament Research and Development Command, and W. W. Gerberich, University of Minnesota

The general nature of fatigue-crack growth and its description using fracture mechanics can be briefly summarized by the example data shown in Fig. 24. This figure, based on the work of Paris *et al* (Ref 3), shows a logarithmic plot of the crack growth per cycle, da/dN, versus the stress-intensity-factor range, ΔK, corresponding to the load cycle applied to a specimen. The da/dN-versus-ΔK plot shown is from five specimens of ASTM A533 B1 steel tested at 24 °C (75 °F). A plot of similar shape is expected with most structural alloys; the absolute values of da/dN and ΔK are dependent on the material. Results of fatigue-crack-growth-rate tests for nearly all metallic structural materials have shown that the da/dN-versus-ΔK curves have the following characteristics: (*a*) a region at low values of da/dN and ΔK in which fatigue cracks grow extremely slowly or not at all below a lower limit of ΔK called the threshold of ΔK, ΔK_{th}; (*b*) an intermediate region of power-law behavior described by the Paris equation (Ref 4):

$$\frac{da}{dN} = C(\Delta K)^n$$

where C and n are material constants; and (*c*) an upper region of rapid, unstable crack growth with an upper limit of ΔK which corresponds either to K_{Ic} or to gross plastic deformation of the specimen.

Testing procedures for measuring fatigue-crack-growth rates are described in ASTM Method E647. This method applies to medium-to-high crack-growth rates—that is, above 10^{-8} m/cycle (3.9×10^{-7} in./cycle). Procedures for growth rates below 10^{-8} m/cycle are under consideration by ASTM. For applications involving fatigue lives of up to about 10^6 load cycles, the procedures of E647 can be used. Fatigue lives greater than about 10^6 cycles correspond to growth rates below 10^{-8} m/cycle, and these require special testing procedures, which are related to the threshold of fatigue-crack growth illustrated in Fig. 24.

ASTM Method E647 describes the use of center-cracked specimens and compact specimens. The specimen thickness-to-width ratio, B/W, is smaller than the 0.5 value for K_{Ic} tests; the maximum B/W values for center-cracked and compact specimens are 0.125 and 0.25, respectively.

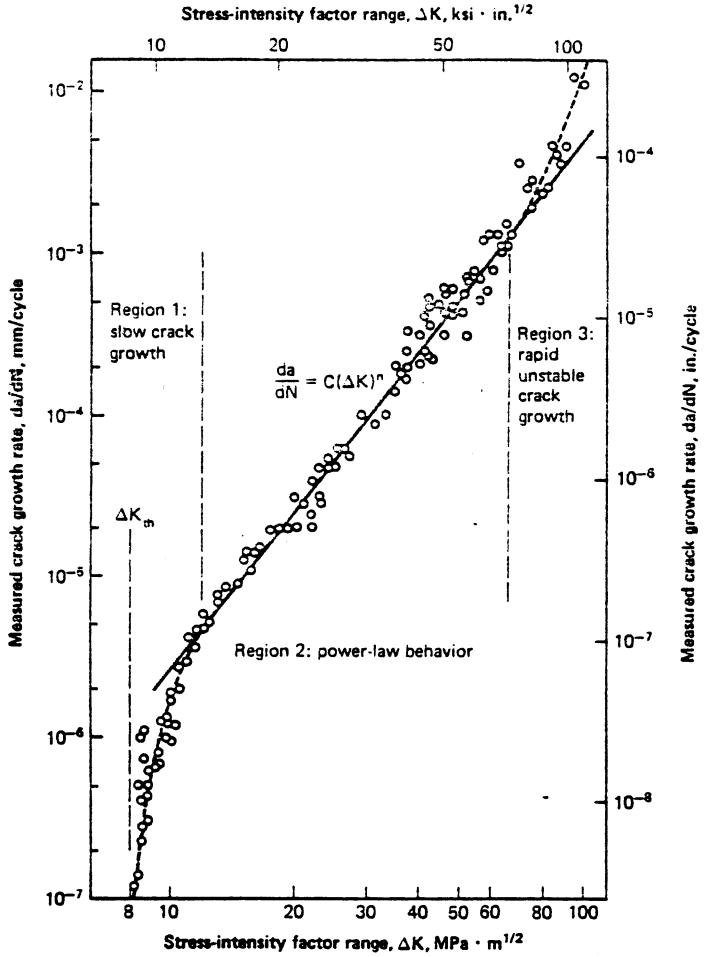

The material was ASTM A533 B1 steel, with a yield strength of 470 MPa (70 ksi). Test conditions: R = 0.10; ambient room air; 24 °C (75 °F).

Fig. 24. Fatigue-crack-growth behavior of A533 steel (Ref 3)

With the thinner specimens, it is feasible to use crack-length measurements on the sides of the specimens as representations of through-thickness crack-growth behavior. The specimens are loaded in the same general manner as for K_{Ic} testing. For tension-tension fatigue loading, the K_{Ic} loading fixtures often can be used. For this type of loading, both the maximum and minimum loads are tensile, and the load ratio, $R = P_{min}/P_{max}$, is in the range $0 < R < 1$. A ratio of $R = 0.1$ is commonly used. Tension-compression loading can be performed with the compact specimen, but it is a more complex type of loading and requires more care.

Testing normally is performed in laboratory air at room temperature; however, any gaseous or liquid environment and temperature of interest may be used in order to determine the effect of corrosion or other chemical reaction on cyclic loading. Cyclic loading may involve various wave forms for constant-amplitude loading, spectrum loading or random loading.

For constant-amplitude loading, a set of crack-length-versus-elapsed-cycle data (a versus N) is collected, with the specimen loading, P_{max} and P_{min}, generally held constant. The minimum crack-length increment, Δa, between data points is required by ASTM E647 to be larger than a certain value. This prevents the measurement of erroneous growth rates from a group of data points which are too closely spaced relative to the precision of data measurement and relative to the scatter of the data. The growth rates may be calculated by either of two methods. The secant method is simply the slope of the straight line connecting two adjacent data points. This method, although simpler, results in more scatter in measured crack-growth rate. The polynomial method fits a second-order polynomial expression (parabola) to typically 5 to 7 adjacent points, and the slope of this expression is the growth rate. The polynomial method, particularly when used with a large number of adjacent points, eliminates some of the scatter in growth rate which is inherent in fatigue testing. The measured values of growth rate typically are plotted as in Fig. 24, where ΔK is calculated from $\Delta P = P_{max} - P_{min}$ (for tension-tension loading) using a K expression such as Eq 16 in the preceding article.

The measured growth-rate data are represented by an equation of the form of the Paris equation:

$$\frac{da}{dN} = C(\Delta K)^n$$

where the material constants C and n apply only within a certain range of da/dN and ΔK values. Other relationships based on the Paris equation, such as the commonly used Forman equation (Ref 5), are used to represent the variation of da/dN with other key variables, including load ratio, R, and the critical K value, K_c, at which fast fracture of the specimen occurs. The Forman equation is:

$$\frac{da}{dN} = \frac{C(\Delta K)^n}{(1 - R)K_c - \Delta K}$$

where C and n are material constants of the same types as those in the Paris equation, but of different values. An advantage of the Forman equation is that it describes the type of accelerated da/dN behavior which is often observed at high values of ΔK and which is not described by the Paris equation. For example, for zero-to-tension loading (in which $R = P_{min}/P_{max} = 0$), as ΔK approaches K_c in the Forman equation, da/dN increases rapidly, and this is often observed in tests. In addition, the Forman equation describes the often-observed decrease in da/dN associated with an increase in R from zero toward one. So when it is necessary to describe the effect of ΔK approaching K_c or the effect of R on da/dN, the Forman equation can be used to represent the da/dN behavior. When only ΔK, the primary variable affecting da/dN, is involved, the less complex Paris equation may be used.

REFERENCES

1. *Mechanical Metallurgy*, 2nd Ed., by G. E. Dieter: McGraw-Hill, New York, 1976, p 403
2. P. G. Fluck: *ASTM Proc.*, Vol 51, 1951, p 584
3. Extensive Study of Low Fatigue Crack Growth Rates in A533 and A508 Steels, by P. C. Paris, R. J. Bucci, E. J. Wessel, W. R. Clark and T. R. Mager: in *Stress Analysis and Growth of Cracks*, Proceedings of the 1971 National Symposium on Fracture Mechanics, Part I, STP 513, American Society for Testing and Materials, Philadelphia, 1972, p 141-176
4. A Critical Analysis of Crack Propagation Laws, by P. C. Paris and F. Erdogan: *Journal of Basic Engineering, Transactions of ASME*, Vol 85, Dec 1963, p 528-534
5. Numerical Analysis of Crack Propagation in Cyclic-Loaded Structures, by R. G. Forman, V. E. Kearney and R. M. Engle: *Journal of Basic Engineering, Transactions of ASME*, Vol 89, Sept 1967, p 459-464

Creep and Creep-Rupture Testing

THE FLOW or plastic deformation of a metal held for long periods of time at stresses below the normal short-time yield strength is known as creep. Although we normally think of creep as occurring only at elevated temperatures, room temperature can be high enough for creep to occur in some metals. In lead, for example, creep at room temperature is common. In many cases, lead pipes must be supported to prevent sagging under their own weight.

The development of steam turbines and jet engines has greatly increased interest in creep because, in these, the metal parts must withstand high loads at high temperatures for long times. The high centrifugal loads tend to cause certain parts to elongate or distort. Tolerances must be kept close to be efficient; yet if the metal parts deform too much, this spacing will be eliminated and failure will occur. In most cases the parts cannot be made sufficiently heavy to prevent all creep because the weight penalty would reduce efficiency too much. Many such parts are therefore designed for a certain expected life span. For this, accurate data are needed to determine how much the metal part can be expected to deform under the conditions of stress and temperature to be encountered in service. Tests which measure the deformation of a metal as a function of time at constant load and temperature are known as creep tests.

CREEP PHENOMENA

A typical creep curve is shown in Fig. 1. The vertical (Y) axis is creep strain and the horizontal (X) axis is time plotted on logarithmic coordinate. The curve consists of three parts: primary, secondary and tertiary creep, or first-, second- and third-stage creep. The strain shown is plastic or permanent strain. When a creep specimen is loaded, there will be some elastic extension of the specimen, but this is not shown in this curve. In the primary stage, the initial creep rate shows a continuous decrease with time. In second-stage creep, the creep rate is considered essentially

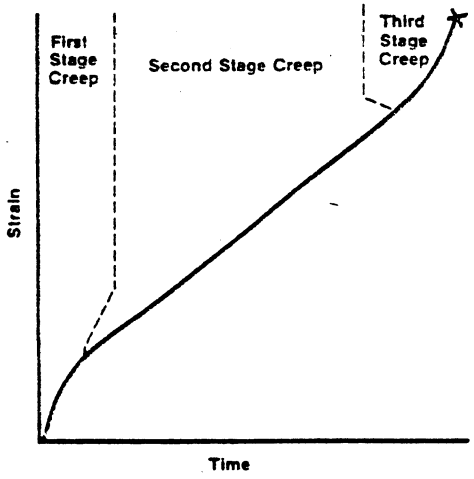

Fig. 1. Idealized creep curve

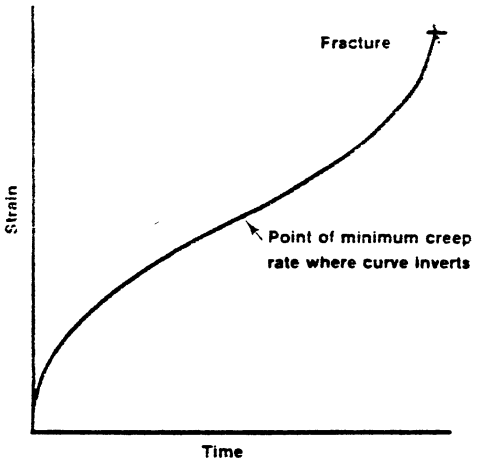

Fig. 2. Creep curve with minimum creep rate and point of inversion

constant. In the third stage, the strain rate increases rapidly to fracture. This increase in the third stage is due, in part, to the reduction in cross-sectional area and thus the increasing true stress. Measurements made of specimen cross section during third-stage creep indicate that the increase in strain rate is not due *only* to necking or reduction in cross-sectional area, however.

Although in the idealized creep curve shown in Fig. 1, the creep rate is shown as constant in the second stage, this does not occur in practice. If the test is long enough to show all stages of creep, the curve will show a continually diminishing rate of creep to a point where the curve inverts and the creep rate starts to increase again (see Fig. 2). The change in rate may be very slight over time; in some cases, the curve may approach a straight line.

RUPTURE TESTS

The rupture test is valuable in determining tendencies of materials that may have to break under an overload. It finds much use in selection of materials for applications where dimensioned tolerances are not critical but rupture could not be tolerated. The rupture test is similar to a creep test except that no strain measurements are made during the test. The specimen is stressed under a constant load at constant temperature as in the creep test, and the time for fracture to occur is measured. Measurements are also made of the elongation and reduction in area of the broken specimen. Stresses are higher than those used for creep tests. An example of a typical application of the rupture test would be for testing boiler pipes. This test is also called the stress-rupture test, or time-to-rupture test.

RELAXATION TESTS

The relaxation test is somewhat similar to the creep test, but the load continually decreases instead of remaining constant. This test is primarily of value in evaluating bolt materials. When a bolt is drawn up tight, a tensile load is present in the bolt and the bolt is elongated slightly. This causes a clamping load on whatever the bolt is mounted on. If the bolt creeps (extends or relaxes) this clamping load will be reduced. If the bolt elongates sufficiently to remove all tension, it no longer fulfills its function. In a relaxation test, the load is reduced at intervals in order to maintain a constant elongation (strain). A relaxation curve thus takes the general shape shown in Fig. 3. Note that the y axis in this curve is stress or load rather than strain (elongation) as in the creep curve.

TYPICAL PROCEDURE FOR MAKING A CREEP TEST

Selection and Preparation of Specimen. The same precautions used in selecting and preparing a specimen for a short-time tension test apply to specimens for creep testing. The specimen should be selected to be truly representative of that which it is supposed to represent. Machining and grinding should follow procedures to produce a surface as nearly stress-free as possible. There should be no undercutting at the fillets, and the gage length should be uniform in cross section or very slightly smaller at the center of the gage length.

The specimen is carefully identified in as much detail as is appropriate—type of metal, heat number, vendor, etc.—and this information is recorded with the specimen's measurements. Sometimes gage marks, for measuring total extension, are made on the specimen. Such marks or scribe lines must be used with care, because the depressions or scribe lines can cause premature failure on some materials. Any operation such as stamping the ends of the specimen must be used with care to avoid any damage to the specimen.

Loading. In mounting the specimen in the adapters and load train, care is needed to avoid straining of the specimen in handling. This can occur when threading the specimen into the adapters and when handling the load train with the specimen in place, especially if the specimen is very small or brittle. The load train (specimen adapters or grips, pull rods, etc.) with the specimen in place should be carefully examined for any misalignment which will cause bending of the specimen under load. The upper load train should be suspended from the lever arm and the compensating weight adjusted so that the lever arm balances. The strain-measuring clamps and extensometer, or the platinum strips, are attached

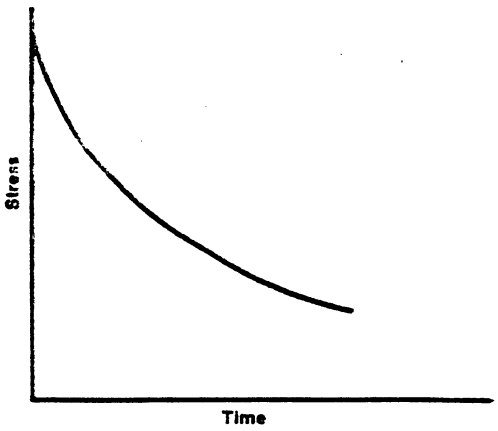

Fig. 3. Relaxation curve

to the specimen, and the load train is inserted into the furnace with the specimen centered. The specimen must be stabilized at temperature before [illegible] and the extensometer should be adjusted [illegible].

Loading of the weight pan should be done smoothly and without excessive shock. If the specimen is to be step loaded, the weight is placed on the weight pan in measured increments and the strain corresponding to each step of loading is recorded. The loading curve thus obtained is used in determining the elastic modulus. If step loading is not used, a method of applying the load smoothly must be used. This can be done by having a support such as a scissors jack under the load pan during loading. When all weights are in place, the supporting jack is smoothly lowered from under the weight pan.

Data Collection. Reading of strain should be made frequently enough to define the curve well. This will necessitate much more frequent readings during the early part of the test than later. The elastic portion of the stress-strain curve can be obtained by measurement of the instantaneous contraction when the load is removed at the end of the test if the specimen has not broken.

Temperature Control. In bringing the specimen to temperature, it is important that the specimen not be overtemperatured. A common practice is to bring the specimen up to about 50 °F (about 30 °C) below the desired temperature in about 1 to 4 h and then spend considerably longer in bringing the specimen to the desired temperature and adjusting for good stabilization. It should be understood that a period of time above the desired temperature is not cancelled in effect by an equal period at a temperature the same amount below the desired temperature. Any rise in temperature above the desired temperature of more than a small amount (such as defined by ASTM Recommended Practice for Conducting Creep and Time for Rupture Tension Tests of Materials) should be rejected. The limits specified in this recommendation are ±3 °F (±1.7 °C) up to 1800 °F (980 °C) and ±5 °F (±2.8 °C) above 1800 °F. At temperatures very much above 2000 °F (1095 °C), the limits are broadened somewhat. Variation of temperature along the specimen from the nominal test temperature should vary no more than these limits at these temperatures. These limits refer to indicated variations in temperature according to the temperature recorder.

Every effort should be made to ensure that the indicated temperature is as close to true temperature as possible. There is the possibility of both thermocouple error and instrument error. Thermocouples, especially base-metal thermocouples, drift in calibration with use or because of contamination. Other possible errors can result from incorrect lead wires or incorrect connection of lead wires, direct radiation on the thermocouple bead or other causes. Representative thermocouples should be calibrated from each lot of wires used for base-metal thermocouples and, except at low temperatures, base-metal thermocouples should not be re-used without slipping back to remove the wire exposed to high temperatures and rewelding. Noble-metal couples are generally more stable. However, they are also subject to error due to contamination and need to be annealed periodically. This can be done by connecting a variable transformer to the two wires and sending enough current through the wire to make it incandescent.

When the thermocouple is attached to the specimen, the junction must be kept in intimate contact with the specimen. The bead at the junction should be as small as possible, and there must be no twisting of the thermocouple elsewhere which could cause shorting. Any other metal contact across the two wires will cause shorting and erroneous readings. Many authorities recommend shielding the thermocouple junction from radiant heating.

Temperature-measuring, controlling and recording instruments must be calibrated periodically against some standard. This is usually done by connecting a precision potentiometer to the thermocouple terminals on the instrument and feeding in millivoltages corresponding to the output of the thermocouple at each of several temperatures. Tables of millivolt output for various types of thermocouples are readily available from manufacturers of precision potentiometers. Most creep and rupture machines are equipped with a switch which automatically shuts off the timer when the specimen breaks. In creep tests, the load is usually selected low enough so that rupture does not occur. The microswitch which shuts off the timer also shuts off or lowers the temperature of the furnace on many other creep-rupture units. In some furnaces the life of the heating element is severely reduced if the furnace is shut off after each test, so for some furnaces the temperature is lowered to some lower control temperature such as 1000 or 1200 °F (540 or 650 °C).

Interrupted Tests. Sometimes, because of a power failure or other problem, it becomes necessary to interrupt a test—that is, the specimen is cooled, then reheated. For many materials, this appears to have little effect on either creep properties or time-to-rupture if the times of cooling and heating are not very great. It cannot be stated, however, that such treatment will not affect any materials. Any interruption of a test should be reported.

PRESENTATION OF DATA

Creep. The usual method for presenting creep data is in the form of a curve showing percent creep strain as the vertical axis and time as the horizontal axis. The time is usually plotted on a log scale to show the early part of the curve in good detail and yet prevent the curve from being excessively long. Sometimes a whole family of curves is plotted on the same coordinates to show the effect of different temperatures or different stresses on the material.

Other methods for plotting data include time to reach a given percent of creep versus load at a constant temperature or time to reach a given percent of creep versus temperature at constant load.

The loading curve, showing the strain versus load as the specimen is loaded, is plotted separately and is used in computing the elastic modulus of the material at temperature.

Rupture. Rupture data are presented in several types of graphs. One has stress as the vertical axis versus log of time-to-rupture (at constant temperature) on the horizontal axis. Usually, stress-rupture data are presented by means of a parameter plot—i.e., stress is plotted against a parameter value which relates it to both time and temperature. Several different parameters have been used. A widely used one, the Larson-Miller parameter, follows the formula $P = (T + 460)(\log t + c)$. This means that the parameter value P equals the Rankine temperature (460 + the temperature in degrees Fahrenheit) times the log (base 10) of the time in hours plus a constant. The constant (c) has various values depending on the material but usually runs from about 17 to 23 for most materials tested. The value of c is determined by plotting log of time versus $1/[T(°F) + 460]$ using rupture data from several tests at constant stress but different temperatures on the same material. This produces a series of straight lines converging as on a single point. At this point $\log t = c$, and this constant is theoretically the best constant to use for the data involved. Figure 4 shows a parameter plot of stress-rupture data.

Shear Testing

IN GENERAL, the amount of existing shear-strength data is seriously less than the published data available for other mechanical properties. Stores of data that deal with mechanical properties such as tensile and yield strength, hardness and ductility for virtually all metals and metal alloys, and in a wide variety of conditions, are readily obtainable.

At least two reasons can be identified to explain the scarcity of shear-strength data. First, the demand is low, because the number of compo-

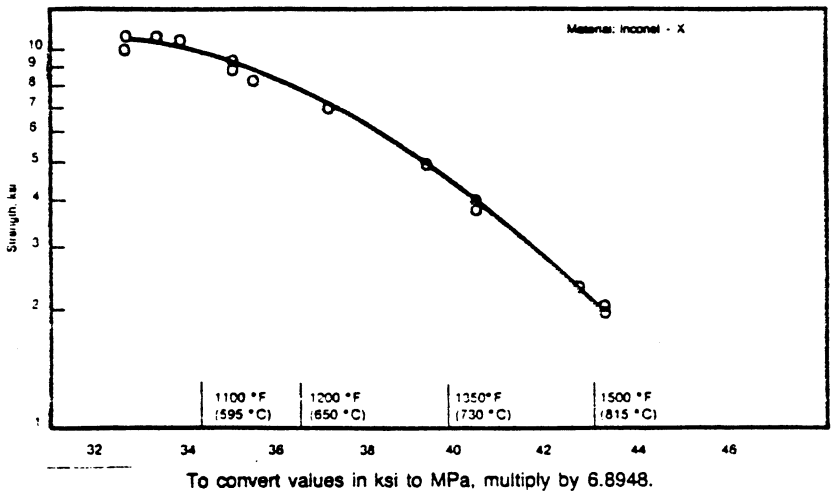

To convert values in ksi to MPa, multiply by 6.8948.

Fig. 4. Plot of stress-rupture data using the Larson-Miller parameter

I line short—

Fig. 5. Shear test fixture of the compression loading type used for single or double shear test (Tinius Olsen Testing Machine Company)

nents that are loaded in shear under service conditions is far less than that of components loaded in tension, compression, bending or torsion. Probably the primary reason for the lack of published data on shear strength is the difficulty in obtaining accurate test data. Shear testing inherently involves a number of variables; thus, the tests are less reproducible than testing for properties such as tensile or yield strength. Therefore, most shear testing has been performed by means of nonstandard equipment and procedures operating on arbitrary bases, thus producing results that are empirical.

The greatest needs for shear-test data are in the designing of structures that are riveted, pinned or bolted together and where service stresses are actually in shear. Notable examples of such structures are found in the aerospace industry. The required standardization is given by ASTM Standard B565.

SINGLE- AND DOUBLE-SHEAR TESTING

In the many tests that have been devised for evaluating shear strength, both single- and double-shear testing have been used. The double-shear technique is far more accurate, however, making those results more reproducible than results for the single-shear technique.

Compression-type loading for a shear fixture is shown in Fig. 5, with a specimen being tested in double shear. This type of fixture may also be used for single-shear tests.

Procedure. The test specimen is assembled in the fixtures, as shown in Fig. 6, and loaded in tension until complete failure occurs. Crosshead speed during the test should not exceed 0.750 in./min (19.1 mm/min), and loading rate should not exceed 100 ksi/min (690 MPa/min). The maximum load in double shear is determined by the direct reading on the testing machine.

CALCULATION OF SHEAR STRENGTH

The calculation of strength in double shear is a simple matter of dividing the machine load by the area of the cross section ($\pi D^2/4$). It follows, then, that single-shear strength is one-half of this value, or:

$$\text{single-shear strength} = \frac{P/2}{\pi D^2/4}$$

where P is load in pounds (kilograms), and D is diameter in inches (millimetres).

As previously stated, shear testing is more vulnerable to the effects of variables than certain other mechanical tests, such as tests for tensile or yield strength. The reader should note from examining Fig. 6 that, even when the fixtures and test specimens meet specified tolerances, some variations are bound to exist in the test-jig assembly that will be reflected as variables in the results.

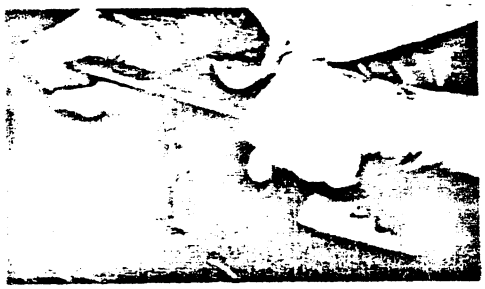

Fig. 7. Torsion testing of a brazed T-joint specimen

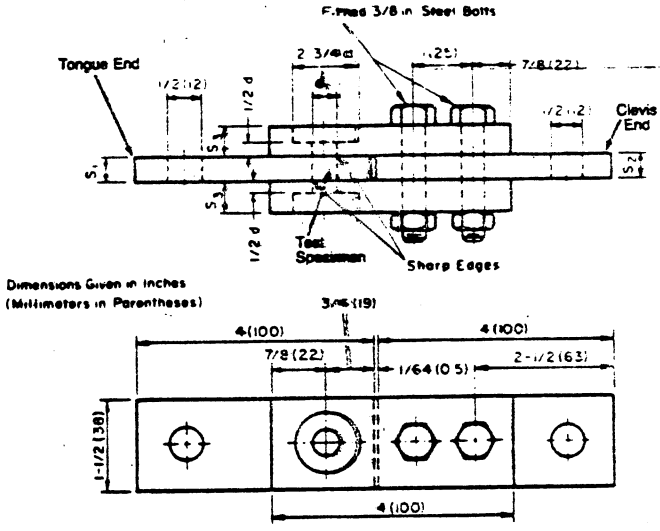

See ASTM B565 for a complete explanation of size requirements.

Fig. 6. Details of test jig used for testing specimens in double shear

The presence or absence of lubricant on the surfaces of the specimens and test fixtures can be responsible for substantial variations in the results. For example, a lubricated specimen may cause a reduction in shear strength of as much as 3%. To minimize this variable, it is recommended that the test fixtures and specimens be carefully cleaned prior to testing — preferably by means of ultrasonic cleaning in a suitable solvent.

Torsion Testing

IN THE TORSION TEST, a specimen is subjected to twisting or torsional loads to simulate service stresses for such parts as axles, crankshafts, twist drills and spring wire. The test has not been standardized, and is rarely specified. However, the torsion test provides information such as modulus of elasticity in shear (sometimes called modulus of rigidity), the shearing yield strength and the modulus of rupture (apparent ultimate shear strength). The torsion test may also be performed as a high-temperature twist test on materials such as tool steels to determine forgeability. The test does not provide meaningful results for very brittle materials such as cast irons, because these materials would fail in diagonal tension before the shear-strength limit was reached.

GENERAL PROCEDURE

In torsion testing, the specimen is clamped in clamping heads so that the specimen remains as straight as possible during testing. The test specimen is then twisted at a slow, uniform rate until it breaks, or until a specified number of turns is obtained. The number of turns is recorded. If the number of turns falls within an acceptable range, the test specimen is considered to have passed the test. Results of the torsion test are largely comparative, and have no standardized values.

Torsion testing is frequently employed to assess the quality of brazed joints for sheet-metal products. A T-joint of sufficient length is brazed and then subjected to two full turns in torsion (Fig. 7). Visual examination is made to determine if failure has occurred in the brazed joint.

One of the only standardized applications of the torsion test applies to torsion testing of wire (ASTM E558).

An example of a torsion-testing machine is presented in Fig. 8.

DATA

Torsion data are usually presented as torque-twist curves, in which the applied torque is plotted against the angle of twist. Torsion produces a state of stress known as pure shear, and the shear stress at yielding can be calculated from the torque at yielding and the specimen dimensions. The maximum stress for a cylindrical specimen (at the surface) can be calculated from the following relation:

$$S = \frac{16T}{\pi d^3}$$

where S is maximum shear stress in psi (MPa), T is torque in lb·in. (N·m) and d is specimen diameter in inches (cm). This formula holds only

1 line short

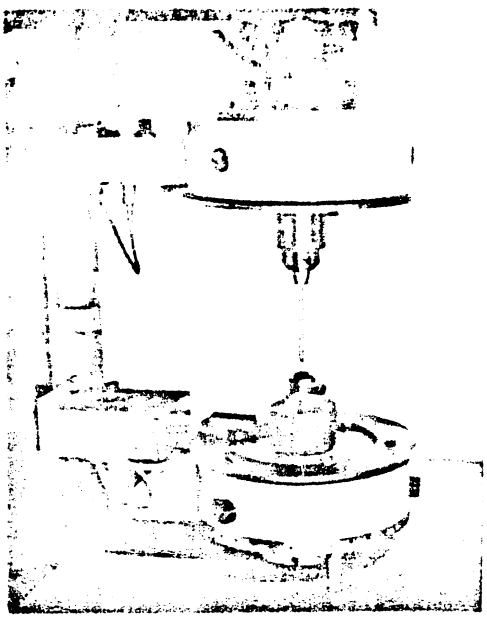

Fig. 8. Close-up of a 10 000 in·lb (1100 N·m) torsion-testing machine with special tooling for Phillips screwdriver bits (Tinius Olsen Testing Machine Company)

when the strain is proportional to stress, but is commonly used for computing higher stresses and for determining modulus of rupture (apparent ultimate shear strength).

The total torsional deformation is measured as angular twist of one end of the gage length in relation to the other. In order to obtain the angular twist per inch of gage length, the total angular twist is divided by the gage length. The angular twist per inch of gage length can then be converted into shear strain, in inches per inch, by multiplying by half the diameter of the specimen.

E_s, the modulus of elasticity in shear (sometimes called the modulus of rigidity), can be calculated from the following formula:

$$E_s = \frac{SL}{r\theta}$$

where S is maximum shear stress, in psi (MPa); L is the gage length of the specimen, in inches (cm); r is the distance from the axis of the specimen to the outermost fiber (half the diameter), in inches (cm); and θ is the angle of twist, expressed in radians, in length L.

The yield strength is generally defined as the maximum stress developed by a torque producing an offset of 0.2% from the original modulus line, analogous to the method used for determining tensile yield strength.

COMPARISON OF TORSIONAL AND TENSION DATA

From the torque-twist diagram it is simple to obtain a shear stress–shear strain diagram. The great advantage of the torsion test over the tension test is that large values of strain can be obtained without complications such as necking. One problem of torsional tests is that the stress is not constant throughout the cross section. This problem can be circumvented by using tubular specimens. If the results of a tension test and a torsion test are plotted for the same low-carbon steel, the two curves will be markedly different. However, if the two curves are normalized by converting the normal stress and longitudinal strain in the uniaxial test and the shear stress and strain in the torsion test into effective stress and strain, the two curves come into close correspondence. The effective stresses and strains are determined by well-known equations (for instance, Eq 1.67 and 1.81 in *Mechanical Metallurgy: Principles and Applications*, by M. A. Meyers and K. K. Chawla, Prentice-Hall, Englewood Cliffs, NJ, 1984.) These results show that the work hardening of the material is a function of the amount of plastic strain and does not depend on the state of stress. Such is not the case for all materials, however. Differences in texture due to different constraints can be responsible for substantial differences in the effective stress-strain curve.

Formability Testing

FORMABILITY is the technical term used to describe the ease with which a metal can be shaped through plastic deformation. Usually, it is synonymous with the term "workability." The evaluation of the formability of a metal involves both measurement of resistance to deformation (strength) and determination of the extent of plastic deformation that is possible before fracture (ductility). The emphasis in most formability tests, however, is on the amount of deformation required to cause fracture.

Because of the diverse geometries of the tools and workpieces and the various ways that forces of deformation are applied, different metalworking processes produce varying stress states. These can be divided into two broad categories: (*a*) bulk-deformation processes, such as forging, extrusion and rolling, where the stress state is three-dimensional; and (*b*) sheet-forming processes, such as deep drawing and stretch forming, where the stress state is two-dimensional and lies in the plane of the sheet. The tests that simulate bulk-formability testing are given in the article on compression testing.

BEND TESTS

Bend tests are among the most frequently used tests for evaluating the ductility of a metal or welded joint by measuring its ability to resist cracking during bending. Bending is the process by which a straight length is transformed into a curved length. The fibers of the metal on the outer (convex) surface of the bend are stretched, thus inducing tensile stresses. Simultaneously, the fibers on the inner (concave) surface of the bend are placed in compression. ASTM methods E190, E290 and E855 provide descriptions of the various procedures.

Bend Radius. For a given bending operation, the bend radius, R, cannot be made smaller than a certain value, or the metal cracks on the outer (tensile) surface. Usually, this *minimum bend radius* (R_{min}) is expressed in terms of multiples of the specimen thickness, t. Thus, a material with a 3t minimum bend radius can be bent without cracking through a radius equal to three times the specimen thickness. It follows, then, that a material with a minimum bend radius of 1t has greater formability; whereas a minimum bend radius of 5t indicates a less formable material.

Test Specimens. Bend-test specimens are usually in the form of a rectangular beam. Wherever possible, as with a plate or a sheet, the full thickness of the material should be used. Generally, the specimen thickness should not exceed 40 mm ($1\frac{1}{2}$ in.). When using a machined specimen of reduced thickness, the as-fabricated surface should be retained as a surface of the bend specimen. This surface should be oriented in the bend fixture as the tensile surface. For specimens cut from plate material, the width should be twice the thickness, but no less than 20 mm ($\frac{3}{4}$ in.). For thin specimens cut from sheet, the width should exceed eight times the thickness. The ratio of width to thickness affects the stress state produced in bending and, therefore, the ductility measured in the test. For this reason, bend-test results made on thin sheet should not be compared with those obtained with thicker plate to avoid erroneous conclusions about the formability of the materials.

The length of a bend-test specimen must be of some minimum that varies with thickness. Length, however, is not critical if the specimen is long enough to accomplish the bending operation. The edges of the specimen may be rounded to a radius not to exceed 1.6 mm ($\frac{1}{16}$ in.) to minimize edge cracking. Flame-cut surfaces should be machined to remove heat-affected metal. Sheared edges should be machined or smoothed on an abrasive belt to remove the sheared edge. Although bend testing usually is performed with specimens of rectangular cross section, round specimens may also be used.

Bend specimens may be cut from sheet or plate to evaluate the basic formability of the material or test the formability of an as-fabricated surface. Because most fabricated products have mechanical properties that are directional (anisotropic), directionality is an important consideration in making the test. Figure 1 shows the orientation of the bend-test specimen with the rolling direction for a longitudinal orientation and a transverse orientation. The transverse orientation generally shows lower ductility, because the tensile bending stresses are oriented perpendicular to the fiber structure developed by the rolling deformation.

The quality of welds often is evaluated by bend testing (ASTM E190). A specimen is cut from the welded assembly with the weld in the center of the specimen. The weld may be either transverse or parallel to the length of the specimen.

Free Bend Tests

A free bend test is one in which the curvature of the bend is left "free" to take its natural shape.

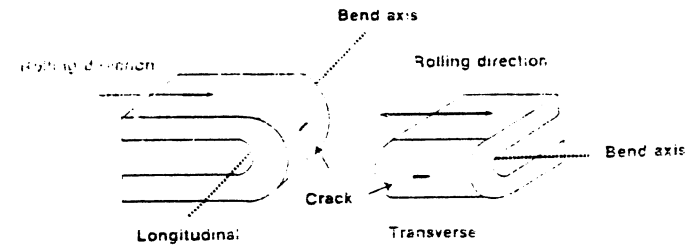

Arrows indicate direction of rolling. Source: Semi-Guided Bend Test for Ductility of Metallic Materials, ASTM E290-80, American Society for Testing and Materials, Philadelphia.

Fig. 1. Relative orientations of specimens for longitudinal and transverse bend tests

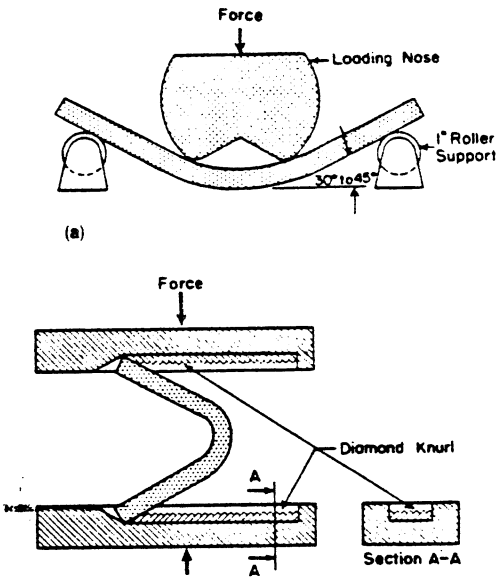

(a) A partial bend is made with the specimen in a horizontal position. (b) The specimen is positioned vertically, and the two knurled jaws are forced together until the specimen fractures or makes a 180° U-bend.

Fig. 2. Free bend tests

As shown in Fig. 2, the specimen is given a preliminary bend in a bending fixture (Fig. 2a) and then is transferred to a free bend fixture (Fig. 2b) where the bend is completed.

For moderately ductile materials, the formability is evaluated by the bend angle (α) that can be achieved before cracking occurs on the tensile face (outside surface) of the bend. For a highly ductile material that can be bent flat on itself ($\alpha = 180°$), the ductility is evaluated on the thickest specimen for which this can be done without cracking.

Restricted (Controlled) Bend Tests

A restricted bend test is one in which the test specimen is made to bend closely around a predetermined radius, R. Various examples of this test are shown in Fig. 3. The test shown in Fig. 3(a) usually is called a guided-bend test. The need for a test fixture sometimes may be eliminated by using a soft metal support to accommodate the punch, as in Fig. 3(b). For thin sheet metal, the bending force may be applied by a hand-operated lever or, alternatively, the sheet may be hammered over the bending die with a plastic or rawhide mallet (Fig. 3c). ASTM E290 describes this test in detail.

Ordinarily a grid pattern is lightly scribed on the tensile surface of the bend specimen before the restricted bend test. This surface is observed during the test, either with a mirror or by bending in small increments, to determine when the cracks first appear. At this point, the angle of bend is recorded, or the elongation of the tensile surface is determined from the grid network. Alternatively, the minimum bend radius that will permit bending through a fixed bend angle is determined as the measure of formability.

Bend Tests on Very Ductile Materials

Bend tests on very ductile materials are less controlled than those discussed above, but they are more severe tests. For a sheet, the basic test is to determine whether the sheet can be bent flat on itself through 180° without cracking. A further test of ductility is to cross-fold the sheet once again across the first fold (Fig. 4a). Bend tests are made on tubes by first flattening the tube, as shown in Fig. 4(b). This applies two separate transverse bends of nearly 180°. Subsequently, the flattened tube can be folded along its longitudinal axis (Fig. 4c).

SHEET-FORMABILITY TESTS

Several tests have been developed to evaluate the formability of sheet metal. Most complex sheet-forming operations can be resolved into a combination of bending plus stretching and drawing. In a pure stretch-forming operation, the edges of the blank strip are clamped, and the shape is produced by multidirectional stretching over the contours of the deforming tool or punch. Sheet-metal drawing, usually called deep drawing, utilizes the radial drawing of the sheet-metal blank into the die under the action of the punch. In deep drawing, the outer portion of the blank shrinks in diameter under circumferential compression. To prevent the blank from buckling, the blank-holder must exert sufficient pressure to prevent wrinkling, but not enough pressure to restrict the sheet from drawing into the die. Thus, in deep drawing, no deformation occurs in the central region of the punch directly under the punch; whereas in stretch forming, the maximum deformation occurs in this region. Figure 5 shows the essential differences between stretching and drawing.

The ability of the metal to undergo stretching is enhanced by a high value of strain hardening. Thus, a high value of the strain-hardening ex-

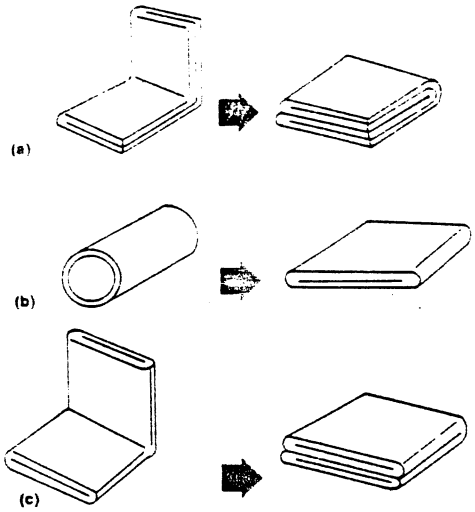

Fig. 4. Fold tests on ductile sheet or tube (see text)

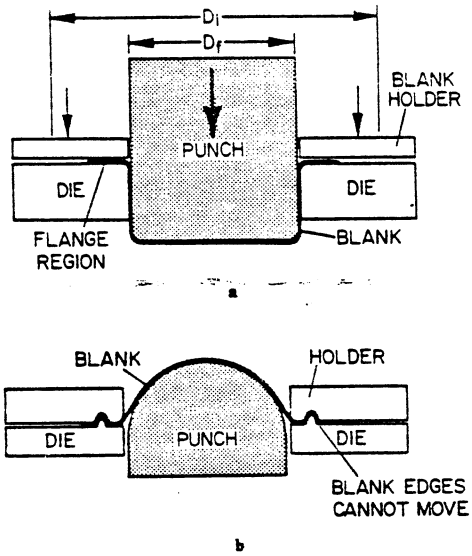

Fig. 5. Two operations that simulate stamping: (a) deep drawing; (b) stretching

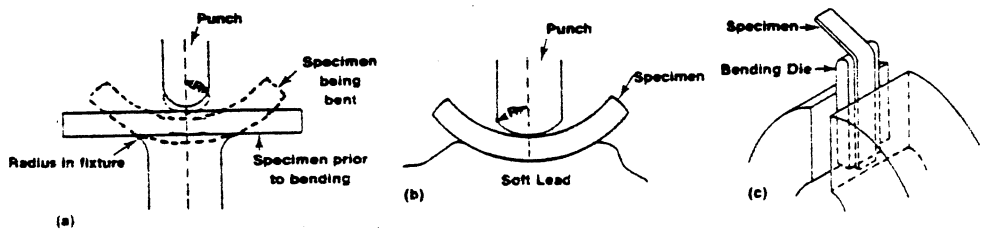

(a) Guided bend test wherein the test material is forced through a fixture of predetermined radius. (b) Modification of guided bend test using soft metal for the fixture. (c) Method of clamping the specimen while bending it over a predetermined radius. Source: same as Fig. 1.

Fig. 3. Restricted bend tests

ponent minimizes failure in stretch forming. The ability to withstand deformation in deep drawing, without failure, derives from the crystallographic texture of the metal sheet produced during rolling. The desired texture is such that the slip systems are aligned to give higher strength in the thickness of the sheet than in the plane of the sheet. As the plastic-strain ratio, r, becomes greater, the limiting draw ratio, LDR, becomes larger. The plastic-strain ratio is obtained by taking a tensile specimen and straining it to the point of necking. The longitudinal, thickness and lateral (width-direction) strains are determined and are, respectively, ϵ_l, ϵ_t and ϵ_w. The plastic-strain ratio is defined as:

$$r = \frac{\epsilon_w}{\epsilon_t}$$

ASTM 517 describes the test used to determine r. The limiting draw ratio (LDR) is the largest ratio of blank diameter to punch diameter for which the blank can be drawn into a cup of diameter D_p without tearing.

Many laboratory tests have been developed to measure and control the formability characteristics of sheet metals. Some, such as the hydraulic bulge test, are fundamental tests, while others attempt to simulate actual sheet-forming operations. Finally, the forming of actual parts on which a grid of circles has been imprinted in combination with the forming-limit curves (or Keeler-Goodwin curves) can be used to measure the formability of a given sheet metal.

In the hydraulic bulge test, metal is tested under uniaxial tension in the tension test and under local compression in the hardness test. In a typical press-forming operation, the metal is deformed under biaxial tension or biaxial tension-compression, in which the metal is strained simultaneously in two directions in the plane of the sheet. The hydraulic bulge test can be used to measure the properties of sheet metal when strained under biaxial conditions.

In the bulge test, a circular sheet is clamped at the edge and deformed by hydraulic pressure into a dome. For an isotropic sheet, essentially uniform biaxial stress and strain exist over an appreciable region at the center of the diaphragm. Failure eventually occurs in this central region.

Another sheet-formability test is the stretch bend test, which measures the ability of a sheet metal to be bent around a sharp radius under tension. It is a more severe test than the simple bend test and, in addition, can be used to measure the sensitivity of a metal to tearing from a stretched cut edge (a major problem in components with hole or stretch flanges).

In the stretch bend test, a sheared strip specimen of the material to be tested is clamped firmly between jaws and bent under tension, burr side outward, over a radiused punch. Normally, an autographic record of punch load and punch travel is obtained during the test. The punch travel—either at maximum load when cracks start to run into the material from the sheared edges, or at failure—is taken as the measure of specimen formability.

Ball Punch Deformation Test (Olsen and Erichsen Tests)

The Olsen test simulates sheet-metal performance under stretching conditions. It is a simple test in which the sheet metal is clamped rigidly in a blankholder, then stretched over a small hemispherical punch 22.2 mm (7/8 in.) in diameter. The stretchability of the sheet is then assessed by measuring the height to which the sheet can be stretched before fracture occurs. In a typical Olsen tester, both the punch travel and punch load are recorded, and the fracture point is established by noting the point at which the load suddenly decreases. Figure 6 shows sheet specimens that were subjected to four different formability tests.

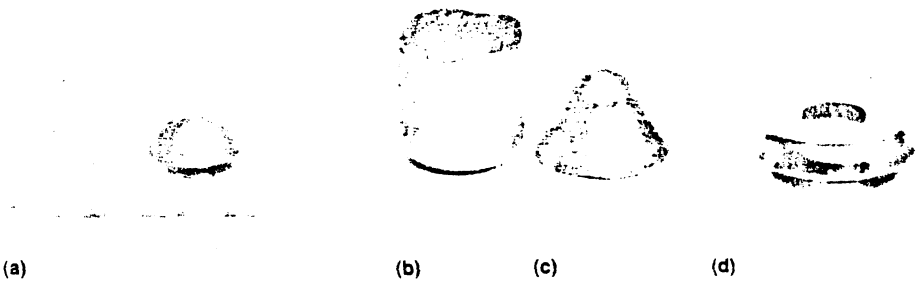

(a) (b) (c) (d)

(a) Olsen and Erichsen tests. (b) Deep draw cup test. (c) Fukui test. (d) Hole-expansion test. Courtesy of Tinius Olsen Testing Machine Co.

Fig. 6. Results typical of ductility tests on sheet-metal blanks

The Olsen test has been replaced by the "ball punch deformation test" standardized by ASTM (ANSI/ASTM E643-78). In this test, many of the test parameters that previously were left to the discretion of the individual performing the test are normalized. The standardized test applies to specimens with thicknesses between 0.2 and 2.0 mm. The machine to which the tooling is attached should have the capability of holding down the specimen (pressure between the top and bottom die) with a force of at least 10 000 N (2200 lbf).

Because the punch surface and the sheet-metal surface are in contact during this test, the friction between the two surfaces has a large effect on the test conditions. To maintain standard friction conditions from one test to the next, the lubricant is standardized. It is commercially available petroleum jelly (vaseline) applied to the punch only. ASTM E643 also states that other lubrication systems (e.g., polyethylene sheet plus oil) may be used as agreed between supplier and user.

The speed of the penetrator shall be between 0.2 and 1 in./min (0.08 and 0.4 mm/s). The end of the test corresponds to the drop in load, which is caused by necking of the sheet. If the machine is not equipped with a load indicator, the end point will be either visible necking or fracture of the test specimen in the dome. The cup height is measured at this point and is the penetrator (punch) displacement.

The Erichsen test, which is common in Europe, where it was standardized, is similar to the Olsen test in principle—that is, the test simulates sheet-metal performance under stretching conditions. The punch diameter for the Erichsen test is slightly smaller than the punch used for the Olsen test (20 mm or 0.79 in.).

The Erichsen test may be performed with or without lubrication, but the use of lubrication introduces a new variable, as described in the above discussion of the Olsen test. A portable instrument for performing the Erichsen test is available and has been widely used for control of formability or drawability in sheet-metal working, especially for quality control of incoming material.

Limiting Dome Height Test

In the Erichsen, Olsen and bulge tests, fracture occurs at conditions that are close to equibiaxial strain (when the strain is the same in the two perpendicular directions). In the uniaxial tension test, fracture occurs at a combination of tensile strain plus a small amount of contraction strain in the width direction. In practical press-forming operations, most fractures occur at close to plane-strain conditions, such as a tensile strain in one direction with zero strain in the other direction—which is somewhere between the conditions in the Olsen, Erichsen and bulge tests on the one hand and conditions in the tension test on the other.

The limiting dome height test has been developed to simulate more effectively the fracture conditions found in most parts. In this test, a large-diameter hemispherical punch, usually 100 mm (4 in.) in diameter, is used, and strips of sheet steel of varying widths are clamped and then stretched over the punch. The strips are marked with a grid of small circles, 2.5 mm (0.1 in.) in diameter, and the width strain at fracture is measured from the circle closest to the fracture. The width strain increases as the width of the sheet becomes greater.

The advantage of the limiting dome height test is that it more closely simulates the fracture conditions in a practical press-forming operation. It is a complex and time-consuming test, however, and the results are critically dependent on sheet thickness. In this test, lubrication is not critical; the standard practice is to perform the test dry (without lubricant).

Swift Cup Test

This test simulates the drawing operation and involves drawing of a small flat- or hemispherical-bottom, parallel-side cup. The sheet is held under a blankholder, as shown in Fig. 7, but is well lubricated with polyethylene and oil to ensure that the blank can be drawn in under the blankholder. Typical Swift cup test forming tools are available in 19-, 32- and 50-mm diameters for use with specimens ranging in thickness from 0.3 to 1.24, 0.32 to 1.30 and 0.45 to 1.86 mm, respectively. For drawing 40-mm-square cups from 80-mm-diam round specimens from 0.2 to 2 mm thick, a 40-mm-square forming tool is recommended.

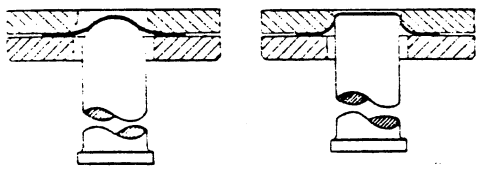

Punch diameter is 50 or 32 mm (2 or 1.3 in.).

Fig. 7. Swift cup test

The drawability of the metal is estimated by drawing a series of blanks of increasing diameter. The maximum blank size that can be drawn without fracture or slipping over the punch nose is used to calculate the limiting draw ratio. For example, 1018 cold-rolled steel disk using a 33-mm forming tool provides an LDR of 2.0. Because the condition of the edge of each blank can have an important effect on the test result, the blank edges usually are turned in a lathe to ensure strain-free, burr-free edges.

The results of this test correlate well with the performance of sheet metal in deep-drawn components, but, because of shape and alignment, reproducibility between laboratories is not good. The main problem with this test, however, is that it is time-consuming, and a large number of blanks of different sizes must be tested to obtain a reliable result.

Apart from measuring drawability, this test also can be used as a quality-control check to measure the tendency toward earing of the sheet metal. In this case, a blank of fixed diameter is drawn, and the height between the peaks and troughs in the cup wall are measured.

The Englehardt or draw fracture test is a variation of the Swift cup test for measuring drawability that overcomes the problems of complexity and time involved in that test. The draw fracture test involves drawing of a cup to the point of maximum drawing load, then clamping the flange and continuing the punch travel to fracture. A load-penetration curve similar to that in Fig. 8 is obtained and the Englehardt value, T, is calculated from the maximum draw and fracture loads, P_d and P_f:

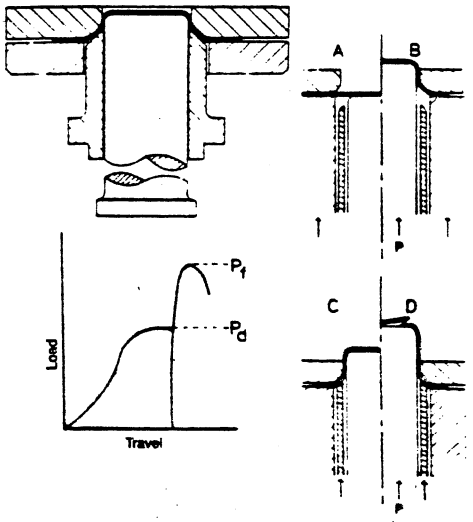

A and B: drawing. C and D: clamping and fracture.

Fig. 8. Draw fracture test

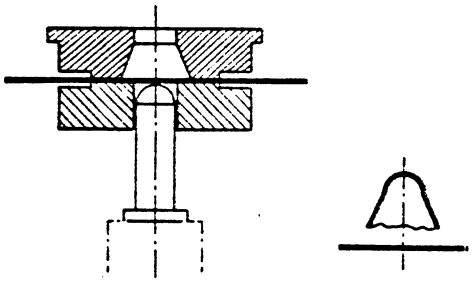

Fig. 9. Fukui conical cup test

Fig. 10. Sheet specimen subjected to punch-stretch test to the point of necking (indicated by clear line). Courtesy of S. S. Hecker, Los Alamos National Laboratory.

$$T = \frac{P_f - P_d}{P_f}$$

This result depends on strip thickness and usually is corrected, using an empirical relationship, to a nominal thickness. Because of its simplicity of operation and reproducibility, the draw fracture test is the most suitable for testing of drawability on a routine basis.

Fukui Conical Cup Test

The Fukui conical cup drawing test (Fig. 9) was developed to assess the performance of a material during forming operations involving both drawing and stretching. The advantage of this test is that no holddown is necessary if the correct relationship between sheet thickness and blank diameter is maintained.

A blank of the appropriate size is laid over a 30° conical entry die and forced into the cavity by a flat-bottom or hemispherical punch. The height of the cup at failure is used as a measure of formability. The test requires various tooling for different sheet thicknesses, and the result is thickness-dependent. It has been demonstrated that the Fukui cup depth is influenced mainly by stretchability, but with some dependence on drawability. Thus, this test does not correlate as highly with uniform elongation and r-values as do other tests that are predominantly stretch or draw, which may explain why the conical cup test has not been as widely accepted as other simulative tests.

Typical tooling commercially available for the Fukui test includes a cutting ring, cutting ram and ball indenter available for specimen thicknesses from 0.5 to 1.6 mm.

FORMING-LIMIT CURVES

The poor correlation often found between results of the common "cupping" test and actual metal performance led investigators to look at some more fundamental parameters. Localized necking requires a critical combination of major and minor strains (along two perpendicular directions in the sheet plane). This concept led to the development of diagrams known as the Keeler-Goodwin or forming-limit curves (Ref 1 and

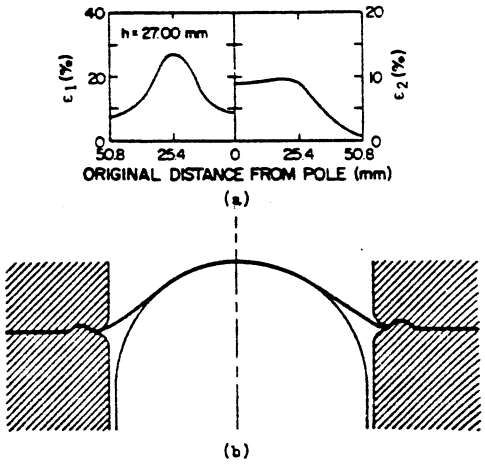

(a) Representation of strain distribution: ϵ_1, meridional strains; ϵ_2, circumferential strains; h, cup height. (b) Geometry of deformed sheet.

Fig. 11. Schematic illustration of sheet deformed by punch stretching

2). The forming-limit curve (FLC) is an important addition to the arsenal of testing techniques in formability.

Hecker (Ref 3) developed a punch-stretch apparatus and technique well suited for the determination of forming-limit curves. This apparatus consists of a punch with hemispherical head 101.6 mm (4 in.) in diameter. The die plates are mounted in a servohydraulic testing machine with the punch mounted on the actuator. The hold-down pressure on the die plates (rings) is provided by three hydraulic jacks (the hold-down load is 133 kN). The bead-and-groove arrangement in the rings eliminates any possible drawing in. The specimens are all gridded with 2.54-mm circles by a photoprinting technique. The load versus displacement is measured and recorded during the test, and the maximum load is essentially coincident with localized instability and the onset of fracture. A gridded specimen after failure is shown in Fig. 10. The circles become distorted into ellipses. The clear circumferential mark is due to necking. The strains ϵ_1 and ϵ_2 are called merid-

ional and circumferential strains, respectively, and are measured at various points when the test is interrupted. Figure 11 shows how these strains vary with distance from the axis of symmetry of the punch, at the point where the punch has advanced a total distance of h = 27 mm. ϵ_1, the meridional strain, is highest at about 25 mm from the center ($\epsilon_1 = 0.25$); ϵ_2, the circumferential strain, shows a definite plateau. By using sheets with different widths and varying lubricants between the sheet and the punch, different strain patterns are obtained. These tests are conducted to obtain different combinations of minor-major strains leading to failure. Figure 12 shows how the FLC curve is obtained. The minor strain (circumferential) is plotted on the abscissa and the major strain (meridional) is plotted on the ordinate axis. Four different specimen geometries are shown. The V-shape curve (FLC) marks the boundary of the safe-fail zone. The region above the line corresponds to failure; the region below is safe. In order to have both major and minor strains positive, a full-size specimen is used. By increasing lubrication, the major strain is increased; a polyurethane spacer is used to decrease friction. The drawings at the lower left- and right-hand corners of Fig. 12 show the deformation undergone by a circle of the grid. When both strains are positive, there is a net increase in area. Consequently, the thickness of the sheet has to decrease proportionately. On the left-hand side of the plot, negative strains are made possible by reducing the lateral dimensions of the blank. This allows free contraction in this dimension. The strains in an FLC are obtained by carefully measuring the dimensions of the ellipses adjacent to the neck-failure region.

These FLC's provide helpful guidelines for press-shop formability. Coupled with circle-grid analysis, they can serve as a guide in modifying the shapes of stampings. Circle-grid analysis consists of photoprinting a circle pattern on a blank and stamping it, determining the major and minor strains in its critical areas. This is then compared with the FLC to verify the available safety margin. The strain pattern can be monitored with changes in lubrication, hold-down pressure, and size and shape of drawbeads and the blank; this can lead to changes in experimental procedure. Circle-grid analysis also serves, in conjunction with the FLC, to indicate whether a certain alloy might be replaced by another one, possibly cheaper or lighter. During production, the use of occasional circle-grid stampings provides valuable help with respect to wear, faulty lubrication, and changes in hold-down pressure.

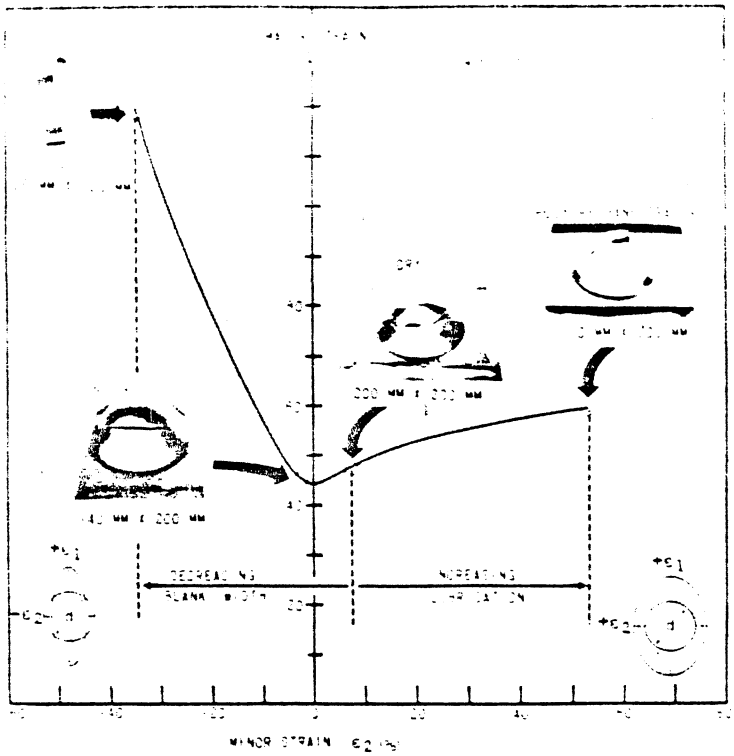

Fig. 12. Construction of a forming-limit curve (or Keeler-Goodwin diagram). Courtesy of S. S. Hecker, Los Alamos National Laboratory.

REFERENCES

1. S. P. Keeler and W. A. Backofen: *Trans. ASM*, Vol 56, 1963, p 25
2. "Application of Strain Analysis to Sheet Metal Forming Problems in the Press Shop," by G. M. Goodwin: SAE Automotive Engineering Congress, Detroit, Jan 1968 (SAE Paper No. 680093)
3. S. S. Hecker: *Met. Eng. Quart.*, Vol 14

Selected References on Mechanical Testing

Hardness Testing

The Hardenability of Steels, by C. A. Siebert, D. V. Doane and D. H. Breen: American Society for Metals, Metals Park, OH, 1977

The Science of Hardness Testing and Its Research Applications, edited by J. H. Westbrook and H. Conrad: American Society for Metals, Metals Park, OH, 1973

Hardness Testing Handbook, by V. E. Lysaght and A. DeBellis: American Chain and Cable Co., 1969

Metals Handbook, 8th Ed., Vol 11, *Nondestructive Testing and Quality Control*: American Society for Metals, 1976

Fracture Testing

Fracture Toughness Testing and Its Applications, STP 381: American Society for Testing and Materials, Philadelphia, 1965

Plane Strain Crack Toughness Testing of High Strength Metallic Materials, STP 410: American Society for Testing and Materials, Philadelphia, 1967

Fracture Toughness, STP 514: American Society for Testing and Materials, Philadelphia, 1972

Fracture Toughness Evaluation by R-Curve Methods, STP 536: American Society for Testing and Materials, Philadelphia, 1973

Fundamentals of Fracture Mechanics, by J. F. Knott: Butterworths, London, 1973

Fatigue Testing

Manual on Low Cycle Fatigue Testing, STP 465: American Society for Testing and Materials, Philadelphia, 1970

Metal Fatigue Damage—Mechanism, Detection, Avoidance, and Repair, STP 495: American Society for Testing and Materials, Philadelphia, 1971

Probabilistic Aspects of Fatigue, STP 511: American Society for Testing and Materials, Philadelphia, 1972

Fatigue and Fracture Toughness—Cryogenic Behavior, STP 556: American Society for Testing and Materials, Philadelphia, 1974

Handbook of Fatigue Testing, STP 566: American Society for Testing and Materials, Philadelphia, 1974

Manual on Statistical Planning and Analysis for Fatigue Experiments, STP 588: American Society for Testing and Materials, Philadelphia, 1975

Fatigue Crack Growth Under Spectrum Loads, STP 595: American Society for Testing and Materials, Philadelphia, 1976

Use of Computers in Fatigue Laboratory, STP 613: American Society for Testing and Materials, Philadelphia, 1976

Creep and Creep-Rupture Testing

Stress Rupture Parameters: Origin, Calculation, and Use, by J. B. Conway: Gordon and Breach, New York, 1969

Time-Temperature Parameters for Creep-Rupture Analysis, by S. S. Manson: Publication No. D8-100, American Society for Metals, Metals Park, OH, 1968

Source Book on Materials for Elevated-Temperature Applications, edited by E. F. Bradley: American Society for Metals, Metals Park, OH, 1979

High Temperature High Strength Nickel Base Alloys, 3rd Ed.: International Nickel Co., New York, 1972

Formability Testing

Formability: Analysis, Modeling, and Experimentation, edited by S. S. Hecker, A. K. Ghosh and H. L. Gegel: TMS-AIME, New York, 1977

Mechanics of Sheet-Metal Forming, edited by D. P. Koistinen and N. M. Wang: Plenum Press, New York, 1978

Formability Topics—Metallic Materials, STP 647: American Society for Testing and Materials, Philadelphia, 1978

Workability Testing Techniques, edited by G. E. Dieter: American Society for Metals, Metals Park, OH, 1984